

**Efficacy Improvement
of
Distribution of F-Latencies (DFL) in the
Diagnosis of Peripheral Neuropathy**



**Thesis submitted to the University of Dhaka
for the Degree of Doctor of Philosophy**

Muhammad Obaidur Rahman

Registration no. 167
Session: 2011 – 2012

Department of Biomedical Physics & Technology

University of Dhaka Bangladesh

October 2015

DECLARATION BY CANDIDATE



This thesis entitled “*Efficacy Improvement of Distribution of F-Latencies (DFL) in the Diagnosis of Peripheral Neuropathy*” is an original work carried out by me under the supervision of Professor K Siddique-e Rabbani of the Department of Biomedical Physics & Technology, University of Dhaka, Bangladesh. I further declare that this thesis has been completed by myself and no part of it has been submitted anywhere else in any form for any academic degree.

Muhammad Obaidur Rahman

Candidate for Ph.D.

Registration No. 167

Session 2011 – 2012

Department of Biomedical Physics & Technology

University of Dhaka, Bangladesh

October 2015

DECLARATION BY THE SUPERVISOR



I hereby certify that the present work entitled “*Efficacy Improvement of Distribution of F-Latencies (DFL) in the Diagnosis of Peripheral Neuropathy*” is an original research work being submitted by Muhammad Obaidur Rahman as a thesis for the award of the Doctorate of Philosophy. He conducted these studies under my close supervision at the Department of Biomedical Physics & Technology, University of Dhaka, Bangladesh.

To the best of my knowledge the work embodied in this thesis or any part thereof has not been submitted anywhere in any form for any academic degree.

Dr. Khondkar Siddique–e Rabbani

(Supervisor)

Professor and Founder Chairperson

Department of Biomedical Physics & Technology

University of Dhaka, Bangladesh

October 2015

Dedicated to

My parents

ACKNOWLEDGEMENT

I wish to express my heartiest gratitude and indebtedness to my supervisor Dr. Khondkar Siddique-e-Rabbani, Professor and Founder Chairperson of Department of Biomedical Physics, and Technology University of Dhaka for his constant guidance, advice, keen interest, encouragement, inspiration, every possible help throughout the research work which contributed in the completion of this thesis.

I am deeply thankful to Dr. Ehsan Alam Chowdhury for his sincere help with his study data in carrying out the DFL tests on the subjects as well as the corresponding MRI. I would like to offer my heartiest gratitude to my junior colleagues and all the members of my Department for their encouragement during this work.

I would like to express my deepest sense of gratitude to the authority of Dhaka University for giving the necessary permission and the ministry of Science and Technology providing financial support for carrying out the research work.

Finally, I would like to extend my indebtedness to all of my family members specially my wife and two of my angels for their relentless moral support and encouragement without which, it would never been possible for me to complete this research work in time.

Above all, I remember and thank Almighty Allah for His Grace, without which I could not have completed this thesis work successfully.

ABSTRACT

The nervous system, consisting of central and peripheral nervous systems, is very important for fast control of our body functions. Therefore, measurement of nerve conduction velocity (CV) is an important tool in the diagnosis of peripheral neuropathy. Distribution of F-latency (DFL) is a nerve conduction parameter introduced by our extended group at Dhaka University and this group has also developed a method for the detection of cervical spondylotic radiculopathy and myelopathy (CRM), a neurological problem causing neck pain, identifying patterns of DFL. The present work was taken up to improve this method of detection, or in other words, to improve the efficacy of DFL in the detection of CRM.

For normal healthy persons DFL has a single sharp peak while for subjects with CRM, DFL may have a broad peak, double or triple peaks as determined for the median nerve for which a large experience has been built upon by our extended group over the years. However, the distinction between the single and the broad peak is very subtle and it is necessary to obtain DFL as accurately as possible for an effective detection of CRM. DFL is a statistical parameter, and we cannot obtain a large number of F-latencies as the process is slightly painful for the patients, about 40 F-latencies being the practical maximum. The present work is related to the accurate determination of the pattern of DFL under such practical limitations.

For most of the studies in the present thesis, DFL data from human subjects obtained by a previous worker in our extended group was used where all the subjects had a standard diagnosis for CRM using MRI, which is the existing 'gold standard'. Of course some data were acquired during the present work as well.

For the accurate determination of DFL effort was made mainly in four directions which are described in brief in the following four paragraphs.

Firstly we tried to obtain a very closely related but more fundamental distribution called Distribution of Conduction Velocity (DCV) from the raw F-latencies to find out if it is useful in the detection of CRM. Our extended group had established earlier that DCV is an approximate mirror image of DFL. The argument behind this relationship also allows us to obtain DCV directly from the CVs corresponding to the multiple F-latencies. However, since a large experience has been built up through earlier work of our extended group in relating the shapes of DFL, obtained from the

median nerve, to CRM, we wanted to obtain DCVs that show similar but laterally inverted (mirrored) shapes. Our extended group used 2ms bin width to obtain DFL, so we tried to determine the most appropriate bin width for computing DCV from CVs so that the above mentioned features are retained. We related the typically used 2ms bin width of DFL for each nerve to the average of the maximum and minimum values, median and mode values of the corresponding CV data. It was found that by relating the median value of CV to the 2ms fixed bin width used for DFL, the best matching of DCV patterns was obtained.

An important part of this study was the sample size of DFL, i.e., to determine how many F-latencies are adequate to make a representative DFL for a particular bin size, particularly to make it effective in the detection of CRM. For this second study, two independent sets of data were used to make the judgment in between normal and abnormal DFL patterns. One used data from 25 median nerves of 16 persons collected earlier by our extended group. These had more than 30 but less than 40 F-latencies each. Further three sets of data were acquired during the present work where a large number (about 200 or more) of non-zero F-latency values were obtained from three median nerves of two subjects. Obtaining random samples with sample sizes of 5, 10, 20 and 30 from both the old and the new data and drawing corresponding DFLs with different bin widths a decision was reached in terms of the sample size, in order to detect CRM reliably. It was found that if the bin width is chosen at 1.5ms or 2.0ms, a minimum sample of 20 F-latencies can give a representative pattern of DFL for the detection of CRM.

The third study revealed a significant effect of the starting point on the DFL pattern where the number of samples is small (20 to 40), and came up with a new method to obtain a better detection of CRM. It was observed that if the starting point of DFL is shifted by half the bin width (by 1ms where the bin width is 2ms, used mostly in the DFL work by our extended group) then the DFL peak pattern may in some cases change from single to broad, broad to double or vice-versa. This observation created a great uncertainty in the prediction of CRM, particularly for the changes between single and broad peak patterns as this changes the prediction altogether. We obtained two sets of DFLs corresponding to each available data set from human subjects with the starting point shifted by 1ms (for a bin size of 2ms). Then we combined the results

through a logical OR and a logical AND operations, where a ‘Yes’ corresponded to the presence of CRM. The predictions were adjudged against MRI findings. It was found from this study that a logical OR operation of the above combination gave the best prediction for CRM, and this has now been introduced in the standard detection algorithm of our extended group.

Finally we tried to find alternative means of characterizing DFL patterns quantitatively, which could lead to objective determination of CRM. We tried two common statistical parameters – Skewness and Full Width Half Maximum (FWHM) – for this purpose. We calculated these values for identified single and broad peaked patterns of DFLs (the two groups under test) obtained from many subjects and performed statistical t-tests to determine significant differences, if any. It was found that skewness could not distinguish the two groups at all while FWHM could do it very well at a very high level of significance. From an observation of the FWHM values from both the groups, a preliminary threshold value was chosen at 2.5ms; a larger value would indicate a broad peak, giving an indication that this is a case of CRM. Of course a study involving a large number of data needs to be carried out to determine a more accurate value of the threshold.

The present study strengthens our confidence in characterizing the DFL patterns both qualitatively and quantitatively for the diagnosis of CRM. DFL can be measured using standard EMG equipment which can be made at a much lower cost in comparison with MRI machines, investigation using which is considered as the ‘gold standard of the day’ in this diagnosis. Portable EMG units based on Laptop computers are also available. Therefore, such portable equipment for measuring DFL can be distributed widely.

The present work builds up sufficient knowledge and confidence in the use of DFL for specific determination of Cervical spondylotic radiculopathy and myelopathy which will go a long way in the diagnosis of neural disorders, contributing to public health, and the society in general.

Table of Contents

DECLARATION BY CANDIDATE	ii
DECLARATION BY THE SUPERVISOR	iii
ACKNOWLEDGEMENT	v
ABSTRACT	vi
Chapter 1: Introduction	13
Chapter 2: Nervous System of the human body and certain relevant disorders	20
2.1. Nervous system	20
2.2. Peripheral Nervous System (PNS).....	22
Median Nerve	26
Ulnar Nerve.....	28
Radial Nerve.....	29
2.3. Action potential and its Propagation	30
2.3.1. Resting potential	30
2.3.2. Nerve action potential.....	31
2.3.3. Muscle action potential.....	35
2.4. Classification of fibers of the PNS.....	36
2.4.1. Distribution of Conduction Velocity (DCV)	37
2.5. Pathology	39
2.5.1. Carpal tunnel Syndrome.....	40
2.5.2. Radiculopathy.....	41
2.5.3. Myelopathy	43
Chapter 3: Measurement of Nerve conduction parameters	44
3.1. Nerve Conduction Velocity (NCV) Measurement through Evoked response	44
3.1.1. Volume conductor effect.....	45
3.1.2. Single Fiber Action Potential (SFAP)	47
3.1.3. Motor Unit Action Potential (MUAP)	47
3.1.4. Compound Muscle Action Potential (CMAP).....	48
3.1.5. Factors determining Conduction Velocity	49
3.2. Techniques for measurement of Nerve Conduction Velocity.....	50
3.2.1. Using surface electrodes	50

3.2.1.1.	Sensory Nerve Conduction (SNC) measurements.....	50
3.2.1.2.	Motor Nerve Conduction (MNC) Measurements	53
3.2.2.	Using Needle electrodes.....	55
3.2.2.1.	Near nerve needle recording techniques (NNRT)	55
3.2.2.2.	Selective nerve fiber stimulation	57
3.3.	<i>F-waves and its measurements</i>	57
3.3.1.	Physiology of F-wave	59
3.3.2.	Measurement of F-wave parameters	60
3.3.3.	Existing Clinical Applications of F-wave.....	62
3.4.	<i>Techniques for measurements of DCV</i>	63
3.4.1.	Experimental	63
3.4.1.1.	Hopf's method	65
3.4.1.2.	Ingram's method.....	66
3.4.1.3.	Kimura's method.....	67
3.4.1.4.	Gilliall et. al.....	68
3.4.1.5.	Harayama's et. al.	68
3.4.2.	Analytical	69
3.4.2.1.	Analysis of a single compound action potential	69
3.4.2.2.	Comparison of two compound action potentials	70
3.5.	<i>Summary of all the methods</i>	71
Chapter 4:	Distribution of F-Latencies (DFL) and its usefulness	74
4.1.	<i>Introduction to DFL and its relationship with DCV</i>	75
4.2.	<i>DFL in Carpal Tunnel Syndrome</i>	77
4.3.	<i>DFL in Radiculopathy and Myelopathy</i>	78
4.4.	<i>Hypothesis for abnormal DFL</i>	82
4.5.	<i>Generalization of Hypothesis</i>	86
Chapter 5:	Statistics related to DCV and DFL.....	88
5.1.	<i>Frequency distributions and its characterization</i>	88
5.2.	<i>Random sampling and Probability distributions</i>	90
5.2.1.	Random sampling	90
5.2.2.	Gaussian distribution.....	91
5.3.	<i>Performance of diagnostic test</i>	92
Sensitivity (SEN)	92

Specificity (SPE).....	92
Positive predictive value (PPV)	93
Negative predictive value (NPV)	93
Accuracy of efficacy	93
Positive likelihood ratio (LR^+)	94
Negative likelihood ratio (LR^-).....	94
5.4. ROC (Receiver Operator Characteristic) Curve	95
Constructions of ROC curve (a plot of SEN to 1 – SPE)	95
PRESENT WORK.....	96
Chapter 6: Distribution of Conduction velocity from Measured F-wave latency and matching with standard DFL	97
6.1. Introduction.....	97
6.2. Methodology.....	100
6.3. Results	103
6.4. Discussions	111
Chapter 7: Study for Sample size and Bin Width for DFL (for detection of CRM)	114
7.1. Introduction.....	114
7.2. Methods, Observations and Results	116
7.3. Discussions	136
Chapter 8: Effect of bin shifting on DFL for the detection of Cervical Spondylotic Radiculopathy and Myelopathy (CRM)	140
8.1. Introduction.....	140
8.2. Methodology.....	142
8.3. Results	144
8.4. Discussions	153
Chapter 9: Quantitative analysis of DFL pattern to identify single and broad peaks	155
9.1. Introduction.....	155
Skewness.....	155
Full Width at Half Maximum (FWHM)	156
9.2. Methodology	157

9.3. Results	157
9.4. Discussions	166
Summary and Conclusion	168
References	171

Chapter 1: Introduction

Human body might be regarded as a complex, elegant and sometimes incomprehensible computer. The central processor of this computer is the brain, and the primary connection to this CPU is the spinal cord. These components are called the *central nervous system* (CNS). The CNS receives data through a set of communication ports, processes it and sends instructions through another set of ports. Collectively these ports and their cabling are called the *peripheral nervous system* (PNS). The output devices control muscle activity through the autonomic and somatic nervous systems. The input devices monitor the performance of the body and keep the CNS aware of the external environment. Hence it is of great importance to understand different functions of the nervous system and its disorders. Scientists all over the world are trying to develop new and improved ways of analyzing the nervous system and its various disorders. Neurophysiology is the branch of biomedical physics which deals with the electrical signals produced by the human nervous system.

The nervous system conveys information by means of action potentials, which originate in the cell body or axon terminals and propagate along the nerve fibres. The brain is supplied with information along sensory or afferent nerves which are affected by sensations such as heat, touch and pain. On the basis of the information being received, the brain can make decisions and pass instructions down the motor or efferent nerves to produce end effect by causing muscle to contract. The basic structural unit of nervous system is a neuron – a nerve cell specialized for system plays a fundamental role in nearly body function.

To assess health of peripheral nerves, Nerve Conduction Study (NCS) is a standard technique. For sensory nerve studies, an artificial electrical stimulation is applied to a nerve trunk at one point and a corresponding evoked potential is recorded from another point on the nerve itself. The resulting response is a combination of action potentials from all nerve fibres in the nerve trunk and is called a compound nerve action potential (CNAP). For motor nerve studies, an artificial electrical stimulation is applied to a nerve trunk at one point and the corresponding evoked muscle action potential is recorded from a supplied muscle group. The resulting potential is called a compound muscle action potential (CMAP). An assessment of the nerve conduction

velocity (NCV) is obtained using these responses for different conduction distances along a nerve trunk.

However, a nerve trunk consists of thousands of nerve fibers with different signal conduction velocities. NCV measured using the above techniques only relate to the fastest nerve fibres as the timing to the response is measured at the onset of a response. The condition of the slower nerve fibres are not revealed through this technique, although information is hidden in the whole of the response. There are several diseases or disorders which may not affect the fast fibres, but the slower ones are affected.

The conduction of all the nerve fibres in a peripheral nerve trunk should conceptually be better assessed through a distribution of conduction velocity (DCV) of the individual nerve fibers which gives the number of fibres as a function of conduction velocity. Normal persons have a typical pattern of DCV with a single peak for motor alpha fibres that are sensitive to external electrical stimulation. It is expected to differ in cases of neural disease or disorder.

For experimental measurement of DCV, a method known as Hopf's technique (Hopf, 1962) with later modifications by others existed earlier, but this uses a complex collision technique which is not very practical in a clinical setting. Besides, it conceptually suffers from inaccuracy as it depends on the subtraction of two large quantities to assess the value of a very small parameter. Some efforts were also made to obtain DCV analytically from CNAP (Barker et al., 1979, Cummins et al., 1979a, Cummins et al., 1979b) but again these suffered from unreliability. Recently the Biomedical Physics group of Dhaka University under the leadership of Professor K Siddique-e Rabbani has made it possible to obtain relative DCV of motor nerves experimentally in a simple way using conventional EMG/EP equipment (Rabbani, 2011a, Rabbani, 2012, Rabbani et al., 2007).

If a motor nerve is artificially stimulated at any point, action potentials are generated within the individual nerve fibres, which travelling directly to the muscle served (orthodromic conduction), elicit a compound muscle action potential, an M-response that reproduces well on repeated supra-maximal stimulation. The onset latency of this M-response is conventionally used for obtaining a measure of nerve conduction velocity (NCV). From the stimulation site the action potentials also travel along the

nerve fibers in the opposite direction (antidromic conduction), towards the cell bodies in the spinal cord. Most of these action potentials die out, but a few percent of the cell bodies backfire after a short delay, and send fresh action potentials down the nerve fibers to the muscle. These in effect produce a delayed compound muscle action potential called F-response (Magladery and McDougal, 1950, Mayer and Feldman, 1967, McLeod and Wray, 1966), which is very much reduced in amplitude with respect to the M-response because of the small number of fibers involved. An important aspect of the F-response is that, unlike the M-response, it varies in shape, amplitude and latency on repeated stimulation; sometimes there will be none. The cause has been ascribed to the randomness of recruitment; which nerve cell will backfire is not previously known, being a random process, recruitment of fibers for F-response would statistically depend on the distribution of conduction velocity (DCV) for motor nerve fibers (Rabbani et al., 2007), specifically of those that contribute to F-responses, and therefore, a frequency distribution of F-latencies (DFL) from such multiple F-responses would be an approximate mirror image of DCV, latency being inversely proportional to the velocity. This was the basis of DFL which was developed by the Biomedical Physics group of Dhaka University, to which the author also belongs. Thus DFL has become a new and improved diagnostic tool in the neurophysiology.

All the studies of our extended group were conducted using a indigenously made computerized Electrophysiology system based on a BBC computer with the help and support of UK scientists (Rabbani et al., 1989). This has been in use at the Biomedical Physics Laboratory since 1988. This system is used to measure different electrical potentials generated within the human body where the data acquisition and analysis are performed using microcomputer. This system was later modified extensively to run on a popular IBM compatible microcomputer. Using microcomputer control, data can be acquired for various time ranges. Recently necessary software was developed to obtain DFL using the above equipment setup, which gives a frequency distribution of F-latency directly (Alam and Rabbani, 2010). The present software allows a maximum of 40 stimulations in 4 blocks of 10 responses (10 responses are plotted on a single computer display). The software is designed to group the data into 2 msec bins which was chosen during the previous work, rather intuitively. Besides this, another commercial Electromyography (EMG) machine, Nicolet EDX system

marketed by CareFusion was used in the present work to acquire additional data. It has the option to stimulate and record a number of more than 200 responses at a time.

The Dhaka University group has also shown that DFL of normal subjects have single peaks while DFL of subjects with Cervical Spondylosis (CS) which will be renamed in our study as Cervical spondylotic Radiculopathy and Myelopathy (CRM) have double peaks or broad peaks (Alam and Rabbani, 2010). Hypotheses have been put forward to explain the occurrence of double or broad peaks in CRM, in both radiculopathy (compression of nerve roots) and Myelopathy (compression of spinal cord) at appropriate vertebral levels (Rabbani, 2011b). The hypotheses have been verified by the Dhaka University group (Chowdhury, 2013, Hossain et al., 2011), a collaborative work by Dhaka and Singapore (Rabbani et al., 2014), and through a double blind experiment on 62 nerve of 31 subjects (Chowdhury et al., 2014). The latest results show that the presence or absence of CRM can be correctly predicted by DFL to an order of 75% to 80% when compared against MRI, the current gold standard in the diagnosis of CRM.

CRM is a disorder which affects people mostly over the age of 50 years, however, younger people have also been diagnosed of CRM which may be caused by poor posture, long working hours on a desktop computer, carrying too much weight, etc., besides lesions caused by tumours and other physical reasons. Such disorders, if allowed to continue, may cause eventual disability through muscle degeneration. Therefore, detection of CRM early is important, so that remedial actions may be taken up before it has caused significant permanent damage. At present the only reliable detection technique of CRM is MRI, which is not available widely. Besides, it is very expensive as well. X-rays can only show up bony growth that may cause radiculopathy, but it cannot detect changes in soft tissue that may also cause both radiculopathy and myelopathy. As the previous results of our extended group have established DFL as being able to predict CRM in about 75% to 80% of cases, DFL has the potential to become a frontline diagnostic method for screening of CRM.

Therefore, if we can improve the efficacy of DFL in the detection of CRM further, it would greatly benefit people the world over. The present work was taken up with this general goal.

The basis of DFL is the random occurrence of F-responses due to stimulations applied to a motor nerve and statistical distributions based on the principles of probability. In the earlier works, 30 to 40 stimulations were applied and a bin size of 2 msec was chosen, rather intuitively, to obtain the frequency distribution of DFL. Whether this choice is justified and whether we would get additional information by applying more stimulations and choosing smaller bin sizes is a worthwhile study at this stage.

The present work will try to improve the efficacy of DFL in the diagnosis of CSN with a limited number of data in a sample (30 to 40 F-responses), as this will be clinically acceptable. The plan of the present work is summarized below:

- i) Distribution of conduction velocity of nerve fibres (DCV) in a peripheral nerve is necessary for a proper assessment of neural health and diagnosis of neuropathy. Earlier work of our extended group at Dhaka University has established that conceptually DFL owes its origin to DCV of motor nerve fibres. On this basis it was claimed that a relative and approximate DCV of motor nerve fibres, particularly for nerve fibres contributing to the F-responses, can be obtained simply through a mirror image of DFL (Rabbani et al., 2007). In the present work we plan to obtain this DCV directly from the Conduction Velocity (CV) values obtained from the individual F-responses, numbering 30 to 40 for each nerve. However, a large experience has been built up on the patterns of DFL in the detection of CRM. Therefore, it will be an important consideration to match the resulting DCVs to the mirror images of the DFLs obtained in the conventional way. The choice of bin width for the distribution is expected to be important in obtaining this pattern matching. Since time (latency) and velocity are inversely related, it will not be straightforward and a few methods for this choice of bin width will be attempted to get the best matching with DFL of many human subjects with and without CRM.
- ii) An important part of this study is the sample size of DFL, i.e., how many F-latencies are used to make a DFL for a particular bin size. The aim would be to find the minimum sample size that would give an acceptable prediction capability of DFL for CRM since supramaximal stimulations given for the F-responses are rather unpleasant for the patient. For this purpose firstly about 40 non-zero F-latency values will be collected from a subject, either normal or

having CRM. DFL obtained using these 40 values will work as the standard reference for the present study. From these 40 data points 30, 20 and 10 data values will be chosen randomly. Comparing the shapes of the DFLs plotted from these separate data sets it will be attempted to find the minimum number of data points (whether 30, 20 or 10) that agrees with the standard pattern (for the 40 data points). These results will then be compared using different statistical formulii to find the best agreement. This sample size minimization (of F-latencies) will provide a relief to the patients from getting too many unpleasant stimulations.

- iii) We would also like to study the above with a large number of data, say, more than 200, which will allow us to have more combinations of sample sizes and also will allow us to choose smaller bin widths for DFL. Since patient cooperation cannot be obtained for such a study, we will perform the same on a few volunteers. This study, if in agreement with the study mentioned above, is expected to give us more confidence in the use of a small number of data points.
- iv) Being a statistical phenomena, it is expected that patterns of DFL will change somewhat if the starting point of the bins are shifted a little, keeping the bin width the same, even for the same data set. This is particularly so since we are limiting our sample size to 20 to 40. Since the detection of CRM is affected by subtle changes in the pattern of DFL, particularly between a single peak and a broad peak, careful attention is to be given to reliability issues. We should try to get as much accurate information as possible from a limited number of data from a particular patient. Therefore we wanted to take up a study of the DFL patterns due to shifting of the starting point by half the bin width. The decisions regarding CRM may be the same or different from these individual DFL patterns. So we need a technique to combine these two results which is expected to give a better performance of DFL. We will try several logical operations, such as OR, AND, etc., for this purpose. Hopefully this work will help improve the prediction capability of DFL significantly.
- v) For quick diagnosis in the field, an objective analysis is much helpful where a large number of subjects are to be screened for CRM. Therefore, further studies will be carried out to find quantitative descriptions of the DFL patterns, particularly using statistical parameters dispersion, chronodispersion

(difference between the longest and the shortest latencies), Skewness, Full Width Half Maximum (FWHM), etc.

As mentioned before, MRI investigation gives most of the information that we need for evaluation of neurological disorders of peripheral nerves, but this equipment is very expensive, and needs a large permanent establishment and infrastructure. The individual investigations are also very expensive. Therefore MRI investigation cannot be made available for widespread use, particularly in low resource countries like Bangladesh. A low cost and easy to measure alternative, if available, can be of immense importance. DFL can be measured using standard EMG equipment which can be made at low cost. Portable units based on Laptop computers are also available. Therefore, such portable EMG equipment for measuring DFL can be distributed widely.

Through the present work, we expect to build up sufficient knowledge and confidence in the use of DFL for specific determination of CRM which will go a long way in the diagnosis of neural disorders, contributing to public health, and the society in general.

Chapter 2: Nervous System of the human body and certain relevant disorders

The task of controlling the various functions of the body and coordinating them into an integrated living organism is not simple. Consequently, the nervous system, which is responsible for the task, is the most complex of all systems in the body. It is also one of the most interesting. Composed of the brain, numerous sensing devices, and a high-speed communication network that links all parts of the body, the nervous system not only influences all the other systems but is also responsible for the behavior of the organism. In this broad sense, behavior includes the ability to learn, remember, acquire a personality, and interact with its society and the environment. It is through the nervous system that the organism achieves autonomy and acquires the various traits that characterize it as an individual.

2.1. Nervous system

A very general look at the anatomy of the brain should be helpful in understanding the functions of the nervous system. Figure 2.1 shows a side view of the brain and the spinal cord which together is called the ‘Central Nervous System’. It also shows representative peripheral sensory and motor nerves together with their respective terminations. There are many such peripheral nerves coming out of the vertebra of the human body.

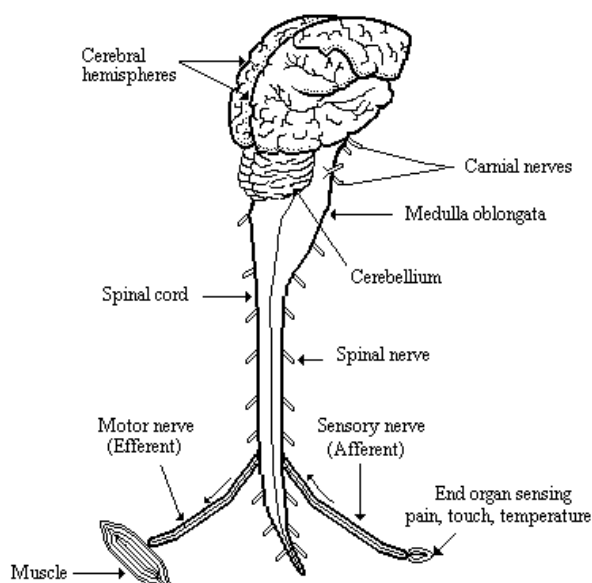


Figure 2.1: General organization of the nervous system

Like all other organ systems the nervous system consists of different types of cells. A neuron is a single cell with a cell body, sometimes called the soma, one or more “input” fibers called dendrites, and a long transmitting fiber called the axon as shown in Figure 2.2. Often the axon branches near its ending into two or more terminals. The portion of the axon immediately adjacent to the cell body is called the axon hillock. This is the point at which action potentials are usually generated. Branches that leave the main axon are often called collateral. Certain types of neurons have axon or dendrites coated with a fatty insulating substance called myelin. The coating is called a myelin sheath and the fiber is said to be myelinated. In some cases, the myelin sheath is interrupted at rather regular intervals by the nodes of Ranvier, which help speed the transmission of information along the nerves. Outside of the central nervous system, another insulating layer sometimes called neurilemma surrounds the myelin sheath. This layer, thinner than the myelin sheath and continuous over the nodes of Ranvier, is made up of thin cells, called Schwann cells.

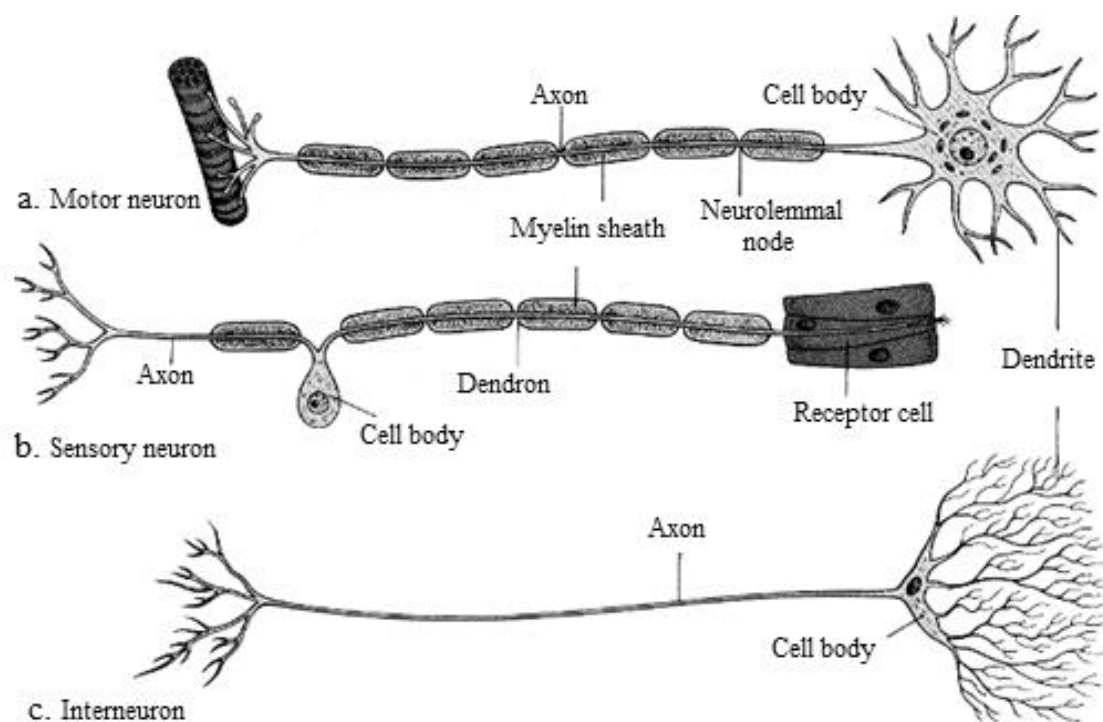


Figure 2.2: Different types of neuron, (a) Sensory neuron, (b) Motor neuron and (c) Interneuron.

As can be seen from Figure 2.2, some neurons have long dendrites, whereas others have short ones. Axons of various lengths can also be found throughout the nervous system. In appearance, it is difficult to tell a dendrite from an axon. The main difference is in the function of the fiber and the direction in which it carries

information with respect to the cell body. Both axon and dendrites are called nerve fibers, and a bundle of individual nerve fibers is called a nerve.

Nerves that carry signals from the brain to operate various muscles are called efferent nerves. The unit of the efferent nerve is motor neurons. Motor neurons, illustrated in Figure 2.2 (a), conduct impulses from the central nervous system to the effected organs, such as muscles and glands. The cell body of a motor neuron is embedded in the central nervous system. The cell body collects impulses from other neurons through its hundreds of tiny fibers, called dendrites. A long, single axon carries these impulses from the cell body to a muscle fiber or a gland. At the point, where an axon of a motor neuron enters a muscle fiber there is a structure called a motor end plate. When impulses reach an end plate they set off chemical reactions which result in electrical action potentials in the connected muscle fibres causing muscular contraction.

Nerves that carry sensory information from the various parts of the body to the brain are called afferent nerves. The unit of the afferent nerve is a sensory neuron. Sensory neurons illustrated in Figure 2.2 (b) conduct impulses from the sense organs to the central nervous system (brain, spinal cord). That is, they conduct impulses from sense receptors in the body such as eyes, ears, nose, taste buds, and touch receptors. Sensory neurons have two long fibers: a dendron which conducts impulses from a sense organ to the cell body of the neuron, and an axon which conducts impulses from the cell body into the central nervous system.

Most nerve fibers, whether dendrons or axons, that lie outside the central nervous system are encased in a sheath of fatty material which insulates them from one another. The main nerves of the body are, in fact, bundles of these insulated fibers wrapped together in a layer of connective tissue, something like a bundle of insulated wires, which make up a nerve trunk, or simply, a nerve.

2.2. Peripheral Nervous System (PNS)

Nerve fibers outside the central nervous system together are bundled into long cable like structures inside the body, called peripheral nerves. This name applies even to fibers from neurons whose cell bodies are contained within the central nervous system. Throughout most of their length, many peripheral nerves are mixed, in that they contain both afferent and efferent fibers. Afferent peripheral nerves that bring

sensory information into the central nervous system are called sensory nerves, whereas efferent nerves that control the motor functions of the muscles are called motor nerves. Peripheral nerves leave the spinal cord at different levels, and the nerves that innervate a given level of body structures come from a given level of the spinal cord.

The peripheral nervous system actually consists of several subsystems. The system of afferent nerves that carry sensory information from the sensors on the skin to the brain is called somatic sensory nervous system. Visual pathways carry sensory information from the eyes to the brain, whereas the auditory nervous system carries information from auditory sensors in the ears to the brain.

Another major division of the peripheral nervous system is the autonomic nervous system, which is involved with emotional responses and controls smooth muscle in various parts of the body, heart muscle, and the secretion of a number of glands. The autonomic nervous system is composed of two main subsystems that appear to be somewhat antagonistic to each other, although not completely. These are the sympathetic nervous system, which speeds up the heart, causes secretion of some glands, and inhibits other body functions, and the parasympathetic nervous system, which tends to slow the heart and controls contraction and secretion of the stomach. In general, the sympathetic nervous system tends to mobilize the body for emergencies, whereas the parasympathetic nervous system tends to conserve and store bodily resources.

Peripheral nerves are defined as the part of the nervous system situated outside the central nervous system (CNS). The division of the nervous system into the PNS and the CNS is to some extent artificial since parts of peripheral neurons are situated within the CNS. Only the thin unmyelinated postganglionic autonomic fibers are located wholly outside the CNS (Berthold and Rydmark, 1995). Even though by definition peripheral nerve disorders are located to the PNS, a number also affect the central parts of the PNS (Asbury and Johnson, 1978, Berger and Schaumburg, 1995).

The dorsal and ventral roots are attached to the spinal cord by a series of filaments. Figure 2.3 shows the anatomy of a nerve. Figure 2.4 shows anatomy of the spinal cord. Each spinal nerve quickly divides into a dorsal and a ventral (primary) ramus. The dorsal rami supply the back; the ventral rami supply the limbs and ventrolateral

part of the body wall. In the cervical and lumbosacral regions, the ventral rami intermingle and form plexuses from which the major peripheral nerves emerge.

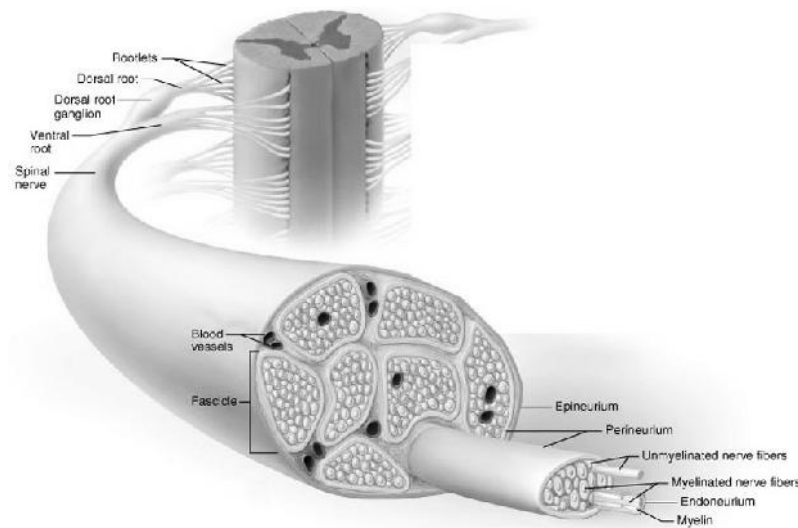


Figure 2.3: Anatomy of a nerve

When the ventral ramus of a spinal nerve enters a plexus and joins other such rami, its component funiculi ultimately enter several of the peripheral nerves emerging from the plexus. Thus, as a general principle, each ramus entering a plexus contributes to several peripheral nerves as shown in Figure 2.5, and each such peripheral nerve contains fibers derived from several ventral rami. Thus each spinal nerve has a pattern of ultimate distribution to that characteristic of peripheral nerves (Hansen and Schliack, 1962, Haymaker and Woodhall, 1953, Sunderland, 1978).

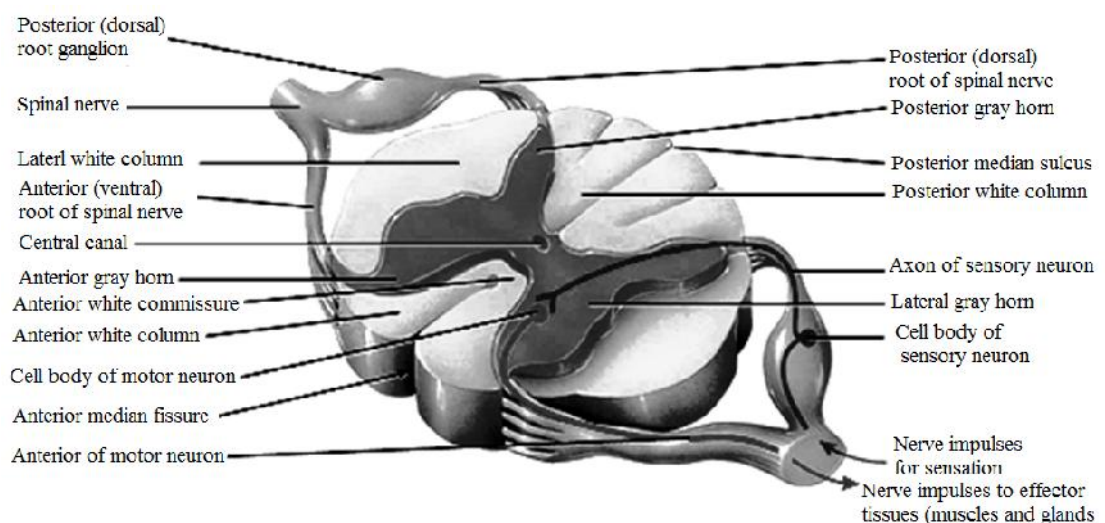


Figure 2.4: Transverse section of a thoracic spinal cord

The ventral rami of the upper four cervical nerves unite to form the cervical plexus. The brachial plexus, which is situated partly in the neck and partly in the axilla, is formed by the ventral rami of the lower four cervical nerves (C5, C6, C7 and C8) and the greater part of the ventral ramus of the first thoracic nerve (T1). Our study mostly focused on the peripheral nerves of the upper limbs containing this brachial plexus. Detail of this plexus is shown in Figure 2.6.

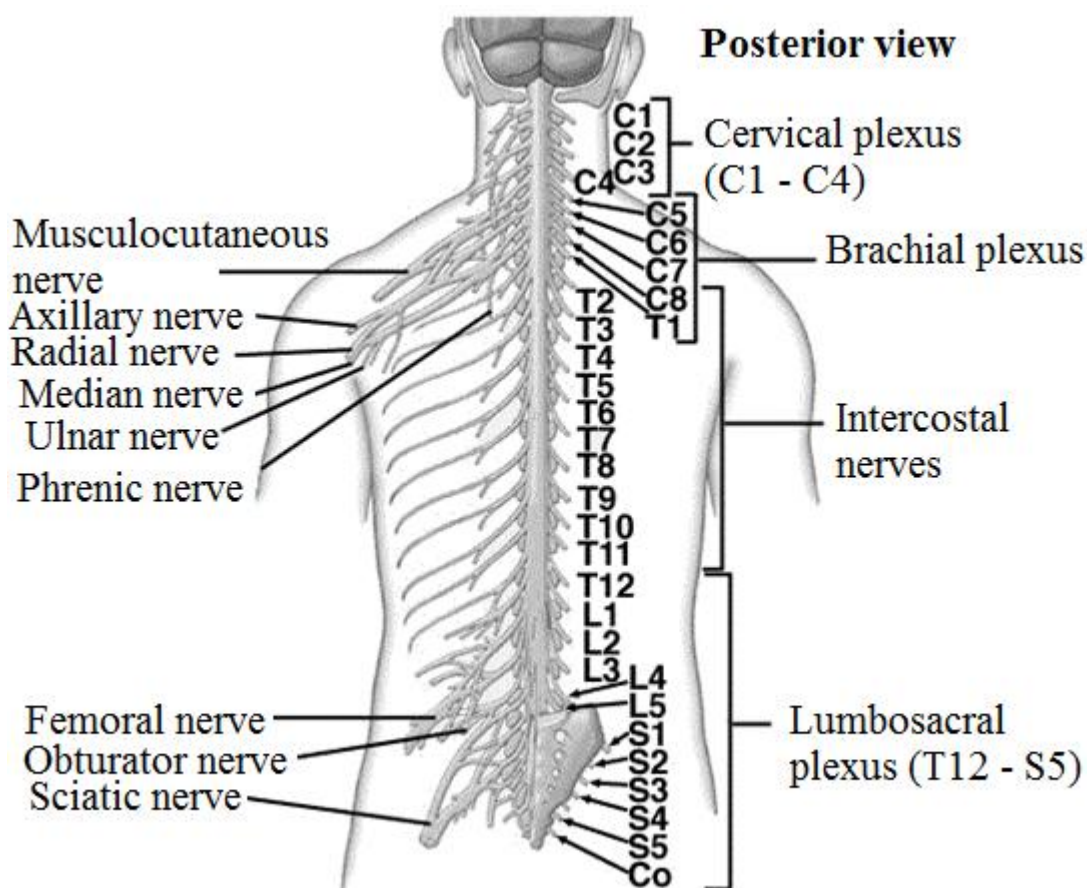


Figure 2.5: Spinal cord, Plexuses and their branches

The common, though not invariable, arrangement of branches is as follows. The ventral rami of the fifth and sixth cervical nerves unite to form the upper trunk, that of the seventh remains single as the middle trunk, and the eighth cervical and first thoracic rami form the lower trunk. Each trunk then divides into an anterior and a posterior division (for the front and back of the limb, respectively). The anterior divisions of the upper and middle trunks unite to form the lateral cord, the anterior division of the lower trunk forms the medial cord, and the three posterior divisions

form the posterior cord. The terminal branches arise from the three cords. These include a number of cutaneous and muscular branches and the important terminal branches, namely the median, ulnar, radial, musculocutaneous, and axillary nerves. Some other branches from these three cords are not discussed here. We focused only the three major nerves, median, ulnar and radial of the upper limbs that are related to our study.

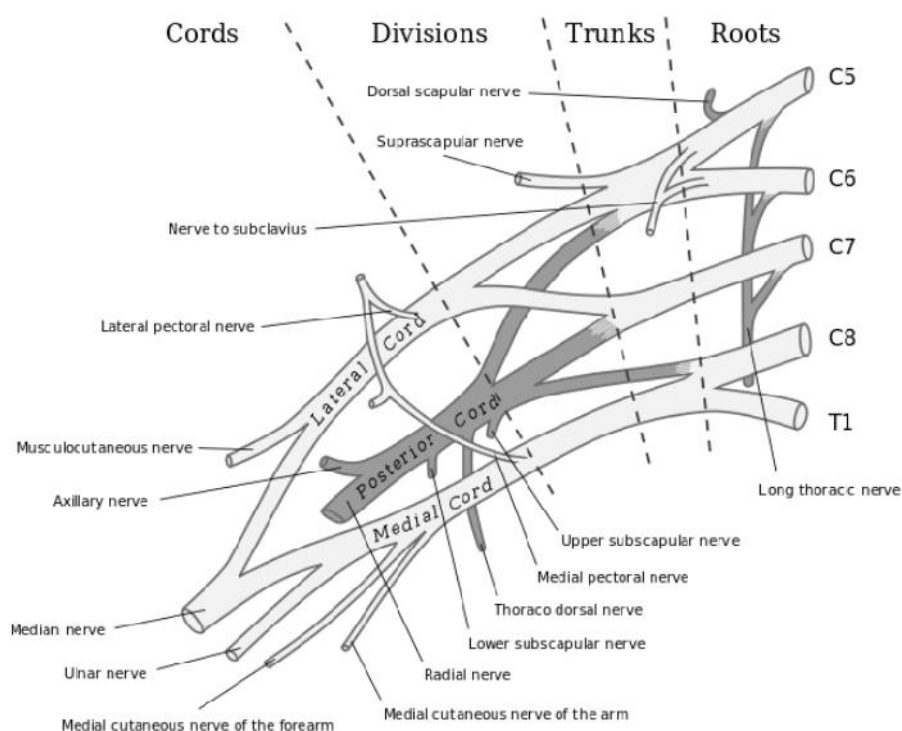


Figure 2.6: Anatomy of a brachial plexus

Median Nerve

The *median nerve* runs relatively superficially in its entire course from the axilla to the palm. The median nerve arises from the lateral and medial cords of the brachial plexus as a mixed nerve derived from C5, C6 to C8 and T1 roots, which unite in a variable fashion (Figure 2.6 and 2.7). It supplies most forearm flexors and the muscles of the thenar eminence. It also sub serves sensation to the skin over the lateral aspect of the palm and the dorsal surfaces of the terminal phalanges, along with the volar surfaces of the thumb, the index and the middle fingers, and half of the ring finger. The sensory fibers of the middle finger enter the C7 root through the lateral cord and middle trunk, whereas the skin of the thumb and the index finger receives fibers from

the C6 or C7 root through the lateral cord and upper or middle trunk. The median nerve innervates no muscles in the upper arm. It enters the forearm between the two heads of the pronator teres, which it supplies along with the flexor carpi radialis, palmaris longus, and flexor digitorum superficialis. It then gives rise to a pure muscle branch called the anterior interosseous nerve, which innervates the flexor pollicis longus, pronator quadratus and flexor digitorum profundus I and II. The main nerve descend the forearm and passes through the carpal tunnel between the wrist and palm. It supplies lumbricals I and II after giving off the recurrent thenar nerve at the distal edge of the carpal ligament (Kimura, 1989).

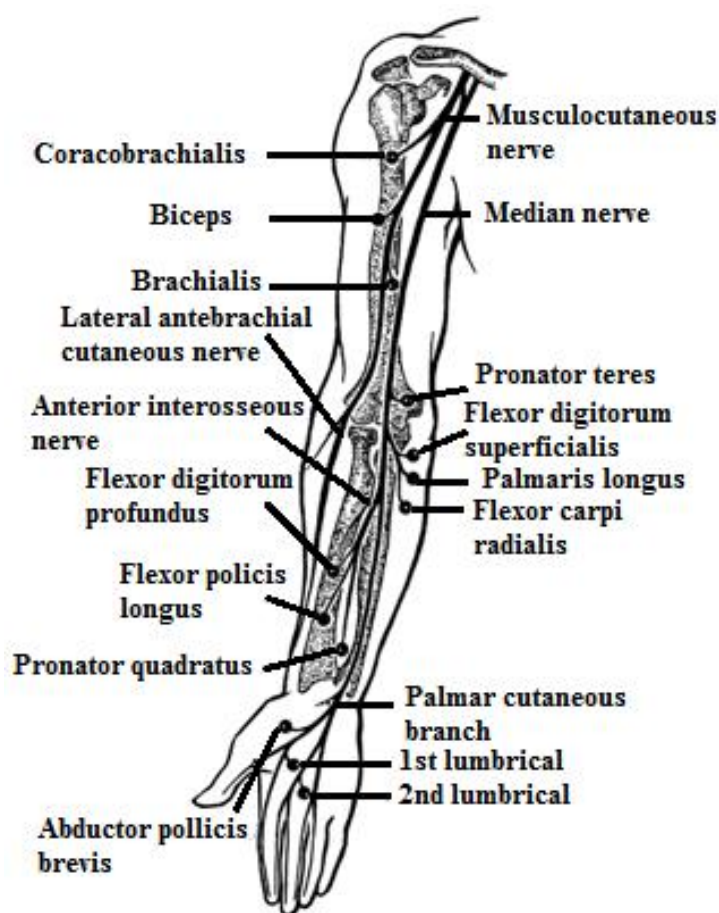


Figure 2.7: Schematic representation of the median nerves with branches. The black dot in each instance represents a muscle or a muscle group. The sequences of muscular branches are the more common ones. Based on studies by Sunderland and Ray (Gardner et al., 1975, Sunderland and Hughes, 1946)

Ulnar Nerve

Like the median nerve, the *ulnar nerve* takes a relatively superficial course along its entire length. Common sites of stimulation include Erb's point, the axilla, the elbow, the wrist and the palm. The ulnar nerve, as a continuation of the medial cord of the brachial plexus, derives its fibers from the C8 and T1 roots (Figure 2.6 and 2.8). It lies in close proximity to the median nerve and brachial artery at the axilla. In this position the ulnar nerve passes between the biceps and triceps, then derives posteriorly at the mid portion of the upper arm and becomes superficial behind the medial epicondyle. After entering the forearm, it supplies the flexor carpi ulnaris and flexor digitorum profundus III and IV. It passes along the medial aspect of the wrist to enter the hand, where it gives off two branches. The superficial sensory branch supplies the skin over the medial aspect of the hand from the wrist distally, including the hypothenar eminence, the fifth digit and half of the fourth digit.

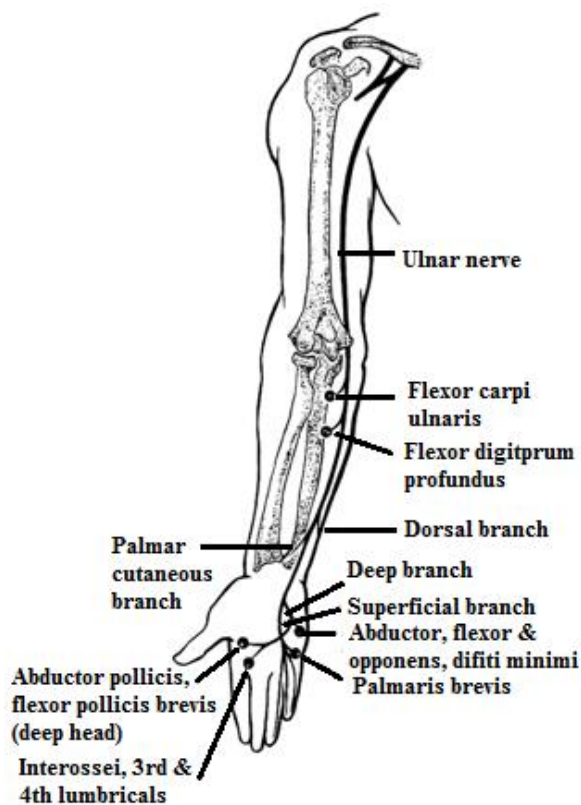


Figure 2.8: Schematic representation of the sequences of muscular and cutaneous branches of the ulnar nerve. The sequences of muscular branches are the more common ones. Based on studies by Sunderland and Hughes (Gardner et al., 1975, Sunderland and Hughes, 1946)

Radial Nerve

The *radial nerve*, as a continuation of the posterior cord, derives its axons from the C5 through T1, or all the spinal roots contributing to the brachial plexus (Figure 2.6 and 2.9). The nerve give off its supply to the three heads of the triceps and the anconeus, which originates from the lateral epicondyle of the humerus as an extension of the medial head. The radial nerve then enters the spiral groove, winding around the humerus posteriorly from the medial to the lateral side.

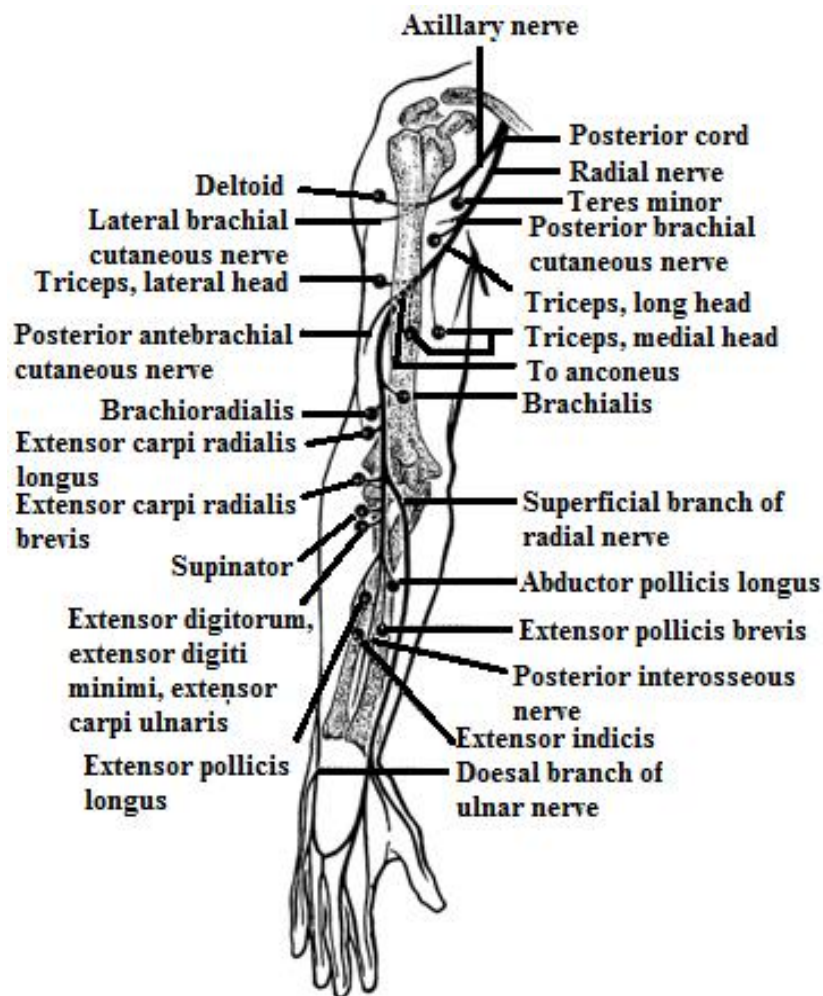


Figure 2.9: Schematic representation of the sequence of muscular branches of the axillary and radial nerves. The sequences of muscular branches are the more common ones. Based on studies by Sunderland (Gardner et al., 1975, Sunderland, 1946)

2.3. Action potential and its Propagation

2.3.1. Resting potential

The resting potential of most mammalian neurons is constant as long as the cell remains inactive due to lack of stimulation. Curtis and Cole in the USA, and Hodgkin and Huxley in England, in the late 1930s revealed the resting potential to be a physico-chemical phenomenon set up and maintained by the differential concentration of ions across the axon membrane and the selective permeability of the membrane to the ions. Analyses of the intracellular fluid of the axon and the extracellular seawater bathing the axon showed that ionic electrochemical gradients exist.

Table 2.1: Ionic concentrations of extracellular and intracellular fluids in squid axon. (Values given are approximations in m.mol/kg H₂O, data from Hodgkin AL (Hodgkin, 1958))

Ion	Extracellular Concentration	Intracellular Concentration
K ⁺	20	400
Na ⁺	460	50
Cl ⁻	560	100
A ⁻	0	370

The axoplasm inside the axon has a high concentration of potassium (K⁺) ions and a low concentration of sodium (Na⁺) ions, in contrast to the fluid outside the axon, which has a low concentration of K⁺ ions and a high concentration of Na⁺ ions. The distribution of ions inside and outside a nerve axon is listed in Table 2.1. Although there are different ions present, Na⁺ and K⁺ contribute the most to the electrical action potentials.

These electrochemical gradients are maintained by the active transport of ions against their electrochemical gradients by specific regions of the membrane known as cation or sodium pumps. These constantly active carrier mechanisms are driven by energy supplied by ATP and couple the removal of Na⁺ ions from the axon with the uptake of K⁺ ions.

The active movement of these ions is opposed by the passive diffusion of the ions, which constantly pass down their electrochemical gradients at a rate determined by the permeability of the axon membrane to the ion. K⁺ ions have an ionic mobility and membrane permeability, which is 20 times greater than that of Na⁺ ions; therefore K⁺

ions loss from the axon is greater than Na^+ ions gain. This leads to a net loss of K^+ ions from the axon, and the production of a negative charge within the axon. The value of the resting potential is largely determined by the K^+ ions electrochemical gradient.

Changes in the permeability of the membrane of excitable cells to K^+ and Na^+ ions lead to changes in the potential difference across the membrane and the formation of action potentials in, and the propagation of nerve impulses along, the axon. Figure 2.10 shows in simplified form the cross section of a cell with its resting potential. A cell in the resting state is said to be polarized.

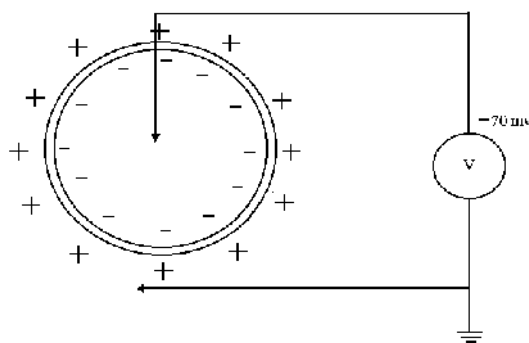


Figure 2.10: Polarized cell with its resting potential

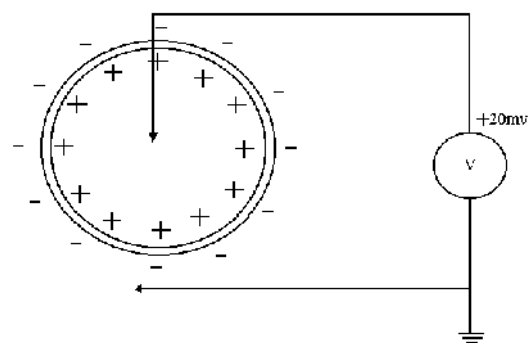


Figure 2.11: Depolarized cell during action potential

2.3.2. Nerve action potential

When a section of the nerve membrane is excited, either by the flow of ionic current or by an externally supplied stimulus, the membrane characteristics change and begin to allow Na^+ ions to enter and K^+ ions to leave the nerve axon. This causes the transmembrane potential to change, which in turn causes further reduces the barrier of the membrane to Na^+ ions. The net result is an avalanche effect in which Na^+ ions literally rush into the cell to try to reach a balance with the ions outside. At the same time K^+ ions, which were in higher concentration inside the cell during the resting state, try to leave the cell but are unable to move as rapidly as the Na^+ ions. As a result, the cell has a slightly positive potential on the inside due to the imbalance of K^+ ions. This potential is known as the action potential and approximately +20mV. A cell has been excited and that displays an action potential is said to be depolarized; The process of changing from the resting state to the action potential is called depolarization. Figure 2.11 shows the cross section of a depolarized cell. The process of depolarization is the beginning of a nerve action potential (NAP).

Because a nerve fiber is immersed in conducting fluids, ionic currents will flow around it from the polarized to the depolarized parts. These external current flow around a nerve fiber is also responsible for the transmission of a nerve action potential along the nerve. The external current flow at the point of depolarization disturbs the transmembrane potential further along the fiber and this causes depolarization to spread. An action potential is transmitted along a fiber with a speed of a few meters each second.

Myelin is an electrical insulator, which prevents current flowing from the nerve axon into the extracellular fluid, and if it were continuous along the nerve then no action potentials would be possible. The myelinated segment of an axon has very low electrical capacitance. The action potential decrease in amplitude as it travels through the myelinated segments. The reduced signal then acts like a stimulus at the node of Ranvier. The myelin is actually in bands with nodes of Ranvier between the bands. External current can flow from the nodes of Ranvier and the effect of the myelin is to speed up the transmission of nerve action potentials, which jumps from one node to the next. This process is called saltatory conduction and it allows action potentials to be transmitted at about ten times the speed which fibers without myelin conduct impulses. The fast nerve fibers, which supply our muscles, are myelinated fibers whereas the slow fibers used to transmit pain sensation are slow non-myelinated fibers.

The speed of transmission of a nerve impulse is actually determined by the capacitance of the membrane and myelin, which separate the axon from the outside fluid, and the resistance of the axon as shown in Figure 2.12. Any resistance and capacitance have a time constant which controls the rate at which the potential across the capacitance can change.

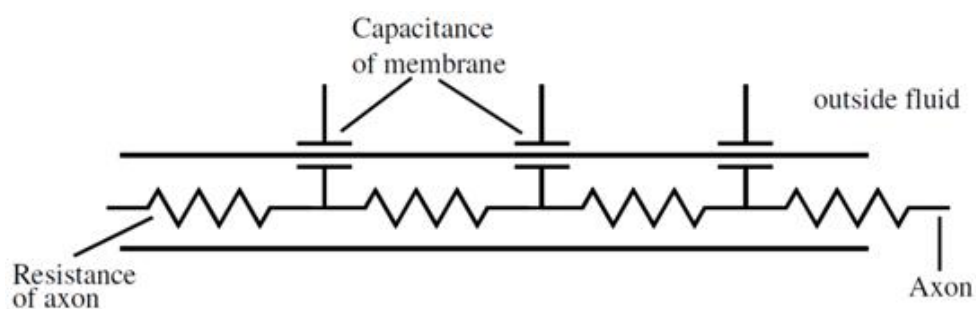


Figure 2.12: Axonal resistance and capacitance control impulse transmission

Depolarization is not a permanent state because the properties of the semipermeable membrane change with time so that, after a short time, the nerve fiber reverses to its polarized state. Figure 2.13 shows how the transmembrane potential changes along a nerve fiber, which is first depolarized and then repolarized. What is shown is a single nerve action potential lasting for about 1 msec. The major change during depolarization is that sodium enters the cell and during repolarization potassium enters the cell. Transmission can be in either direction. Muscle fibers can also transmit action potentials, which result in a contraction of the muscle.

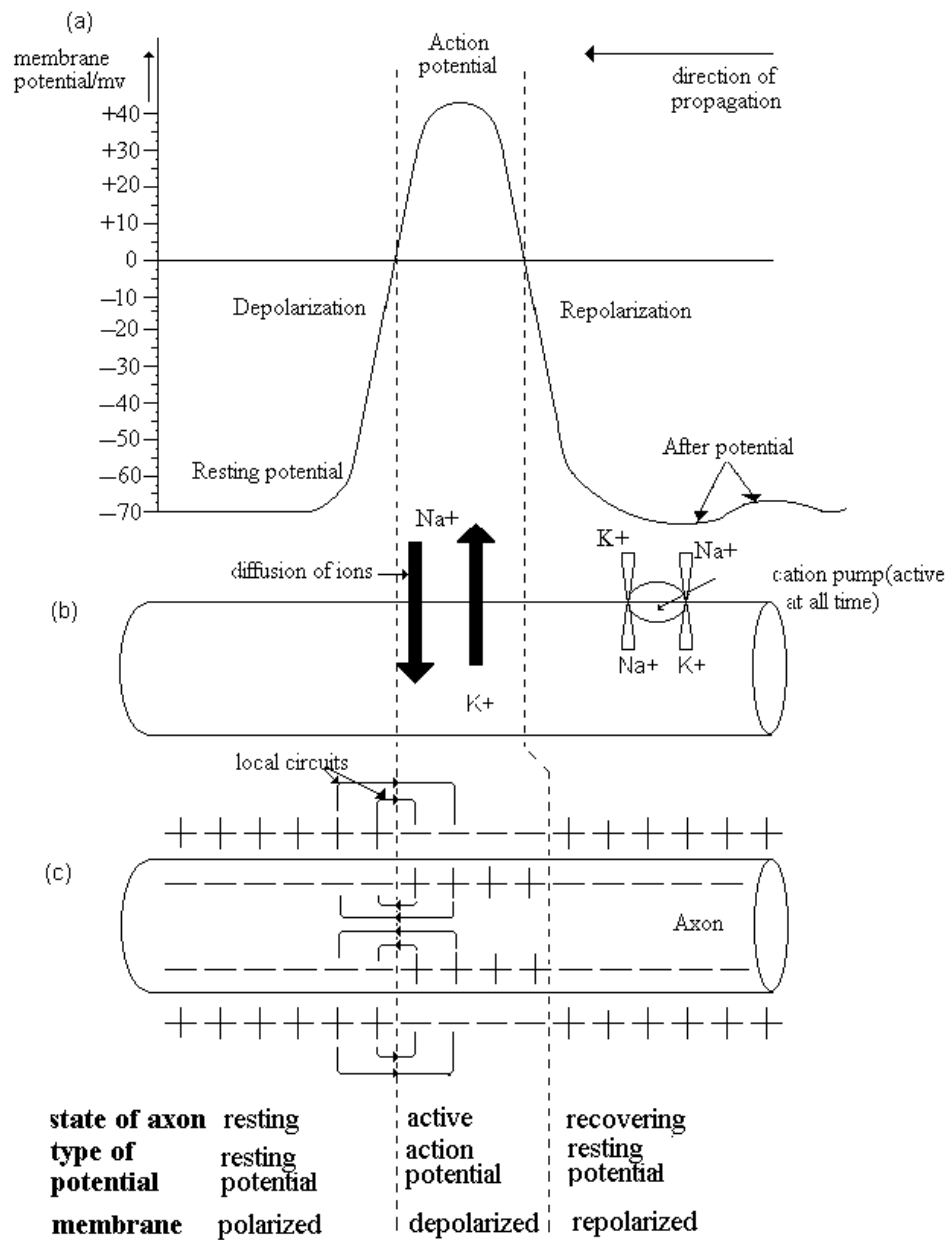


Figure 2.13: Diagram showing the events accompanying the production of local circuits within the axon and the propagation of an action potential in a non-myelinated axon

- a) action potential and direction of propagation
- b) ionic movement across the axon membrane
- c) current flow in the local circuits

Once the rush of Na^+ ions through the cell membrane has stopped (a new state of equilibrium reached). The ionic currents that lowered the barrier to Na^+ ions are no longer present and the membrane reverts back to its original, selectively permeable condition, wherein the passage of Na^+ ions from the outside to the inside of the cell is again blocked. By an active process, called a sodium pump, the Na^+ ions are quickly transported to the outside of the cell, and the cell again becomes polarized and assumes its resting potential. The process is called repolarization. Although little is known of the exact chemical steps involved in the sodium pump, it is quite generally believed that sodium is withdrawn against both charge and concentration gradients supported by some form of high-energy phosphate compound. The rate of pumping is directly proportional to the sodium concentration in the cell. It is also believed that the operation of this pump is linked with the influx of potassium into the cell, as if a cyclic process involving an exchange of sodium for potassium existed. Figure 2.13 shows a typical action potential waveform, beginning at the resting potential, depolarization, and returning to the resting potential after repolarization. The ionic movements across the axon membrane and current flow in local circuits are also shown.

The time scale for the action potential depends on the type of cell producing the potential. In nerve and muscle cells, repolarization occurs so rapidly following depolarization that the action potential appears as a spike of as little as 1 ms total duration. Heart muscle, on the other hand, repolarizes much more slowly, with the action potential for heart muscle usually lasting from 150 to 300 ms.

Regardless of the method by which a cell is excited or the intensity of the stimulus (provided it is sufficient to activate the cell), the action potential is always the same for any given cell. This is known as the all-or-nothing law. The net height of the action potential is defined as the difference between the potential of the depolarized membrane at the peak of action potential and the resting potential.

Following the generation of an action potential, there is a brief period of time during which the cell cannot respond to any new stimulus. This period, called the *absolute refractory period*, lasts about 1 ms in nerve cells. Following the absolute refractory period, there occurs a *relative refractory period*, during which another action potential can be triggered, but a much stronger stimulation is required. In nerve cells, the

relative refractory period lasts several milliseconds. These refractory periods are believed to be the result of after-potentials that follow an action potential.

2.3.3. Muscle action potential

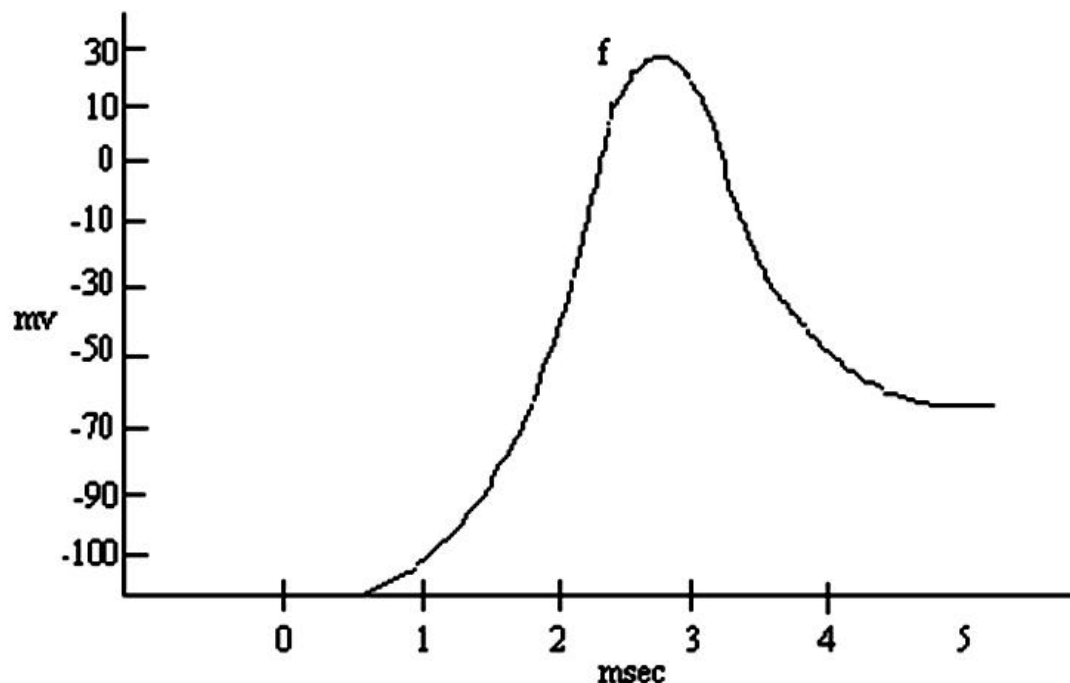


Figure 2.14: The microelectrode recording of a single muscle action potential

A motor unit is composed of a motoneuron and all the muscle fibers that the neuron innervates. The function of the neuromuscular junction is to transfer impulses from the very small motor nerve endings to the much larger muscle fibers, thus initiating muscle fiber contractions. When a nerve impulse is initiated, it travels down to its non-myelinated terminals and starts up an impulse in the muscle fibers. The electrical activity of the nerve impulse arriving at the terminal is sufficient itself to depolarize the muscle fiber directly by its action current; instead a chemical mediator Acetylcholine (Ach) is transferred across the synaptic cleft, probably by diffusion. There the Ach react with the receptor molecules in the postsynaptic membrane and alters the properties of the membrane so that it becomes highly permeable to small cations. The result is a local depolarization of the postsynaptic membrane known as the endplate potential (EPP).

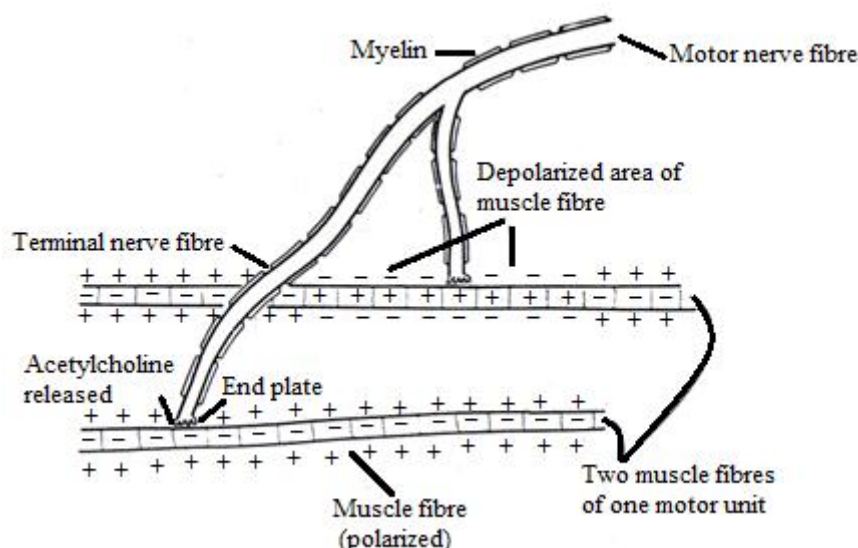


Figure 2.15: Two striated muscle fibres which are supplied from one motor nerve fibre.

In the process of depolarization the EPP reaches a critical threshold. A propagated action spike develops along the length of the muscle fiber, resulting in a shift of the internal potential from negativity to positivity. This is the muscle action potential that spreads in both directions along the muscle fibers away from the endplate and triggers mechanical contraction. Until sufficient internal negativity is restored the muscle fiber remains refractory to a subsequent impulse. As seen in Figure 2.14, the recording at the endplate reveals the EPP with the muscle action potential superimposed. At 1 or 2 mm from the endplate the effect of the EPP become less evident since it is not propagated. The time sequence of neuromuscular transmission is of interest. Following the arrival of the nerve impulse is seen in the muscle fiber for 0.5 to 0.8 ms. Figure 2.15 illustrates the process of the muscle action potential.

2.4. Classification of fibers of the PNS

The compound nerve action potential elicited by supramaximal stimulation consists of several peaks, each representing a group of fibers with a different conduction velocity. The distribution of peripheral nerve fibers are classified according to morphology and function. The afferent system consists of myelinated and unmyelinated fibers that innervate different types of sensory receptors and accordingly convey different sensory modalities (Gardner et al., 2000). Myelinated fibers are grouped according to diameters into types A α - δ in cutaneous nerves (touch, vibration, temperature, pain), whereas they are named I-III in muscle nerves (proprioception, pressure, pain)

(Pearson and Gordon, 2000), and unmyelinated fibers consist of type C in cutaneous nerves and group IV in muscle nerves that innervate pain and temperature receptors. It is now known that unmyelinated fibers have different subtypes (Serra et al., 1999). The efferent system is divided in myelinated α -, γ - and δ -fibers that innervate extrafusal muscle fibers, muscle spindles and both, respectively. Autonomic postganglionic fibers are unmyelinated.

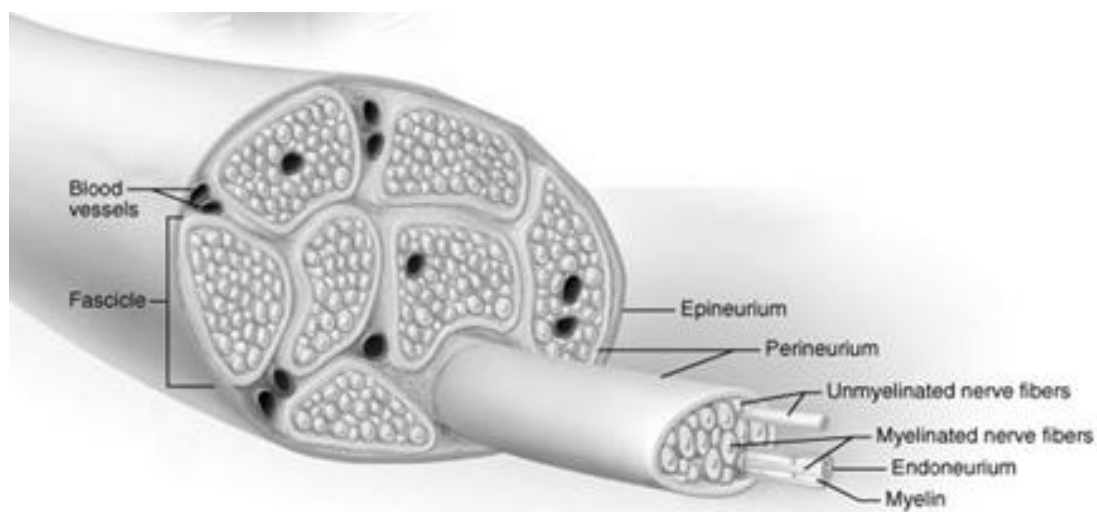


Figure 2.16: Nerve trunk consists of thousands of nerve fibres.

2.4.1. Distribution of Conduction Velocity (DCV)

Peripheral nerves consists of thousand of nerve fibers with individual diameters and myelin sheaths (Figure 2.16). Because the conduction velocity of myelinated fibers is mainly determined by their myelin sheaths, nerve conduction studies are well established to detect and characterize neuropathies that affect the peripheral myelin. However, the routinely measured maximum nerve conduction velocity (NCV) reflects only a small proportion of the total nerve-fiber population, namely the fastest conducting fibers. Theoretically, the conduction velocity distribution must be somehow calculated or estimated from compound action potentials, the summation of nerve fiber action potentials recorded from a nerve trunk. For clinical purposes, it is necessary to know whether a conduction velocity distribution is normal or not. Methods to measure the full conduction velocity distribution require considerable mathematical processing of the bioelectric signals recorded from the patients. Methods that do not provide the full conduction velocity distribution but some

important parameters of it, are currently available for the use in a clinical setting. Small myelinated and unmyelinated nerve fibers cannot be studied with the available electrodiagnostic methods, the following discussion concerns only large myelinated nerve fibers are concerned.

Mean fiber diameter distribution from normal sural nerve (n = 10) (Behse, 1990)

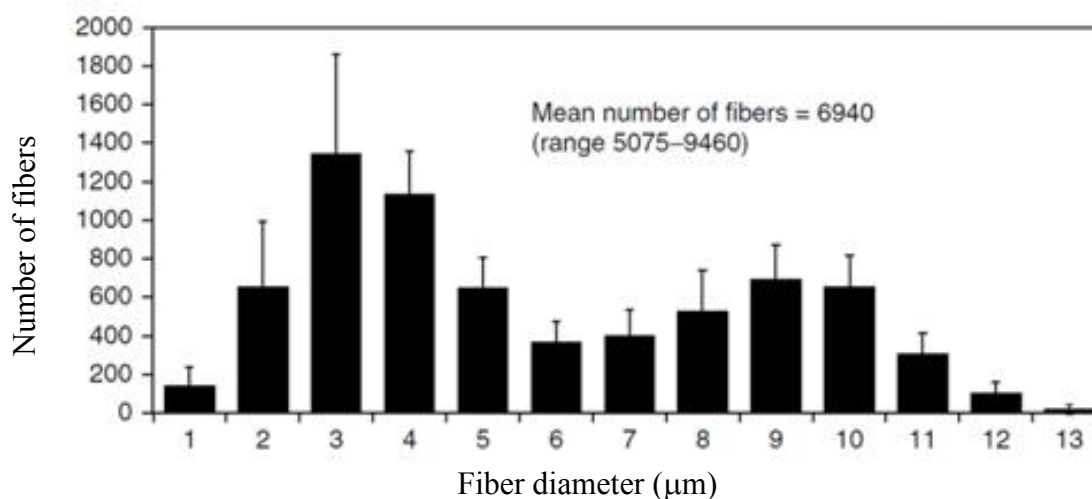


Figure 2.17: Fiber diameter distribution from 10 normal sural nerves. The total number of myelinated fibers was calculated from sampling of 200–300 fibers in whole nerve biopsies multiplied by the total fascicular area. The bars indicate the mean number of fibers in each bin (1 μm) and the error bars indicate the standard deviation Calculated from data in (Behse, 1990).

The distribution of motor and sensory myelinated fibers in humans is bimodal (Figure 2.17), with motor fibers classified as small 1–8 μm γ -fibers, and large 8–15 μm α -fibers (Lee et al., 1975), and sensory fibers ranging from small 1 μm A δ fibers to large 18 μm A α and A β fibers (Figure 2.16) (Behse, 1990, Berthold and Rydmark, 1995, Buchthal and Rosenfalck, 1966, Caruso et al., 1992). Unmyelinated fibers have small diameters of 1–2 μm. Generally two systems are used for categorization of PNS nerve axons. The Gasser and Erlanger (Gasser, 1941, Gasser and Erlanger, 1927) system is used to categorized both afferents and efferents. Whereas the Lloyd and Hunt scheme is used completely to define the afferent axons. The above description has been summarized in the following table (Table 2.2) according to these two systems.

Table 2.2: Classification of peripheral nerve fibers

Fiber (type/group)	Mean diameter (μm)	Mean conduction velocity (m/S^2)	Function
Erlanger/Gasser classification (type)			
A α	15	100	Motor neurons
A β	8	50	Skin touch afferents
A γ	5	20	Motor to muscle spindles
A δ	4	15	Skin temperature afferents
B	3	7	Unmyelinated pain afferents
C	1	1	Autonomic postganglionic neurons
Lloyd/Hunt classification (group)			
I	13	75	Primary muscle spindle afferents
II	9	55	Skin touch afferents
III	3	11	Muscle pressure afferents
IV	1	1	Unmyelinated pain afferents

2.5. Pathology

The purpose of the clinical neurophysiological examination is to localize, identify, and specify pathophysiological abnormalities as consistent with disease affecting the peripheral nervous system (PNS), neuromuscular transmission or muscle and after integration with clinical and other paraclinical information to establish a specific diagnosis. To accomplish these goals, it is necessary to have a clear notion of the physiological characteristics of the individual systems, which methods are needed to study these systems, and how particular deviations from normal function reflect pathological abnormalities. In addition, recently it has become apparent that axon membrane function is fundamental for phenomena such as fasciculations, cramps and neuromyotonia (Heidenreich and Vincent, 1998, Kiernan et al., 2001b, Mogyoros et al., 1997, Mogyoros et al., 1998, Newsom-Davis, 1997, Vincent et al., 1998).

The main outcome of the neurophysiological studies is to determine whether there is loss of nerve fibers or whether their function is abnormal or both. The main parameters in routine electrophysiological studies include conduction velocity and amplitudes of the evoked responses, and it is necessary to consider to what extent abnormalities associated with these parameters may be used to determine loss or

abnormalities of function. We discussed here only the three nerve abnormalities related with our study are Carpal tunnel syndrome, Radiculopathy and Myelopathy.

2.5.1. Carpal tunnel Syndrome

Carpal tunnel syndrome (CTS) is a medical condition in which the median nerve is compressed as it travels through the wrist at the carpal tunnel and causes pain, numbness and tingling, in the part of the hand that receives sensation from the median nerve. Anatomy of the carpal tunnel showing the median nerve passing through the tight space it shares with the finger tendons (Figure 2.18).

The mechanism is not completely understood but there are a variety of contributing factors. Some of the individual predisposing factors include: diabetes, obesity, pregnancy, hypothyroidism, and a narrow-diameter carpal tunnel. CTS may also result from an injury that causes internal scarring or mis-aligned wrist bones. Occupational causes involve use of the hand and arm, such as heavy manual work, work with vibrating tools, and highly repetitive tasks even if they involve low force motions.

The main symptom of CTS is intermittent numbness of the thumb, index, and middle (long) fingers and the radial (thumb) side of the ring finger. The numbness often occurs at night, with hypothesized reasons related to sleep position, such as the wrists being held flexed during sleep or sleeping on one's side. It can be relieved by wearing a wrist splint that prevents flexion. Long-standing CTS leads to permanent nerve damage with constant numbness, atrophy of some of the muscles of the thenar eminence, and weakness of palmar abduction.

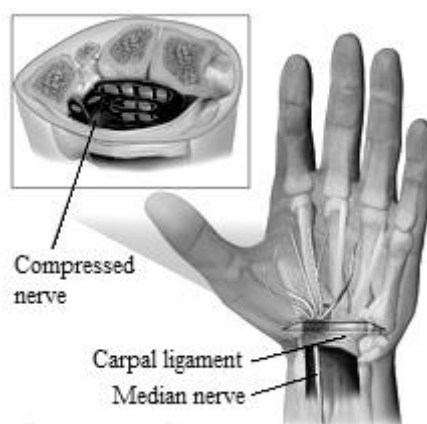


Figure 2.18: Compression of Median nerve at wrist

There is no consensus reference standard for the diagnosis of carpal tunnel syndrome. A combination of described symptoms, clinical findings, and electrophysiological testing may be used. Historically, diagnosis has been made with the combination of a thorough history and physical examination in conjunction with the use of electrodiagnostic testing for confirmation. Additionally, evolving technology has included the use of ultrasonography in the diagnosis of CTS. DFL (detailed of these method is described in Chapter 4) can be used to detect this neuropathy.

2.5.2. Radiculopathy

Radiculopathy refers to a set of conditions in which one or more nerves are affected and do not work properly (a neuropathy). The location of the injury is at the level of the nerve root (*radix* = "root"). This can result in pain (radicular pain), weakness, numbness, or difficulty controlling specific muscles.

In a radiculopathy, the problem occurs at or near the root of the nerve (Figure 2.19), shortly after its exit from the spinal cord. However, the pain or other symptoms often radiate to the part of the body served by that nerve. For example, a nerve root impingement in the neck can produce pain and weakness in the forearm. Likewise, an impingement in the lower back or lumbar-sacral spine can be manifested with symptoms in the foot. *Polyradiculopathy* refers to the condition where more than one spinal nerve root is affected.

Radiculopathy is a mechanical compression of a nerve root usually at the exit foramen or lateral recess. It may be secondary to degenerative disc disease, osteoarthritis, facet joint degeneration/hypertrophy, ligamentous hypertrophy, spondylolisthesis, or a combination of these factors. More rare causes of radiculopathy may include radiation, diabetes mellitus, neoplastic disease, or any meningeal-based disease process.

Radiculopathy is a diagnosis commonly made by physicians in primary care specialities, orthopedics, physiatry, and neurology. The diagnosis may be suggested by symptoms of pain, numbness, and weakness in a pattern consistent with the distribution of a particular nerve root. Neck pain or back pain may also be present. Physical examination may reveal motor and sensory deficits in the distribution of a nerve root. In the case of cervical radiculopathy, Spurling's test may elicit or reproduce symptoms radiating down the arm. In the case of lumbosacral

radiculopathy, a Straight leg raise maneuver may exacerbate radiculopathic symptoms. Deep tendon reflexes (also known as a Stretch reflex) may be diminished or absent in areas innervated by a particular nerve root.

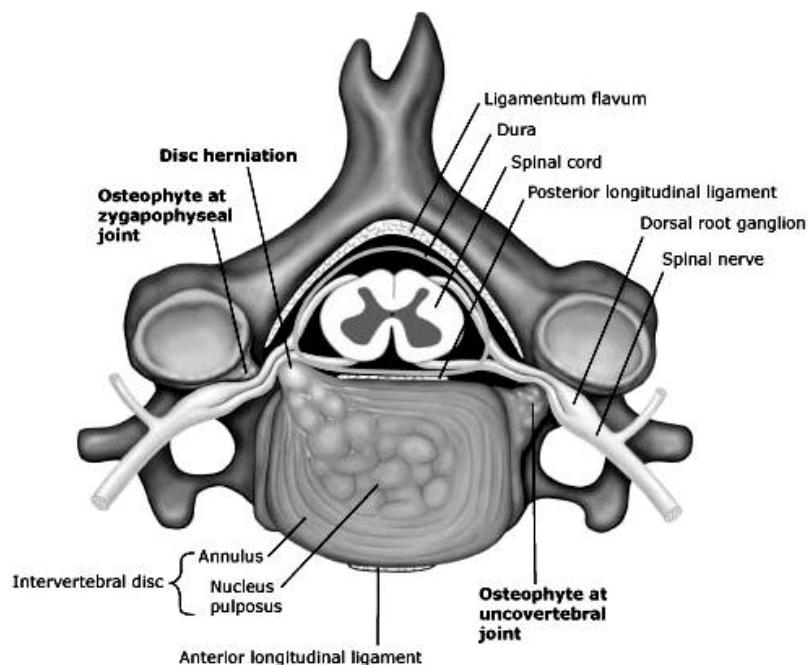


Figure 2.19: Vertebral section showing radiculopathy (compression of nerve root).

Two additional diagnostic tests that may be of use are magnetic resonance imaging and electrodiagnostic testing. Magnetic resonance imaging (MRI) of the portion of the spine where radiculopathy is suspected may reveal evidence of degenerative change, arthritic disease, or another explanatory lesion responsible for the patient's symptoms. Electrodiagnostic testing, consisting of NCS (Nerve conduction study) and EMG (Electromyography), is also a powerful diagnostic tool that may show nerve root injury in suspected areas. On nerve conduction studies, the pattern of diminished Compound muscle action potential and normal sensory nerve action potential may be seen given that the lesion is proximal to the Posterior root ganglion. Needle EMG is the more sensitive portion of the test, and may reveal active denervation in the distribution of the involved nerve root, and neurogenic-appearing voluntary motor units in more chronic radiculopathies. Recently the Dhaka University Biomedical Physics group conceived and developed a method named Distribution of F-latencies (DFL) through which cervical spondylotic radiculopathy can be diagnosed very easily with low cost. A detailed of these method is described in Chapter 4.

2.5.3. Myelopathy

Myelopathy refers to pathology of the spinal cord (Figure 2.20). Due to trauma, it is known as spinal cord injury. To inflammatory, it is known as myelitis. Disease that is vascular in nature is known as vascular myelopathy.

Clinical signs and symptoms depend on which spinal cord level (cervical, thoracic or lumbar) is affected and the extent (anterior, posterior or lateral) of the pathology, and may include: upper motor neuron signs (weakness, spasticity, clumsiness, altered tonus), pathological hyperreflexia and inverted Plantar reflex (positive Babinski sign), sensory deficits, bowel/bladder symptoms and sexual dysfunction.

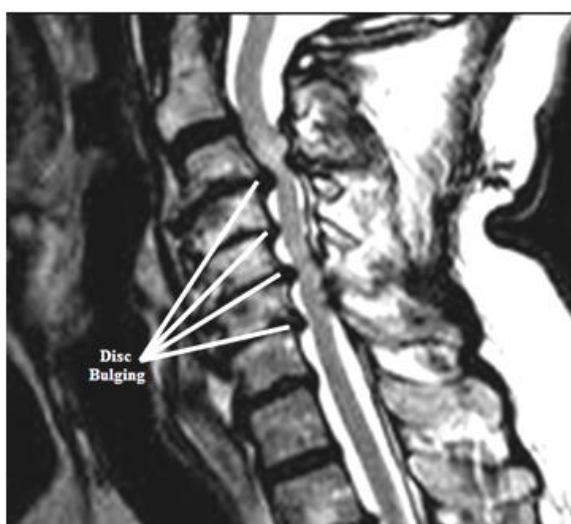


Figure 2.20: Compression of spinal cord due to disc bulging (myelopathy)

Magnetic resonance imaging (MRI) of the cervical spine is the procedure of choice during the initial screening process of patients with suspected cervical spondylotic myelopathy. MRI is noninvasive and provides images of the spine and spinal cord in several planes (Figure 2.20). In addition to giving an assessment of the degree of spinal canal stenosis, an MRI can identify intrinsic spinal cord lesions that can also present with myelopathy (e.g., tumors). High signal changes seen in the spinal cord of patients with cervical spondylotic myelopathy may indicate myelomalacia or permanent spinal cord damage. DFL (detailed of these method is described in Chapter 4) can also detect cervical spondylotic myelopathy easily with low cost as Like Radiculopathy.

Chapter 3: Measurement of Nerve conduction parameters

The purpose of the clinical neurophysiological examination is to localize, identify, and specify pathophysiological abnormalities as consistent with disease affecting the peripheral nervous system (PNS), neuromuscular transmission or muscle and after integration with clinical and other paraclinical information to establish a specific diagnosis. To accomplish these goals, it is necessary to have a clear notion of the physiological characteristics of the individual systems, which methods are needed to study these systems, and how particular deviations from normal function reflect pathological abnormalities.

The main outcome of the neurophysiological studies is to determine whether there is loss of nerve fibers or whether their function is abnormal or both. The main parameters in routine electrophysiological studies include conduction velocity and amplitudes of the evoked responses, and it is necessary to consider to what extent abnormalities associated with these parameters may be used to determine loss or abnormalities of function.

3.1. Nerve Conduction Velocity (NCV) Measurement through Evoked response

To measure the conduction in a nerve it is artificially stimulated at a particular point and the resulting evoked response is recorded from another point, either on the nerve for sensory conduction velocity, or from a supplied muscle, in the case of motor conduction velocity. For artificial stimulation an electrical pulse is driven through two electrodes typically placed over the skin with the target nerve underneath at a subcutaneous site. The nerve is stimulated at one, two or more points along its course, with a cathode to anode distance of 2 or 3 cm. Depolarization under the cathode results in the generation of an action potential in the nerve whereas hyperpolarization under the anode tends to block the propagation of the nerve impulse. With the cathode at the best stimulating site one stimulates the nerve with an intensity that stimulates all the nerve fibres that can be stimulated in the nerve trunk. Usually, with skin surface electrodes it is only the A-alpha group of fibres that are stimulated. Techniques for the determination of sensory and motor nerve conduction velocity are described separately in section 3.2.1.1 and 3.2.1.2.

3.1.1. Volume conductor effect

A signal recorded at a distance relates to the signal at its source can be obtained by considering the circulating currents around a single neuron. In Figure 3.1 a neuron is polarized, i.e. inactive. Because all points on the surface of the neuron are at the same potential there are no circulating currents and therefore no potential changes in the volume conductor. An inactive source, even though it is polarized, does not cause any potential change in the surrounding tissue and cannot be detected at a distance.

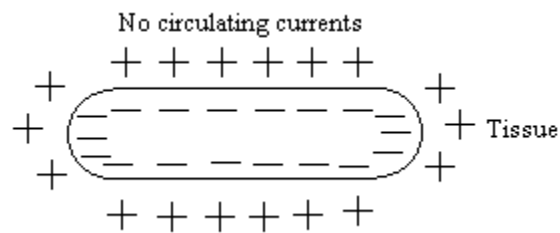


Figure 3.1: A single polarized neuron in a volume conductor.

If the neuron is depolarized completely, then again all parts of its surface will be at the same potential and there will be no potential change in the surrounding tissue. However, at the point where the semipermeable membrane becomes depolarized and also at the point where it becomes repolarized, the surface of the neuron is not all at the same potential and therefore external current will flow. Figure 3.2 illustrates this effect.

The second important point is therefore: potential changes in the tissue surrounding a neuron only occur at the points where the transmembrane potentials are changing.

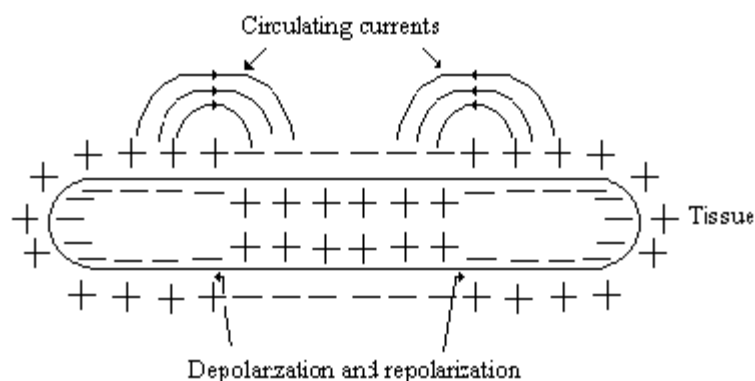


Figure 3.2: An active neuron (containing both polarized and depolarized parts) in a volume conduction gives rise to circulating currents

Figure 3.3 shows the currents circulating around a nerve fiber which is first depolarized and then repolarized. The current paths are rather like the field pattern around two bar magnets placed with like poles end to end. Also shown are the transmembrane potential changes and the changes in V_p , the potential away from the nerve, as the recording electrode is moved from left to right. In practice it is the nerve action potential which moves and not the recording electrode so that the waveform shown as V_p would be the shape of a recorded signal as an action potential passed beneath a fixed electrode. It is very difficult to calculate V_p , but a rough rule of thumb is that V_p is approximately equal to the second differential of the transmembrane potential. As NAP travels along a nerve, or a muscle action potential (MAP) along a muscle fiber, a triphasic waveform would be expected to record rather like V_p .

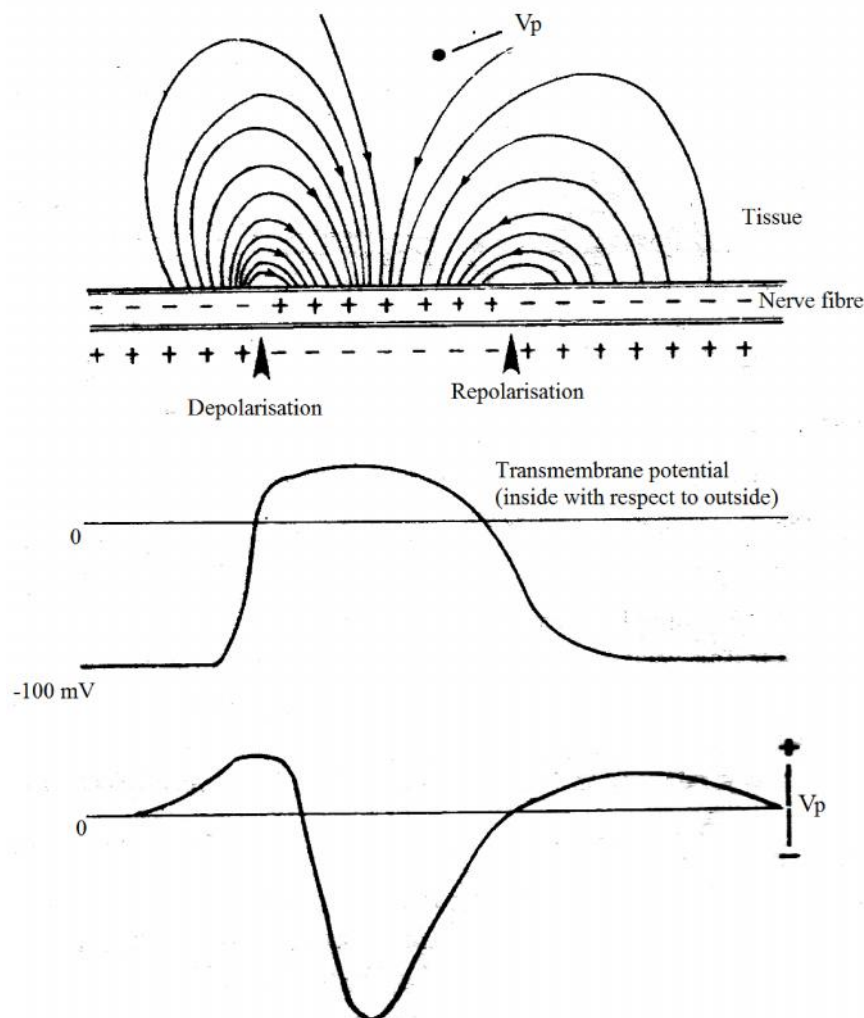


Figure 3.3: The upper part of the diagram shows the currents which flow around an active nerve fiber. The middle graph shows the transmembrane potential along the nerve fibre. The lower graph shows the potential which will be recorded at the point V_p which is moved parallel to the nerve fibre.

As the recording electrode is moved away from the source, the amplitude of the signal will fall and the shape of the signal will change. As the action potential approaches an electrode the potential is first positive, then negative, and finally positive again. The positive action potential is shown as an upward deflection. However, many recordings of NAPs and MAPs show a negative potential as upward deflection.

3.1.2. Single Fiber Action Potential (SFAP)

When an electrical impulse travels down a single nerve fiber the transmembrane potential between the inside and the outside of the fiber will be monophasic in form. This action potential can be detected in the external surface of the fiber as a transmembrane current, which has been shown analytically by Lorente de No (Lorente de No, 1947), to be proportional to the second derivative of the transmembrane voltage. The potential that can be detected some distance from the active fiber will be a function of the triphasic transmembrane current and the electrical properties of the surrounding medium in the vicinity of the fiber and the recording electrode, known as volume conductor.

3.1.3. Motor Unit Action Potential (MUAP)

The motor unit is composed of a motor neuron and all the muscle fiber that the neuron invites. The function of neuromuscular junction is to transfer to impulses from the very small motor nerve ending to the much larger muscle fibers, thus initiating muscle fiber contraction.

When a nerve impulse is initiated, it travels down to its own-myelinated terminals and starts up an impulse in the muscle fibers. The electrical activity of the nerve impulse arriving at the terminals is insufficient in itself to depolarize the muscle fiber directly by its action current; instead a chemical mediator Ach is transferred across the synaptic cleft, probably by diffusion. There the Acetylcholine (Ach) reacts with receptor molecules in the post synaptic membrane and alters the properties of the membrane so that it becomes highly permeable to small actions. The result is local depolarization of the post synaptic membrane known as end plate potential (EPP). In the process of depolarization the EPP reaches a critical threshold. A propagated action spike develops along the length of the muscle fiber resulting in a shift of the internal potential from negatively to positively. This is the muscle action potential that spread in both directions along muscular fiber away from the endplate and hence shows a

greater dispersion than a single fiber potential alone. The single motor unit action potential originates from one motor unit. A normal MUAP will have an initial positive peak followed by a negative peak. The amplitude of MUAP varies from muscle to muscle. The amplitude is lower in the facial muscle and higher in muscle of the extremities.

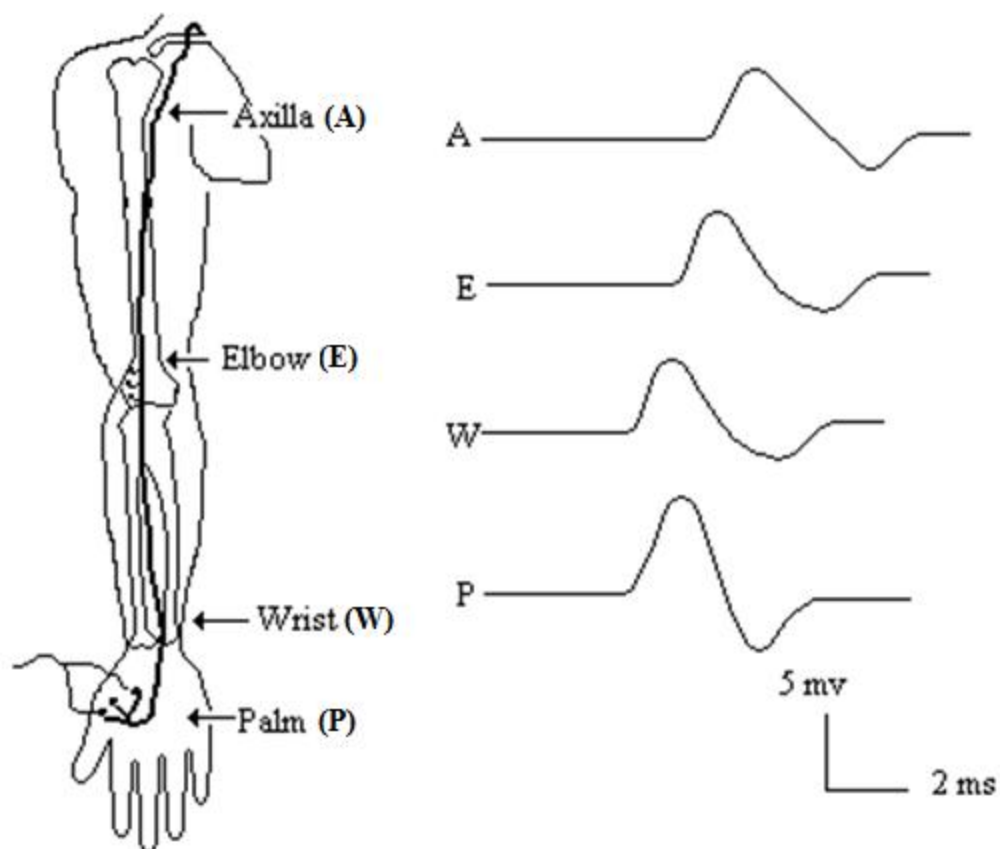


Figure 3.4: compound muscle action potentials are recorded with surface electrodes placed on the thinner eminence.

3.1.4. Compound Muscle Action Potential (CMAP)

The compound muscle action potential generally obtained in clinical study is simply the combination of single muscle fiber action potentials obtained from individual motor neurons. The clinical observation of CMAP shows that it is biphasic in shape and more dispersed than CAP obtained directly from sensory study. Figure 3.4 shows the shape of CMAP obtained from motor nerve conduction study of the median nerve. The sites of stimulation includes axial, elbow, wrist and plam (Kimura, 1989). The compound muscle action potentials are recorded with surface electrodes placed on thinner eminence.

3.1.5. Factors determining Conduction Velocity

A number of factors affect the time necessary for generation of action potentials, which in turn determines the conduction velocity of an axon. The most important factors that should be taken into consideration when interpreting physiological findings in peripheral nerves are age and temperature.

Age

Increasing age affects nerve conduction as well as Electromyography (EMG). In newborn, the conduction velocities of both motor and sensory fibers are low and gradually increase to normal range at the age of 3–4 years (Cai and Zhang, 1997, Devries, 1996, Rabben, 1995, Wagner and Buchthal, 1972) and may be used to assess the development of preterm infants (Pierrat et al., 1996). Developmental changes of myelinated fibers occur in parallel (Ouvrier et al., 1987). A large number of studies have confirmed that the amplitudes of the SNAP, and to a lesser extent, the CMAP decrease with age in the adult (Behse and Buchthal, 1971, Buchthal and Rosenfalck, 1966, Horowitz and Krarup, 1992, Rosenfalck and Rosenfalck, 1975, Trojaborg, 1992, Trojaborg et al., 1992), and in about 10% of elderly subjects without neuromuscular disease.

Temperature

By far the most important environmental factor that influences the results of conduction studies is temperature. Low temperature causes depolarization of the membrane potential and prolong refractoriness (Burke et al., 1999, Kiernan et al., 2001a). The exact correction factor for the effect of temperature is unknown, so the convention of adding 2 m/sec/°C in clinical studies is at best an approximation (Cummins and Dorfman, 1981, Franssen and Wieneke, 1994, Stegeman and De Weerd, 1982, Trojaborg et al., 1992). Low temperature has profound effects on the SNAP and single-fiber action potential rise times and duration (Paintal, 1965, Paintal, 1966). The distance between electrodes may also be a determining factor in how the amplitude of the SNAP is influenced by temperature (Alfonsi et al., 1987, Ashworth et al., 1998, Letz and Gerr, 1994, Pitt, 1996, Rutkove, 2001), since cooling is associated with slowing of conduction and less interaction and cancellation of phases with different polarity. At bipolar recording the amplitude increases at low temperature due to the prolonged duration and reduced phase cancellation at low

conduction velocity. At monopolar recording the temperature had little and variable effect on the SNAP amplitude (Buchthal and Rosenfalck, 1966, Stegeman and De Weerd, 1982). In pathological nerve, in particular when subject to demyelination, low temperature may mask abnormalities since the prolongation of the SFAP may allow conduction across segments of nerve fibers with reduced safety factor (Bostock et al., 1981, Bostock et al., 1978, Franssen et al., 1999, Kaji, 2003).

Other biological variables that have been found to influence nerve conduction parameters include gender and height. The amplitudes of the sural nerve SNAP are greater in females than in males when recorded with a near-nerve needle, which may reflect differences in subcutaneous tissue composition (Horowitz and Krarup, 1992), whereas surface recordings of the orthodromic SNAP in median and ulnar nerves did not differ in men and women (Shehab et al., 2001). Height has been found to be negatively correlated with conduction velocities in motor as well as sensory nerves in large population based studies (Letz and Gerr, 1994, Rivner et al., 2001, Solders et al., 1993), whereas other studies with fewer subjects but better control of environmental factors such as temperature have not confirmed this relationship (Trojaborg et al., 1992). Body mass index has been found to be correlated with conduction velocities in some studies but the relationship is weak.

3.2. Techniques for measurement of Nerve Conduction Velocity

3.2.1. Using surface electrodes

3.2.1.1. Sensory Nerve Conduction (SNC) measurements

Sensory nerve conduction studies, as currently performed measure conduction along the myelinated group I, A α nerve fibers. Impulses are propagated along these fibers by saltatory conduction. Sensory nerve conduction studies differ from motor nerve conduction studies in that, no neuromuscular junction or muscle is involved. With the use of carefully standardized techniques and the availability of signal averaging devices, more and more sensory nerve are now being adequately studied.

Here we consider sensory conduction studies in the upper extremities. Stimulation of the digital nerves elicits an orthodromic sensory potential at a more proximal site. Alternatively stimulation of the nerve trunk evokes the antidromic digital potential proximally. For example, shocks applied to the median or ulnar nerve at the wrist give

rise to an action potential along the nerve trunk at the elbow. Generally sensory fibers with large diameters have lower thresholds and conduct faster than motor fibers by about 5 to 10 percent (Dawson, 1956). Thus mixed nerve potentials allow determination of the fastest sensory nerve conduction velocity.

For routine clinical recordings surface electrode provides adequate and reproducible information non-invasively. Some electromyographers prefer needle recording to improve the signal to noise ratio, especially in assessing temporal dispersion (Rosenfalck, 1978). Here a signal averaging provides a sensitive measure of early nerve damage by defining small late components that originated from demyelinated, remyelinated or regenerated fibers (Gilliatt, 1978). The basic instrumental setup for recording nerve conduction velocity is similar to that of motor nerve conduction study. Only the points of electrode placing are different. Following stimulation of the nerve fiber, nerve impulses will be conducted in both directions along the nerve fibers; conduction up the sensory nerves in the normal direction is termed orthodromic conduction and conduction in the opposite direction is called antidromic conduction. With the use of surface electrodes the antidromic potentials from digits generally have greater amplitude than the orthodromic response from the nerve trunk because the digital nerve lies nearer to the surface. For recording antidromic sensory signal conduction from digital nerves, ring electrodes are generally used. They are normally placed over the proximal and distal interphalangeal joints of a finger. For example, for recording median nerve antidromic conduction the recording ring electrode pair is placed over the digital nerve branches of the index or middle finger. The stimulating electrodes can be placed at wrist or elbow at the same sites used for motor nerve conduction studies. Figure 3.6 shows the process in which the compound action potential is recorded during antidromic sensory conduction studies of the digital median nerve recording ring electrodes are placed around the proximal and distal interphalangeal joints of the second digits.

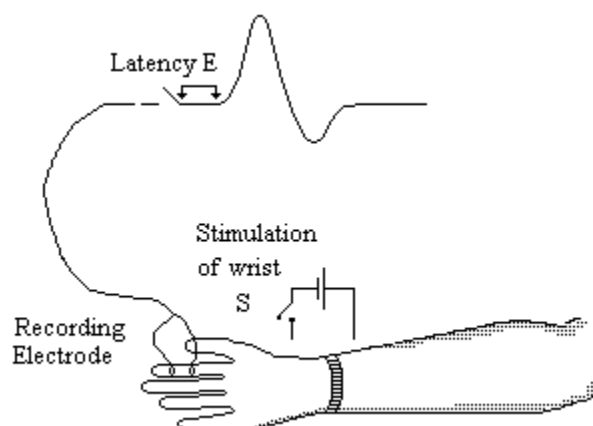


Figure 3.6: Recording of CNAP from median nerve from wrist.

The amplitude of the sensory potential measured either from the baseline to the negative peak or between the negative and positive peaks, varies substantially among subjects and to a lesser extent between the two sides in the same individual. The density of sensory innervation in each finger determines the amplitude of the digital nerve potential. Most of the electromyographers measure the duration of the nerve action potential from the initial deflection to the intersection between the descending phase and the baseline. Some use the negative and positive peak as the point of reference and still others resort to the less definable point where the tracing finally returns to baseline.

Unlike motor latency, which includes neuromuscular transmission, sensory latency consists only of the nerve conduction time from the stimulus point to the recording electrode. Therefore stimulation of the nerve at a single site suffices for calculation of conduction velocity. In measuring the latency of orthodromic sensory potentials, some electromyographers use the initial positive peak as the point of reference (Joynt, 1983). With the digital potential recorded antidromically, the onset latency measured to the initial take off of the negative peak corresponds to the conduction time of the fastest fibers. The use of peak latency has little, if any, justification with antidromically recorded digital potentials, which considerably exceed orthodromic potential in amplitude.

The position of the recording electrodes alters the waveform of a sensory nerve action potential (Andersen, 1985). A small initial positive phase clearly seen in the antidromic is absent in the antidromic digital potential recorded with a pair of ring electrodes. An initially positive triphasic waveform characterizes the orthodromic

potential recorded with an active cathode on the nearer and a reference electrode at a remote site.

3.2.1.2. Motor Nerve Conduction (MNC) Measurements

For motor nerve conduction (MNC) studies, the nerve is stimulated at two or more points along its course, with a cathode to anode distance of 2 to 3 cm with the anode proximal to the cathode. Depolarization under the cathode results in the generation of a NAP whereas hyperpolarization under the anode tends to block the propagation of the nerve impulse. With the cathode at the best stimulating site one then defines the maximal intensity that just elicits a maximal potential. Increasing the stimulus further should result in no change in the size of the MAP. The use of a 20 to 30 percent supramaximal intensity guarantees the activation of all the nerve axons innervating the recording muscle. Recording action potential requires a pair of surface electrodes, an active lead and an indifferent lead placed on the belly of the muscle with 2 or 3 cm separation between them. After cleaning the skin site properly a reference electrode is attached at a suitable location. A ring type electrode can be used at the wrist instead of lead electrode. The leads to the electrodes should be secured to the arm so that the movement of the arm does not cause electrode movement.

As for example a loosely placed reference electrode can introduce an enormous amount of noise at the output. With this arrangement, the MAP originated under the stimulating cathode will travel down the nerve, along the nerve fibers, across the neuromuscular junction and then cause a MAP to spread along the muscle fibers. This MAP when reaches underneath the recording active lead located near the motor point will record a potential shape. The incoming MAP will have a simple biphasic shape with initial negativity. By using an inverting amplifier this negative peak can be seen as positive deflection on the monitor. The usual measurements include amplitude from the baseline to the first negative peak or between negative and positive peaks, duration from the onset to the negative or positive peak or to the final return to the base line and latency. Latency consists of two components:

- (1) Nerve conduction time from the stimulus point to the neuromuscular junction
- (2) Neuromuscular transmission time, from the axonal terminal to the motor end plate including the time required for generation of MAP through chemical neurotransmitter.

Onset latency is a measure of the velocity of a group of fastest conducting motor fiber velocities. To measure the MNC time, it is better to consider the latency difference between the two responses elicited by stimulation at the two separate points. In this way the time for neuromuscular transmission and generation of MAP can be excluded as common factor for both cases. The latency differences represents the time required by the nerve impulse to travel between the two stimulus points. The conduction velocity is defined as the ratio between the distance from one point of the stimulation to the next and the corresponding latency difference. Mathematically

$$\text{MNCV} = \frac{D \text{ mm}}{(L_p - L_d) \text{ ms}} = \frac{D}{(L_p - L_d)} \text{ m/s.}$$

Where D is the distance between the two stimuli points in millimeters. Distance is measured between the stimulation cathodes because the action potential is initiated underneath the cathode. L_p is the latency from proximal site. The proximal means the point closest to the point of attachment. Latency is generally measured to the start of the MAP. But in some cases latency is considered to extend up to the major negative peak.

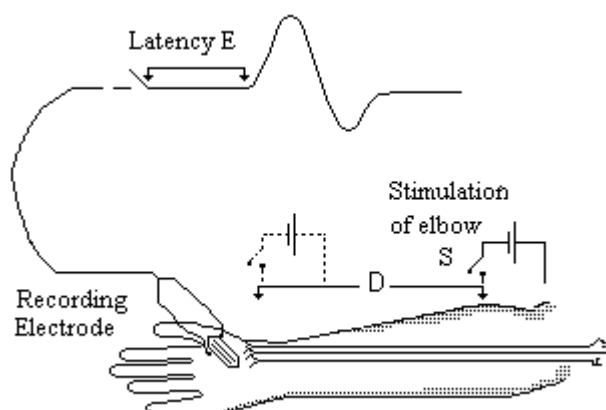


Figure 3.5: Recording of CMAP from median nerve at wrist and elbow.

Figure 3.5 shows a process of recording compound muscle action potential (CMAP). The CMAP is recorded from the thenar eminence muscle below the thumb after stimulation of the median nerve at the elbow. The nerve conduction time from the elbow to the wrist equals the latency difference between the two responses elicited by the distal and proximal stimulation. The motor nerve conduction velocity (MNCV) is calculated by dividing the surface distance between the stimulus points by the subtracted times, concerning the fastest fibers.

The reliability of the results depends on the occurrence in determining the length of the nerve segments, estimated with the surface distance along the course of the nerve. Excessive stimulus intensity can cause an erroneously short latency because the spread of stimulus current depolarizes the nerve few millimeters away from the cathode. The surface length measured between the two cathodal points under this condition does not precisely correspond to the conduction of the nerve segment under study.

When recorded with high sensitivity, a small negative peak sometimes precedes the main negative component of the MAP. This small potential is to be disregarded in latency determination. This peak probably originates from small nerve fibers near the motor point. With awareness of this possibility one can avoid miscalculation.

Position of the stimulating electrodes plays an important part. Placing them over a cross over between median and ulnar in the forearm give rise to the CMAP of dissonant waveform. Responses may be absent or unexpectedly small in amplitude if the stimulus is misdirected despite adequate current strength. In this situation one must relocate the stimulating electrode and press it firmly closer to the nerve and if necessary increase the intensity or duration of the shock.

3.2.2. Using Needle electrodes

3.2.2.1. *Near nerve needle recording techniques (NNNRT)*

Abnormalities of the conduction velocity distribution can be characterized with this method qualitatively. The occurrence of late components of the compound action potentials represent subpopulations of abnormally slow conducting nerve fibers. This serves as an example for the principle that certain determinants of the conduction velocity distribution can be derived from compound action potentials. The NNNRT is a relatively simple and minimally invasive method of sensory nerve testing in the assessment of polyneuropathy (Claussen et al., 1996, Oh et al., 1992) and entrapment syndromes (Odabasi et al., 1999).

The method consists in orthodromic sensory nerve stimulation with an intensity of 0.5 to 1 mA for a stimulus of 0.2 m/s, and 1–5 mA for stimulus of a 0.05 msec duration. Recordings are made using a Teflon-coated steel needle electrode with an uncoated tip area of 2 mm and a reference electrode with an uncoated tip of 3.5 mm (Figure

3.7). The recording electrode is placed near the nerve, and the reference electrode at 3–4 cm of transverse distance. The high frequency filter is set at 5–10 KHz to allow recording of fast components. This induces noise is hard to eliminate, but can be improved by averaging 500–1000 responses. Near nerve needle recording technique allows the study of slow myelinated fibers with velocities as low as 15 m/s (Behse and Buchthal, 1971), and is useful in the diagnosis of peripheral neuropathies in which the SNAPs are not recordable with surface electrodes (Oh, 2002). This method also helps to diagnose involvement of large myelinated fibers in patients with apparent “small fiber neuropathy” that have normal routine SNCS. In these, the NNNRT could show slowing and dispersion of the slow components, indicating demyelination (Oh et al., 2001).

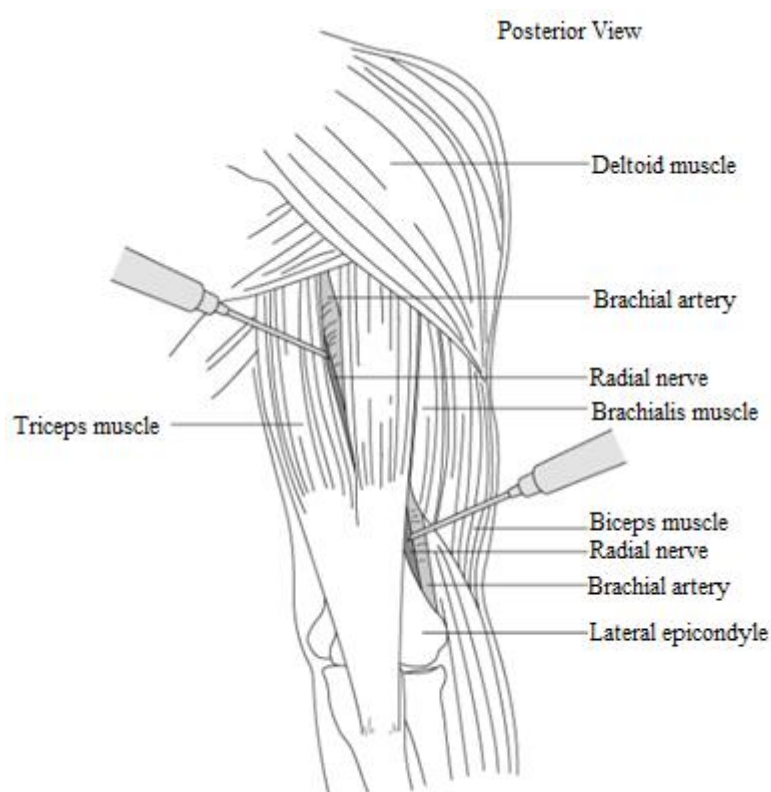


Figure 3.7: Near Nerve Needle recording technique

The NNNRT has been valuable to diagnose patients suspected to have demyelinating neuropathy not supported by standard motor conduction tests (Claussen et al., 1996, Oh et al., 2001), and to diagnose tarsal tunnel syndrome, plantar neuropathy and interdigital neuropathies of the foot (Oh et al., 2001, Oh et al., 1985) and, as discussed, to localize ulnar nerve entrapments (Odabasi et al., 1999).

3.2.2.2. Selective nerve fiber stimulation

Dengler et al. (Dengler et al., 1988) measured conduction velocities of single motor axons innervating human hand muscles by recording from single motor units with special tungsten microelectrodes. The electrodes were inserted into the muscle during steady voluntary innervation. Then the position was adjusted until action potentials of a single motor unit could be recorded optimally. This position of the recording electrode was carefully maintained during subsequent electrical nerve stimulation. Stimulus intensity and position of the stimulus electrode that was positioned at the wrist, were manipulated until action potentials of the previously identified motor unit could be recorded and their latencies measured. Thereafter, the stimulation procedure was repeated with the stimulus electrode at the elbow. The axonal conduction velocity was calculated from the distance between both stimulation sites and the difference of the latencies. The axons of 94 motor units from 9 muscles could be studied. Their conduction velocity distribution ranged from 40 to 63 m/s, with a peak between 53 and 53 m/s. Nearly half of the axons had conduction velocities in the range from 52 to 55 m/s. Although the conduction velocity of single motor axons can be measured with this method, it should be noted that only 10 axons per muscle could be studied on average. This is a relatively small sample of the whole population of the motor axons of a muscle, which introduces the methodological issue of sampling bias. Therefore, and because of its substantial requirements to both examiner and patient, the method is not suitable for clinical routine measurements.

The interesting thing is that the above mentioned methods can only provide us a small portion of the whole nerve trunk population. A technique is required to find the whole scenario of the nerve bundle.

3.3. F-waves and its measurements

F-waves are considered to be late waveforms of muscle action potentials, produced largely by recurrent responses of motor neurons to antidromic supramaximal stimulation. They occur after the M-wave or direct (orthodromic) muscle response to the stimulation of a peripheral nerve (Figure 3.4). F-waves are indirect responses, their latency is decreased by more proximal stimulation, since this shortens the afferent (antidromic) part of the loop, and increased by more distal stimulation, which lengthens the afferent part of the loop. In contrast, the latency of M-waves, and of any

of their late components if they are dispersed, increases with more proximal stimulation and decreases with more distal stimulation.

F-waves were described in humans by Magladery and McDougal (Magladery and McDougal, 1950). They recorded from eight young adults with surface electrodes, or unipolar needles insulated to the tips, from the hypothenar eminence, short flexor muscles of the foot, or from antero-lateral or calf leg muscles. They stimulated with monopolar cathodal shocks of about 0.5 ms duration, at not less than 1 Hz, six to twenty times. On stimulating the ulnar nerve they found that, in addition to the M-wave, a smaller potential change appeared later, at about 30 ms latency. This potential tended to increase in amplitude with increasing strength of the stimulus up to supra-maximal stimulus intensities for the M-wave. This distinguished it from the H-wave, described by Hoffman (Hoffman, 1922), which decreased in amplitude as the stimulation strength increased. This F-wave, as Magladery and McDougal called it, could have a large amplitude or could be apparent only at relatively high magnification. In one of the examples shown in their paper the F-wave has a peak to

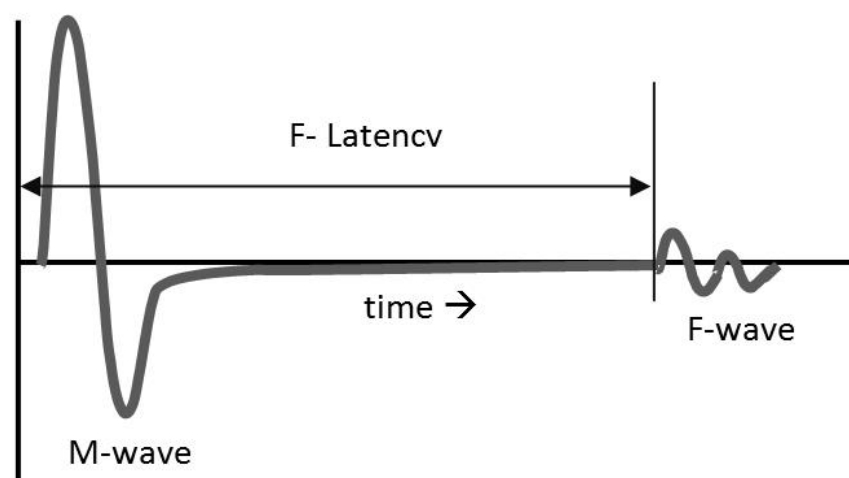


Figure 3.8: M-wave and F-wave in evoked EMG response

peak amplitude of about 0.1 mV. It is believed that the name F-wave was invented by Magladery and McDougal because these late responses were easily recordable from the foot muscles (Kimura, 1989).

Considerable progress has been made in refining the methodology and techniques and in defining the clinical applications of F-waves since their description in humans (Magladery and McDougal, 1950). The initial reports of the clinical use of F-wave measurements (Conrad et al., 1975, Eisen et al., 1977a, Eisen et al., 1977b, Kimura,

1974, Kimura and Butzer, 1975, Kimura et al., 1974, King and Ashby, 1976, Panayiotopoulos and Scarpalezos, 1977, Panayiotopoulos et al., 1977) were followed by a number of criticisms regarding, in particular, the variability of the responses and the assumptions made in the calculations of conduction velocities (Bradley, 1978).

Since those initial controversies, and with further experience and work in this area, the technique has gradually become widely used in departments of clinical neurophysiology throughout the world, and is considered by most to be a routine procedure in nerve conduction studies. It is now accepted to have a particular value in assessing motor conduction in proximal segments of peripheral nerves, including plexii and nerve roots. It seems also to be the most sensitive technique to detect motor conduction abnormalities in peripheral nerve diseases because of the length of the peripheral motor pathways tested (Andersen et al., 1997, Kimura et al., 1979, Kohara et al., 2000). The latency variability, once thought to be a major limitation for clinical use (Kimura, 1983), can be measured and has been called chronodispersion (Panayiotopoulos, 1979). This latency variability of F-waves can be used to look at the spectrum of conduction velocities of motor axons of a population of motor units in a muscle (Guiloff and Modarres-Sadeghi, 1991), which has been called tacheodispersion (Chroni and Panayiotopoulos, 1993a, Chroni and Panayiotopoulos, 1993b). Latency variability seems to be a very sensitive parameter of disease in peripheral nerves (Weber, 1998), as predicted initially (Panayiotopoulos, 1979).

3.3.1. Physiology of F-wave

After supra-maximal stimulation of a motor nerve, action potentials travel in two directions: orthodromically to the muscle, causing the M-response, and antidromically to the anterior horn cells. Very few anterior horn cells react to the arrival of the action potentials by “backfiring,” i.e., by generating an action potential, which travels orthodromically back to the muscle (Figure 3.9 (a) and 3.9 (b)). The muscle response to the action potentials generated by backfiring is called the F-wave. Its latency represents the fastest conducting axon among those contributing to the F-wave. The conduction velocity (V) of this axon can be calculated from the M-latency, the F-latency and the distance (d) between the stimulation site and the motor neurons,

$$FWCV = \frac{2 \times d}{(F-M-1)}$$

Because F-waves following successive stimuli are generated by different motor neurons, it makes sense to measure the F-wave conduction velocity distribution after a series of successive stimuli. Each of the F-wave is a compound potential of a few individual motor unit action potentials (MUAP), each motor unit being supplied by a single nerve fibre. The F-wave latency measured from the onset of the response relates only to the fastest of the few nerve fibres involved in the particular event. Since the backfiring events are random, there will be a random selection of MUAPs coming at different times in each F-wave, which explains the variation in latency, shape and size of the F-wave obtained from multiple stimulations. It was used as

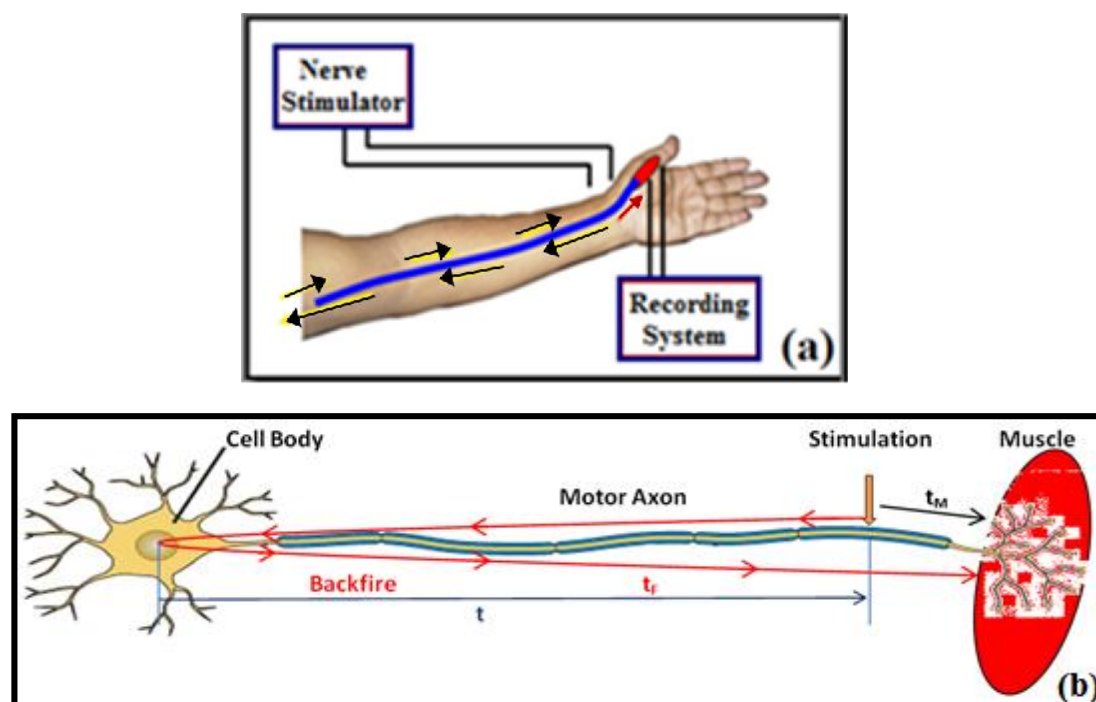


Figure 3.9: F-wave pathway

representative of the conduction velocity distribution of the entire nerve (Panayiotopoulos, 1979, Panayiotopoulos and Chroni, 1996, Rabbani et al., 2007).

3.3.2. Measurement of F-wave parameters

A supramaximal electric stimulus applied at practically any point along the course of a nerve elicits the F-wave. Placing the anode distal to the cathode or off the nerve trunk avoids anodal blocking of the antidromic impulse (Daube, 1996, Delisa et al., 1994, Fisher, 1992, Fowler, 1993, Kimura, 1989, Kimura, 1993, Liveson and Ma, 1992, Oh, 1993). However, others point out that in routine clinical practice F-waves are elicited with cathode distal stimulation (Young and Shahani, 1978). A surface

electrode placed over the motor point of the tested muscle serves as the active lead against the reference electrode over the tendon. An optimal display of F-waves requires an amplifier gain of 200 or 500 $\mu\text{V}/\text{cm}$ and an oscilloscope sweep of 5 or 10 ms/cm , depending on the nerve length and stimulus point.

These recording parameters truncate and compress the simultaneously recorded M response into the initial portion of the tracing. Thus, one must study the M response and F wave separately, using different gains and time bases.

F-wave latencies measured from the stimulus artifact to the beginning of the evoked potential vary by a few milliseconds from one stimulus to the next. Hence for an adequate study, more than 10 F-waves must be clearly identified among 16 to 20 trials. In addition, determination of the minimal and maximal latencies reveals the degree of scatter among consecutive responses, providing a measure of temporal dispersion (Panayiotopoulos, 1979). Electronic averaging of a large number of responses permits easy analysis of mean latency, although phase cancellation sometimes defeats its own purpose (Eisen et al., 1984, Fisher, 1982, Fisher, 1983, Marra, 1987).

The population of F-waves can be seen as a sample of the population of motor neurons innervating a muscle and their axons. Thus, the estimated conduction velocities of all the individual F-waves in a representative sample of the population of F-waves should be a sample of the conduction velocities of the population of motor axons in a nerve. The incidence of the F-wave may favour the larger motor neurons with faster conducting axons. This in turn provides a rationale for using the minimal latency of the F-wave as a measure of the fastest conducting fibers. Kimura showed that the antidromic maximal conduction velocity of the F-wave is the same as the orthodromic conduction velocity of the M-potential in a given nerve segment (Kimura et al., 1974). The conduction velocity of the F-wave, as measured with the shortest F-wave latency, is similar to the maximal motor conduction velocity (Barwick and Fawcett, 1988, Gilloff and Modarres-Sadeghi, 1991, Nobrega et al., 2000, Panayiotopoulos et al., 1977). It has been assumed that the motor unit indexing the latency to the onset of the compound muscle action potential is often the same as, or has a similar CV to the fastest F-wave obtained with 50 or more supra-maximal stimuli (Burke et al., 1989).

Some other parameters, such as minimal latency, maximal latency, mean latency, dispersion or chronodispersion (difference between the longest and the shortest latencies), persistence (number or percent rate of F waves generated by consecutive stimuli), amplitude of F waves, ratio of F/M amplitudes and tachodispersion (difference between the fastest and the slowest conduction velocities) are used to evaluate F waves. Some of these reflect proximal conductive properties of motor nerves whereas others provide information on the excitability of motor neuron pool (Andersen et al., 1997, Bischoff et al., 1992, Drozdowski et al., 1998, Fisher et al., 1994, Fraser and Olney, 1992, Tsai et al., 2003, Weber, 1998).

3.3.3. Existing Clinical Applications of F-wave

Clinical uses of the F-wave suffer from inherent latency variability from one trial to the next. Determination of the shortest latency after a large number of trials can minimize this uncertainty. Recording as many as 100 F-waves at each stimulus site proved useful in special studies (Panayiotopoulos et al., 1978) but is not practical in routine clinical test. Determining the latency differences between two sides or between two nerves in the same limb serves as the most sensitive means of examining a patient with a unilateral disorder affecting a single nerve. Absolute latencies suffice for evaluating the entire course of the nerve in a diffuse process. Calculation of the central latency, the F-wave conduction velocity (FWCV), and the F-ratio provides additional information not otherwise available, especially in the comparison of proximal and distal segments.

Conventionally measurement of F-wave latencies are used in identifying disorders involving proximal segments of peripheral nerves. The determination of F-wave latencies is thought to be particularly valuable in evaluating neuropathies in which focal, proximal pathology may be seen, as in Guillain-Barre syndrome and neuropathy associated with rheumatoid arthritis.

The inherent variability of the latency and configuration makes the use of F-wave less precise than that of the direct compound muscle action potential or M-response determination. Nonetheless, the technique usefully supplements the conventional nerve conduction studies, especially in characterizing demyelinating polyneuropathies, in which the delay of the F-wave often clearly exceeds the normal range. In addition to determination of F-wave latencies and calculation of conduction

velocities provides a measure of motor neuron excitability, which presumably dictates the probability of a recurrent response in individual axons.

The F-wave is commonly abnormal in hereditary motor sensory neuropathy (Kimura, 1974, Kimura et al., 1975, Panayiotopoulos et al., 1978), acute or chronic demyelinating neuropathy (Kimura, 1978, Kimura and Butzer, 1975, King and Ashby, 1976), diabetic neuropathy (Conrad et al., 1975, Kimura et al., 1979), uremic neuropathy (Ackil et al., 1981, Panayiotopoulos and Lagos, 1980, Panayiotopoulos and Scarpalezos, 1977), alcoholic neuropathy (Labbok, 1937, Lefebvre d' Amour et al., 1979) and a variety of other neuropathies (Lachman et al., 1980). Other categories of disorders associated with F-wave changes include entrapment neuropathies (Eisen et al., 1977b, Wulff and Gilliat, 1979), amyotrophic lateral sclerosis (Argyropoulos et al., 1978) and radiculopathies (Eisen et al., 1977a, Fisher et al., 1978).

Studies of the F-wave help in characterizing polyneuropathies in general and those associated with prominent proximal disease in particular. In the early diagnosis of more localized nerve lesions such as radiculopathies, the remaining normal segment tends to dilute a conduction delay across the much shorter segment.

For clinical purposes, the F-wave dispersion was used to characterize abnormal conduction velocity distributions. It is defined as the difference between the maximal and the minimal F-wave latencies (chronodispersion) or between maximal and the minimal F-wave conduction velocity (tacheodispersion) of a series of F-waves. Parameters, such as minimal latency, maximal latency, mean latency, persistence (number or percent rate of F-waves generated by consecutive stimuli), amplitude of F-waves and ratio of F/M amplitudes are used to evaluate F-waves. Normative data vary considerably between different laboratories (Table 3.1), which reflects that F-wave methodology is less standardized than conventional nerve conduction studies. So, F-waves are useful to demonstrate abnormal conduction velocity distributions in patients, when a standard methodology will be developed.

3.4. Techniques for measurements of DCV

3.4.1. Experimental

Collision testing was suggested by Thomas et al. (Thomas et al., 1959) and fully developed by Hopf (Hopf, 1962) to measure the conduction velocity distributions of

peripheral motor nerves. The collision technique involves the interaction of two action potentials propagated toward each other from opposite directions on the same nerve fiber. In routine clinical practice, collision testing is used most commonly during motor nerve conduction studies to allow for distinction between separate components of an evoked response that are conveyed via two different nerve pathways. Stimulations may be delivered simultaneously or separated by a time delay, termed interstimulus interval (ISI). In motor nerve conduction studies assessing for anatomic variants, the first stimulus is often applied to a distal nerve segment from which the clinician wishes to suppress (abolish) an evoked response. The second stimulus is applied to a more proximal nerve segment from which an evoked response is being assessed. Assuming appropriate timing, the nerve will be in the refractory period, when the volley from the second stimulation arrives, preventing further propagation and preventing the recording of a response derived from this nerve fiber. The recorded response, therefore, will reflect only those components that are conveyed via an alternate route.

Table 3.1: F-wave chronodispersion: Upper limits (95%) of normal

Nerve	Upper limit (ms)	N	
Median	8.9	10	(Weber, 1998)
	4.1	20	(Puksa et al., 2003)
Ulnar	8.7	10	(Weber, 1998)
	6.7	64	(Nobrega et al., 2001)
	3.9	10	(Weber, 1998)
Tibial	9.5	10	(Puksa et al., 2003)
	5.9	20	(Puksa et al., 2003)
Peroneal	7.5	20	(Panayiotopoulos, 1979)
	10.6	10	(Weber, 1998)
	6.9	20	(Puksa et al., 2003)

N, Number of F-waves from which the chronodispersion was calculated.

A simple collision technique to assess conduction velocity combines supramaximal proximal stimulus with a simultaneous submaximal distal stimulus, to preferentially excite large diameter, fast conducting fibers. This allows for collision to occur only in the fast fibers, and only a response conveyed via the slow fibers will be recorded. Unfortunately, technical factors preclude this method from being accurate as the

location of individual fascicles in relation to the stimulating electrode is another important factor in determining the order of activation of nerve fibers (Kadrie et al., 1976, Kimura, 2001, Preston et al., 1994).

3.4.1.1. Hopf's method

In 1962, Hopf described a technique that involves a series of paired supramaximal stimuli that are delivered with increasing ISIs. Stimuli with a short ISI cause collision of all the fibers. As the ISI increases, some faster fibers will escape collision. The minimal ISI at which the full M wave is restored allows for an indirect calculation of the slowest fibers (Hopf, 1962).

At the start of the examination consecutively a single distal S1, a single proximal S2 and a simultaneous distal S1 and proximal S2 stimulus (Figure 3.10) were applied to produce control CMAPs. A supramaximal stimulus S1 delivered at the wrist evokes a CMAP1 response and an antidromic CNAP1. As CNAP1 approaches the elbow, a second supramaximal stimulus S2 delivered at this site fails to generate a CMAP2 because the orthodromic CNAP2 is extinguished by collision with antidromic CNAP1. At longer S1-S2 ISI, faster-conducting fibers whose CNAP1 action potentials have passed the elbow and which are no longer refractory are activated by S2 and propagate to the muscle, producing an incremental CMAP2 component of the composite CMAP12. The size of CMAP2 is proportional to the number of unblocked motor nerve fibers. With increasing ISI, slower-conducting fibers are progressively recruited into CMAP2, until CMAP2 = CMAP1. The cumulative response function of ISI vs CMAP2 (amplitude, area, or $[CMAP12 - CMAP1]/CMAP2$ cross-correlation in ascending order of sophistication) may be differentiated to yield the latency response density function, which is readily transformed into the DCV (Leifer, 1981, Leifer et al., 1977).

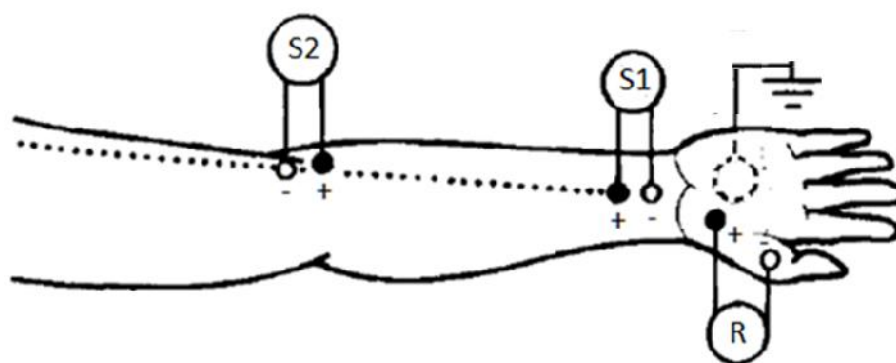


Figure 3.10: Hopf Collision technique

In collision neurography, the responsiveness of motor fibers to the S2 stimulus depends not only upon their CV, but also on their refractory characteristics. The initial distal-proximal ISI_{dp} was set to the latency difference from the normal MNCV measurement rounded down to the nearest 0.5 msec. The initial step size was 0.5 msec. Step size was reduced to 0.25 or 0.2 msec in the range of 70-95% response amplitude, judged from an on-line graph produced during the examination. For this purpose the test response was isolated by subtracting the response to the single distal stimulus acquired at the start of the examination. After the CMAP amplitude had regained more than 95% of its control value, step size was increased to 0.5 msec again. The examination ended when the amplitude of the CMAPs was stable in an ISI range of 1.5-2 msec.

3.4.1.2. *Ingram's method*

Ingram et al. (Ingram et al., 1987) proposed an alternative method, and mentioned 4 major objections to Hopf's method which would result in a limited accuracy:

- i. First, in Hopf's method allowance must be made for the refractory period.
- ii. The test compound muscle action potential (CMAP) would be distorted,
 - a. firstly due to transient slowing of the proximal orthodromic nerve impulse associated with the nerve subnormal period and
 - b. secondly due to velocity recovery in muscle fibres (Stålberg, 1966).
- iii. Finally, in Hopf's method the part of the distribution of motor nerve conduction velocity (DMCV) associated with the slowest fibres' MNCV is marked by full recovery of the CMAP, which cannot be easily established.

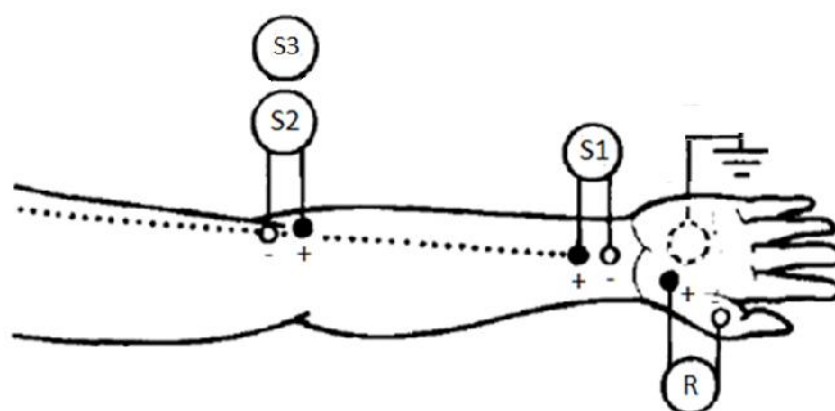


Figure 3.11: Ingram Collision technique

Ingram et al. stated that their method obviated the problem of CMAP distortion in particular and allowed accurate measurement of the MNCV of the slowest fibres in the nerve bundle.

A single distal S1, a single proximal S2 and a simultaneous distal and proximal stimulus were applied consecutively (Figure 3.11). Subsequently a series of combined proximal-distal-proximal stimuli were applied. The ISI between the first proximal (S2) and the distal (S1) stimulus (ISI_{p1-d}) is variable. The ISI between the distal (S1) and second proximal (S3) stimuli (ISI_{d-p2}) was fixed at the conduction interval from the conventional MNCV minus 1 msec. At least two stimulus sequences with a short ISI_{p1-d} were applied which produced maximal test CMAPs.

3.4.1.3. Kimura's method

Kimura (Kimura, 1983) described a method that allows for a direct calculation of the slowest fiber velocities, by colliding the fastest fibers (Figure 3.12). This paradigm uses supramaximal stimulations. A proximal stimulation, e.g. axilla S(A1), is followed with a varying ISI by a distal stimulation, e.g. wrist S(W). A third proximal

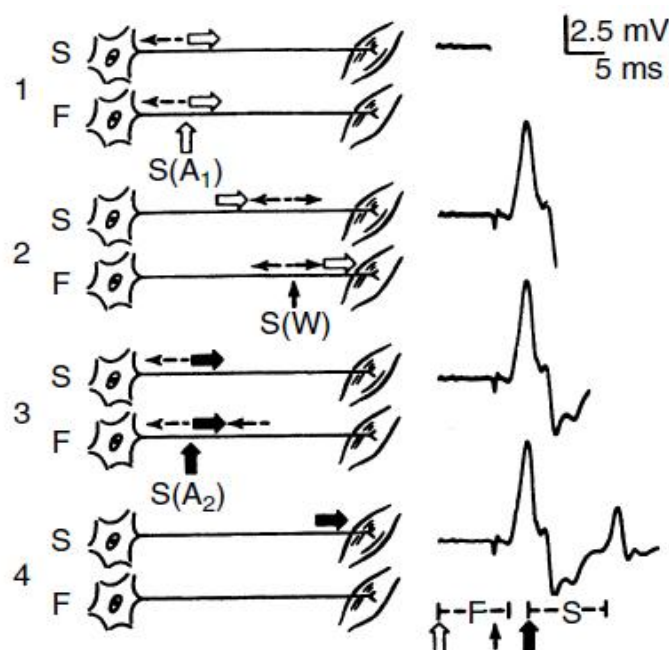


Figure 3.12: Kimura's method

stimulation S(A2) is then delivered at an ISI fixed to the wrist stimulation. The interval between S(A1) and S(W) varies between approximately 6 and 8 ms, which is sufficiently long to cause collision from the S(W) only in the slow fibers, allowing the S(W) elicited impulses in the fast fibers to continue propagating proximally. S(A2) is

then delivered at 6 ms following S(W). The impulses from S(A2) then collide only with the S(W) elicited impulses in the fast fibers, allowing the slower fibers to continue to propagate. With increasing ISIs, the M-response amplitude declines and latency increases, as only the slowest of fibers contribute to the response. The conduction velocity of the slowest fibers can then be calculated from the M-response elicited with the highest ISI before the response became absent.

3.4.1.4. Gilliatt et al.

Gilliatt et al. (Gilliatt et al., 1976) described a collision method in animal studies that was then adapted in animals by Nakanishi et al. (Nakanishi et al., 1986), and later in humans by Nakanishi et al. (Nakanishi et al., 1989). This stimulation method involves a submaximal distal stimulation and two different proximal stimulation sites. The method also uses a computerized subtraction for analysis. Using this method, normal maximal and minimal conduction values have been described (Arasaki et al., 1991), the findings in ALS have been described (Nakanishi et al., 1989), and the normal values in F and S type motor units have been described (Arasaki, 1992).

3.4.1.5. Harayama's et al.

Harayama et al. (Harayama et al., 1991) described a method of measuring conduction velocity distributions using a combination of techniques. In essence, the Hopf method (Hopf, 1962) is used primarily. Then a correction for the distortion in CMAP size caused by the velocity recovery effect (Stålberg, 1966) is applied using a modification of Kimura's refractory period collision method (Kimura, 1976). In addition, another correction, based on an equation, is applied to correct for the refractory period of the nerve at the point of stimulation.

As most collision studies involved motor nerve conduction, typically the recorded response is a CMAP. In addition to the typically measured parameters of latency, amplitude, and area, the shape of the response should also be subjectively interpreted. Visual comparison of waveform morphology is important to ascertain whether there has been stimulus spread, and whether collision has occurred.

3.4.2. Analytical

3.4.2.1. Analysis of a single compound action potential

Figure 3.13 (a) illustrates that a compound sensory nerve action potential (SNAP) is the sum of the action potentials of the single fibers of that nerve. It is obvious that the compound SNAP can be calculated from the single fiber action potentials, simply by summation. If the *inverse problem* was solved, namely to calculate the single fiber action potentials from the compound SNAP, the conduction velocity distribution could be measured easily. Figure 3.13 (b) illustrates that the inverse problem can be solved if the single fiber action potentials are very short. In this case the contribution of each single potential to the compound SNAP is apparent. In general, the inverse problem can only be solved if the single fiber action potentials meet certain conditions or if certain assumptions are made about them.

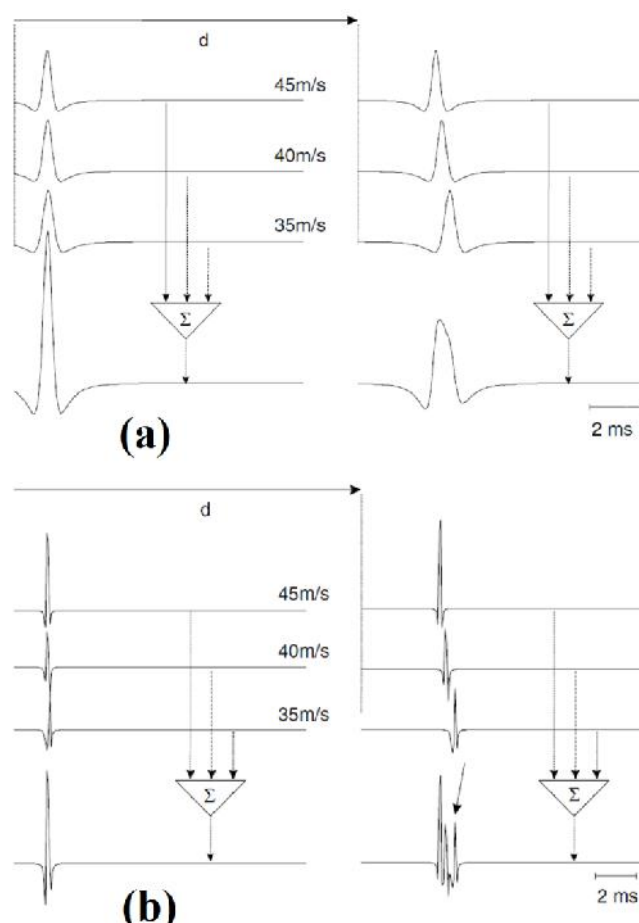


Figure 3.13: Construction of a compound sensory action potential by the summation of three sensory nerve fiber action potentials (computer simulation, surface electrodes (a), needle electrodes (b)). Left column: action potentials immediately upon nerve stimulation. Right: action potentials after propagation through a 15-cm nerve segment d . Different arrival times at the recording electrode due to different conduction velocities of the fibers. The conventional NCV is 45 m/s but a late component with a NCV of 35 m/s can be identified (arrow).

3.4.2.2. Comparison of two compound action potentials

For Sensory Nerves

Cummins et al. (Cummins et al., 1979a) introduced this principle and studied how the assumptions about the single fiber action potentials influence the resulting conduction velocity distributions. In this method, the nerve is stimulated at one point and CNAPs are recorded at two sites separated by known distances from each other and from the stimulation site as shown in Figure 3.14.

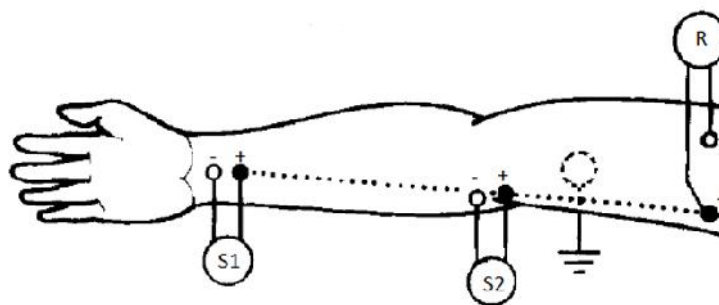


Figure 3.14: Cummins et. al. CNAP method

In the methods of Barker et al. (Barker et al., 1979) and Caddy et al. (Caddy et al., 1981), one recording site and two stimulation sites are employed (Figure 3.15). These methods all have the advantageous property that knowledge of the SFAP waveform is not required. In fact, the SFAP may be explicitly estimated, together with the DCV.

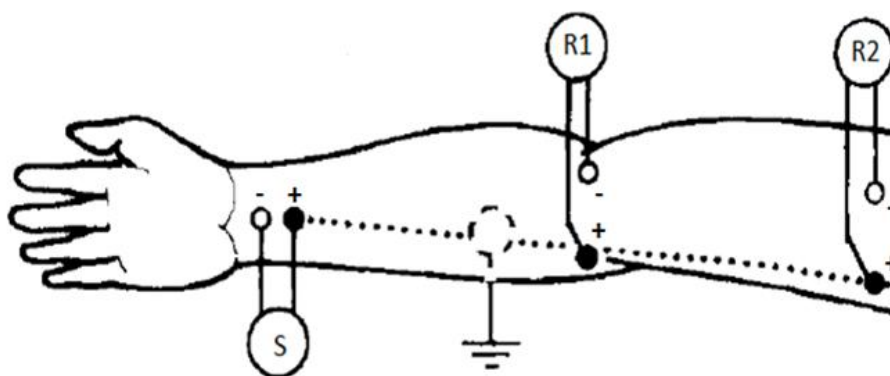


Figure 3.15: Barker et. al. CNAP method

For Motor Nerves

Caddy et al. (Caddy et al., 1981) and by Dorfman et al. (Dorfman et al., 1982) explored the deconvolution of the evoked CMAPs. When the nerve to a muscle is stimulated at two points (Figure 3.16), as is commonly done clinically to measure maximal motor CV, the shapes of the evoked CMAPs differ – reflecting the effects of dispersive conduction in the motor axon population. Their results corresponded reasonably well with results obtained with the collision method.

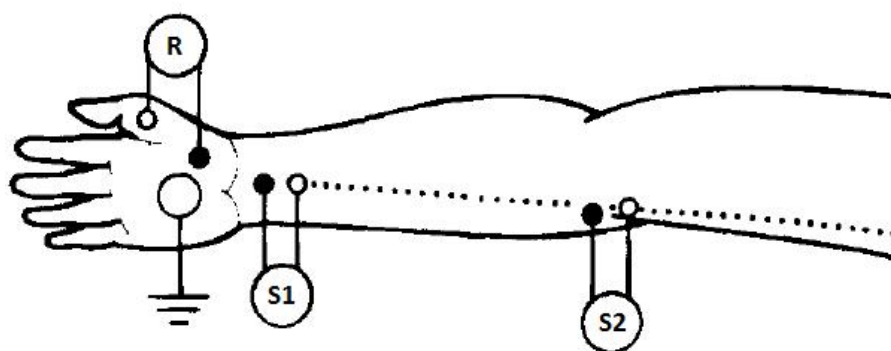


Figure 3.16: Method based on CMAP's

Motor DCVs obtained using the deconvolution method tend to indicate a relatively narrow range of active fiber CVs (about 12-24 m/sec) compared to mixed-nerve DCVs (about 30-50 m/sec). This reflects the fact that in normal subjects there is usually only a small change in CMAP configuration from a distal to a more proximal stimulus site.

3.5. Summary of all the methods

All methods discussed above have the potential to provide more information about the pathophysiological state of a nerve or a nerve segment. However, each method has specific shortcomings, which may have hindered its widespread use in electrodiagnostic laboratories. The shortcomings are obvious with near nerve recording or with collision testing.

For clinical purposes, the discomfort and the cost of a diagnostic method must be balanced against its diagnostic sensitivity and specificity. The patient's discomfort is definitely higher upon one of these studies than upon a routine nerve conduction study. Moreover, both methods are more time consuming than routine studies (Table

3.2). The time consumption especially has led to a gradual decrease in the number of studies done.

Some of the methods described here essentially are nothing else as numerical post-processing of waveforms obtained during routine nerve conduction studies, namely the F-wave dispersion and the deconvolution methods. The F-wave dispersion has the advantage that it can be measured without sophisticated computer programs but has the disadvantage of low test-retest reliability. The opposite is the case in the deconvolution methods, which have high test-retest reliability but require specialized computer programs.

The necessity of looking into the DCV of the fibers was felt a long time back but no satisfactory method exists till today for obtaining this distribution from measured compound nerve action potentials (CNAP's) or compound muscle action potentials (CMAP's). Different workers attempted obtaining DCV's and most of the work concentrated on the CNAP.

Table 3.2: Overview of methods to characterize nerve conduction velocity distribution

Method	Fibre type	CVD	Gain in Diagnostic sensitivity*	Pain**	Time***	Skills****	Remarks
Near Nerve recording	s, x	p	11% (Oh et al., 2001b)	>50	<1 h	Yes	Invasive method
Nerve fibre stimulation	m	p	n. d.	>60	>1 h	Yes	Invasive method
Collision testing	m, s	f	18% (Bertora et al., 1998)	>20	0	Yes	
Deconvolution of compound SNAPs	s, x	f	7%-21% (Cummins and Dorfman, 1981b, Dorfman et al., 1983)	0 (<0.5 h)	0	No	Special software needed
Deconvolution of CMAPs	m	f	n. d.	0	0	No	Special software needed
F-wave dispersion	m	f	0-22% (Chroni and Panayiotopoulos, 1993a, Nobrega et al., 2001, Weber, 1998)	20	0	No	Nerve segments cannot be studied

n. d., not determined; m, motor; s, sensory; x, mixed; CVD, result of the method is a full conduction velocity distribution (f) or parameters of it (p)

* percentage of abnormal findings in a group of patients with (suspected) polyneuropathy but normal NCV. It should be noted that the structure of the groups of patients varies between studies.

** estimated number of electrical stimuli exceeding those required for a conventional nerve conduction study (NCS).

*** time required in addition to what is necessary to do a conventional NCS.

**** special training required in addition to what is necessary to do a conventional NCS.

Conventional clinical measures of motor, sensory, or mixed-nerve conduction velocity (CV) have tended to focus primarily upon the faster conducting fibers in the

nerve bundle. This approach has been remarkably productive and has demonstrated a high degree of clinical relevance, considering the small proportion of the total nerve-fiber population which contributes to these measures (Dorfman et al., 1982). In part, this is because many pathophysiological processes affect all nerve fibers comparably, or preferentially affect the faster-conducting (largest diameter) ones. Many developmental and disease processes affect nerves nonuniformly,” and for this reason it is desirable to be able to describe the population conduction characteristics of a nerve more completely. Attempt was also taken by the Dhaka University Biomedical Physics group during the last 20 years for assessing the conduction velocity distribution using a new technique Distribution of F-latencies (DFL), describe in the next chapter.

Chapter 4: Distribution of F-Latencies (DFL) and its usefulness

A peripheral nerve consists of thousands of nerve fibers with varying conduction velocities. If a motor nerve is artificially stimulated at any point, action potentials are generated within the individual nerve fibers, which travelling directly to the muscle served (orthodromic conduction), elicit a compound muscle action potential, an M-response that reproduces well on repeated supra-maximal stimulation and whose onset latency is conventionally used for obtaining a measure of NCV. From the stimulation site, the action potential also travel along the nerve fibers in the opposite direction (antidromic conduction), towards the cell bodies in the spinal cord. Most of these action potentials die out, but a few percent of the cell bodies backfire after a short delay, and send fresh action potentials down the nerve fibers to the muscle. These in effect produce a delayed compound muscle action potential called the F-response (Figure 4.1), which is very much reduced in amplitude with respect to the M-response because of the small number of fibers involved.

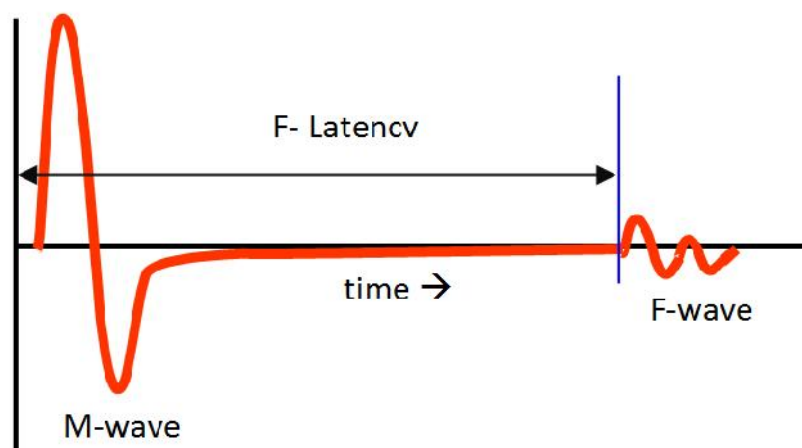


Figure 4.1: M-wave and F-wave in evoked EMG response

An important aspect of the F-response is that, unlike the M-response, it varies in shape, amplitude and latency on repeated stimulation (Figure 4.2); sometimes there will be none. The cause has been ascribed to the randomness of recruitment; which nerve cell will backfire is not previously known. It is likely to be a random process. Being a random process, it was hypothesized that, recruitment of fibers for F-response would statistically depend on the distribution of conduction velocity (DCV) for motor nerve fibers specifically of those that contribute to F-responses, and therefore, a frequency distribution of the onset F-latencies (DFL) from such multiple F-responses

would be approximate mirror image of DCV, latency being inversely proportional to the velocity (Rabbani, 2011a, Rabbani et al., 2007).

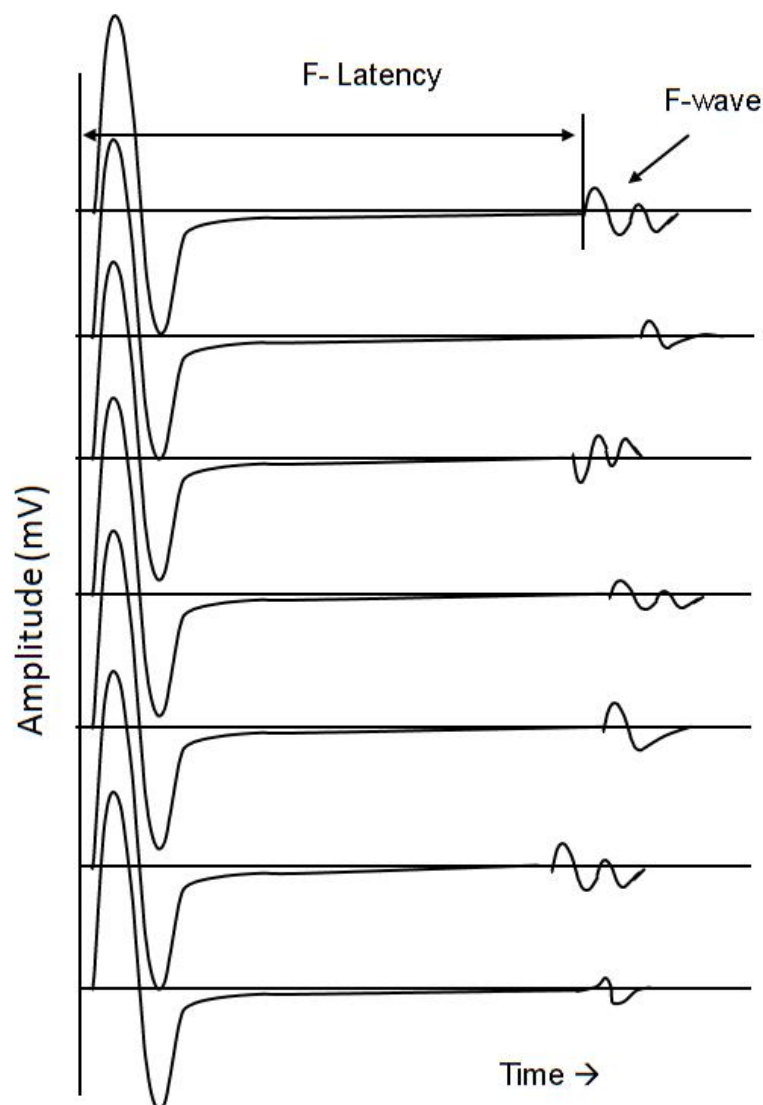


Figure 4.2: F response variation on repeated stimulation

4.1. Introduction to DFL and its relationship with DCV

In Dhaka University Biomedical Physics laboratory DFL was obtained by grouping F-latency data into 2ms bins and then plotting a frequency polygon. The resulting polygon shapes are sorted into two categories: i) single peak and ii) broad peak or multiple peaks. The first category was taken to represent normalcy while the second category was taken to represent abnormality. Different types of DFL typically obtained are shown in Figure 4.3 – 4.6. In comparison of polygon pattern, DFL with

multiple peak(s) is/are completely different from the bimodal nature of DCV. Because DCV pattern was obtained directly with respect to the diameter of individual nerve fibres, whereas DFL was obtained by grouping the onset F-latencies into 2ms bins.

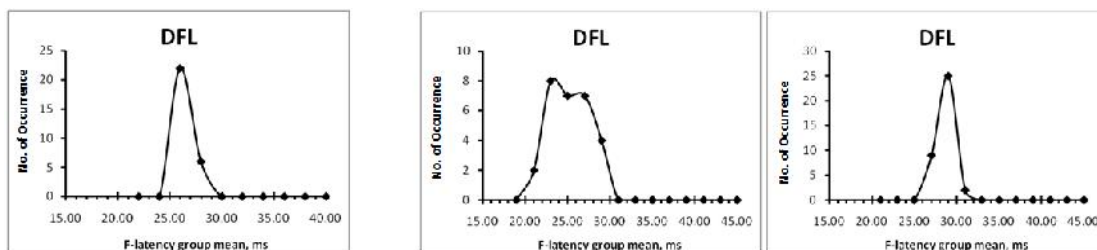


Figure 4.3: Single Peak

Figure 4.4: Broad Peak

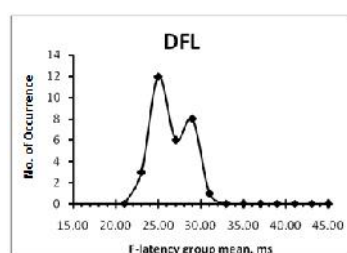


Figure 4.5: Double Peak

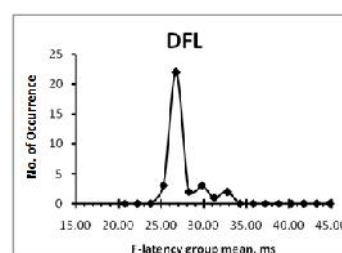


Figure 4.6: Triple Peak

The polygon shape considered as broad peak where the adjacent frequency of occurrence was greater than one third of the peak frequency, or where non-zero frequency exists at 4 ms difference from the position of the peak.

First, obtaining DFL from many human subjects, it was shown that, this is a reproducible parameter for a nerve trunk of a subject, and hence reveals a new physiological phenomenon (Rabbani et al., 2007). DFL has a single peaked distribution for normal subjects, which is also expected for the DCV of a normal healthy motor nerve. To validate its hypothesized relationship to DCV, DFLs were obtained from both median nerves of patients with unilateral carpal tunnel syndrome (CTS). The patterns of DFL from both sides remained almost the same except for a delay shift equal to that in between the two M-responses, which lends support to this hypothesis (Rabbani et al., 2007). As DCV is suggested to be mirror image of DFL, it appears to change systematically with certain known disorders such as Cervical spondylotic Radiculopathy and Myelopathy (CRM), even at a subclinical stage (Alam and Rabbani, 2010). Earlier it was named as Cervical Spondylosis (CS). There appears significant differences between the DFLs of normal subject and that of a CRM patient. Normal subjects having no neurological complaints show a single peaked distribution, whereas, patients having CRM show double or triple peaks in

their DFLs. Some subjects demonstrated rather broad plateau with slight indication of dual peaks, although, they did not complain of any neurological problem. This clearly indicates that, DFL may become a new and improved investigative diagnostic tool in neurophysiology.

A study was conducted by Rabbani et al. (Rabbani et al., 2007) to establish DFL as a physiological phenomenon on ten adult subjects, aged between 23 and 45. They stimulated each of the median nerves of these subjects about with 40 supramaximal electrical stimulations at the wrist in sequence. The time sequence of the collected F-latencies from each nerve was maintained and recorded. From this protocol, 20 data sets for multiple F-latencies were collected from the right and left median nerves of 10 subjects. According to the above grouping, respective DFLs were obtained for all the 20 data sets. They also test the reproducibility of the DFLs. They separated the raw F-latency data from each nerve into odd and even data points in terms of time sequence of collection, and fresh DFLs were plotted for those odd and even data sets following the latency grouping. The correlation coefficients between the respective odd and even DFLs were 0.81 confirming them about their hypothesis that DFL is a physiological parameter and is an approximate mirror image of the DCV of nerve fibres.

4.2. DFL in Carpal Tunnel Syndrome

Carpal tunnel syndrome (CTS) is a well-understood disorder in which the median nerve is compressed at the wrist, causing a conduction delay through all the nerve fibres. The entrapment is expected to affect all the nerve fibres equally due to pressure transmission in a fluid, and it has also been demonstrated well through a shift in the M-response towards longer latencies (delays) without any significant change in its shape, unless other abnormalities are involved. This also results in a delay of the shortest F-latency. An experiment was performed by Rabbani et. al. (Rabbani KS 2011) to validate that DFL is a simple reflection of DCV. In many subjects CTS occurs only in one hand while the other hand has normal conduction. So the new multiple F-latency technique was used to obtain DFLs from both hands of such patients, particularly those who demonstrated similar shapes of M-responses from the two hands except for the delay. This disorder is expected to shift the DCV towards lower velocities in the affected side without significant change in the relative

distribution pattern. Since DFL is related to DCV as suggested by Rabbani et.al. (Rabbani KS 2011), then DFL was shifted to longer latencies without significant change in shape, and the lateral time shifted almost the same as the difference between the latencies of the M-responses (Figure 4.7).

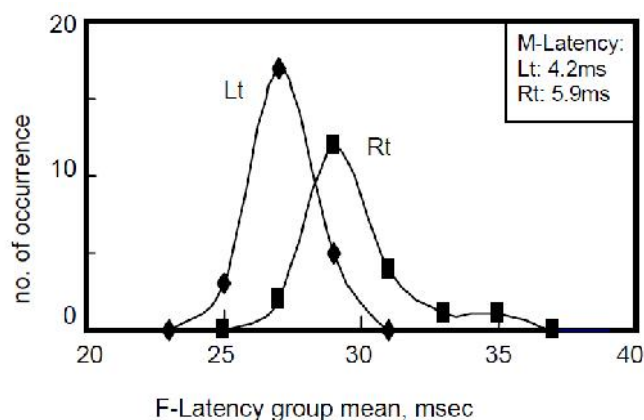


Figure 4.7: DFL for median nerve for a subject with CTS on right hand, but normal left hand. The M-latency values from the M-responses are quoted in the box (upper right corner). DFL peak shifts by the same amount as that for the M-latencies (Rabbani KS 2011a).

In the course of routine clinical work one of the authors also had observed double or broad peaks of DFL for the median nerve for many patients who had symptoms of CRM (Rabbani, 2011b, Rabbani, 2011a, Rabbani, 2012). Similarly, double or broad peaks of DFL were also be observed for Tibial or Common Peroneal nerves for cases with Lumbo-sacral spondylosis.

4.3. DFL in Radiculopathy and Myelopathy

CRM usually has two main causes. One is called Radiculopathy in which nerve branches coming out of the spinal cord are compressed in the narrow channels or gaps created by the vertebral bones. This compression may be caused by bony growth in the vertebra (osteophyte), or herniation of inter-vertebral disc as shown in Figure 4.8. Either of these compressions leads to CRM, and this condition is known as Radiculopathy.

The other cause of CRM is Myelopathy in which one side of the spinal cord is directly pressed onto, mostly by a bulging intervertebral disc, as shown in Figure 4.9. This affects nerve fibres located in the pressed region of the spinal cord. For the median nerve DFL is usually obtained from the Thenar muscle (Abductor Policis Brevis, APB) at the base of the thumb, by stimulating the nerve at the wrist.

As mentioned before, for a normal healthy nerve trunk having many fibres, the DCV has a single peak, which gives rise to a DFL with a single peak as well. The same may be expected for the separate DCV of the fibres within each of the nerve branches C7, C8 and T1 that combine in the median nerve to serve the thenar muscle. That is, the relative DCV may expect from each of the nerve branches to be the same, having approximately the same conduction velocity values. This means DFLs due to the nerve fibres in the three branches will also have similar distributions with approximately the same latency values. The combined DFL due to all the nerve fibres together would be simply a sum of all the three branch distributions, which will also have a similar pattern with a single peak at the same latency value, as shown schematically in Figure 4.10 (left). This explains why DFL for a normal healthy nerve has a single peak.

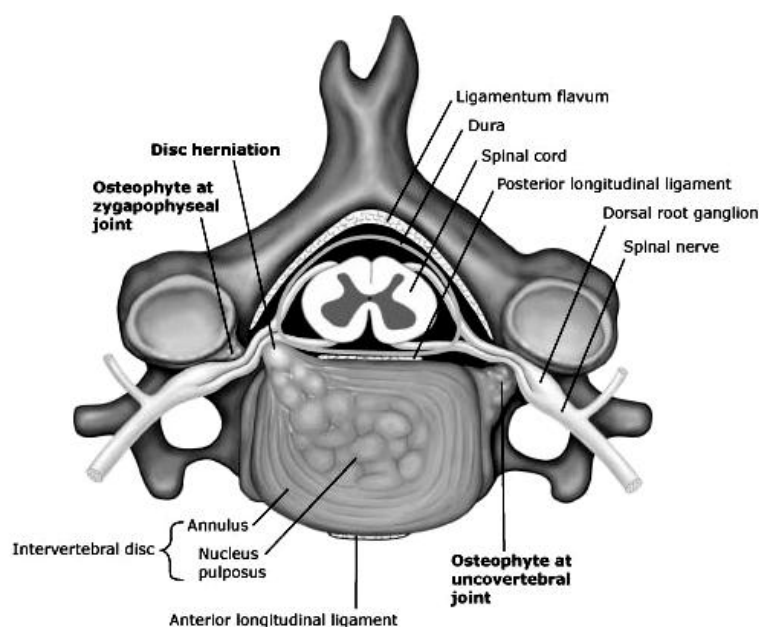


Figure 4.8: Vertebral section showing radiculopathy (compression of nerve root).

Now suppose one of the nerve branches, say, C7 is compressed due to radiculopathy at the vertebral region while the other two, C8 and T1 are uncompressed. Therefore, all the nerve fibres within the C7 branch will be similarly compressed at the point of compression following the same argument as given before for CTS. Therefore, the contribution of nerve fibres from this branch to the measured DFL will have a delay shifted pattern, same as that occurring in CTS. On the other hand, there will be no delay in the DFL for the other two uncompressed nerve branches C8 and T1.

Therefore the combined DFL due to nerve fibres from all the three branches will essentially be a sum of the three distributions, and will have a double peak. This is shown schematically in Figure 4.10 (right). This also will mean that the first uncompressed peak, being from two branches, will be larger than that from the second delayed peak, being from a single branch. This hypothesis was the first to explain the double peak of DFL in CRM. It is interesting to note that most of the experimentally observed DFLs with double peaks had the first peak larger than the second one, matching the above explanation. So this hypothesis suggests that compression of any one of the three nerve branches, C7, C8 and T1, will contribute to a DFL with double peaks (Rabbani, 2011b).



Figure 4.9: Compression of spinal cord due to disc bulging (Myelopathy)

Now with the less degree of the above compression as happens in the early stage of radiculopathy, the delay shift of DFL will also be less, and the two peaks of the two distributions may not get resolved in the combined DFL. So they will result in a broad peak. With an increasing degree of compression, the delay will also increase, and two humps may just be noticeable. With further compression, there will be more delay; the two peaks will be resolved and clear double peaks will be noticeable. Therefore, it was hypothesized that a broad peak of DFL indicates an early stage of radiculopathy (Rabbani et al., 2007). The subject usually does not feel anything at this stage, i.e., it is a sub-clinical phase, and this offers the possibility of early indication of neuropathy.

Now, if two of the nerve branches of the three (C7, C8 and T1) are compressed to different degrees, triple peaks may be obtained, following the same arguments as above. Therefore the same hypothesis given by Rabbani KS also explains the occurrence of triple peaks in DFL (Rabbani, 2011b).

The same arguments would hold for Common Peroneal nerve and Tibial nerve in the legs due to similar differential compression of the nerve branches in the Lumbo-sacral region of the vertebra.

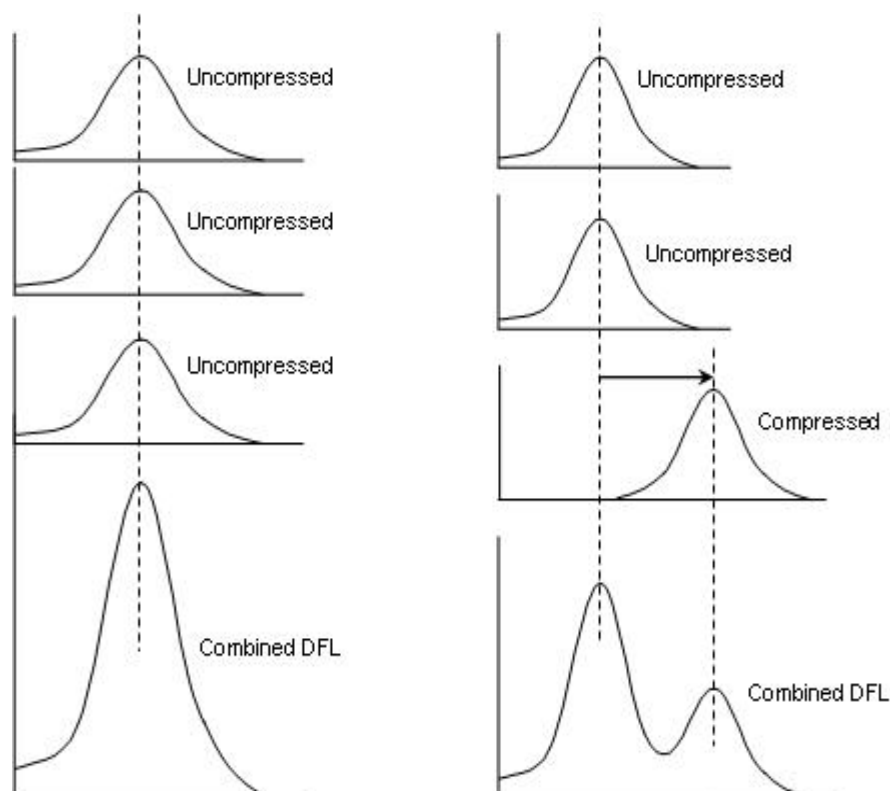


Figure 4.10: DFL due to uncompressed nerve roots (left) and due to compression in one of the three roots (right), the latter causing a double peak (Rabbani, 2011b).

Conventional neurophysiological techniques have so far not produced any method to give a positive diagnosis of CRM except for excluding other peripheral nerve disorders. Using a train of 200 stimuli (Peioglou-Harmoussi et al., 1987) studied the frequency of occurrence of F-responses from ulnar nerves, frequency of identical responses and F-wave shapes, to relate these to CRM. None of these led to any clear-cut method to identify CRM, as the distinctions were not well marked; however, there appears to be a correspondence with one of their observations with the observation of DFL. They found that the F-wave appeared complex visually compared to those from controls. In the above findings, DFL is a simple distribution with a single peak for

normal subjects; therefore the backfiring nerve cells have less dispersion in latency among them, contributing to simple F-waves on combination of the individual motor unit responses. On the other hand, in case of CRM, DFL has more dispersion with double peaks, meaning that latencies from back firing nerves may have wider separation among them, leading to more complex patterns on combination.

4.4. Hypothesis for abnormal DFL

After the indication of the relationship between CRM and multiple peaks of DFL by Alam and Rabbani, further studies were taken up to establish this observation on firmer grounds.

In one study DFL was obtained from the median nerves of 20 subjects with age varying between 25 and 65 (Hossain et al., 2011). Firstly the DFL results were correlated to clinical findings reported by the volunteers themselves, whether they had diagnosed CRM or neck pain (which was also taken as a case of CRM). As expected, the 6 normal subjects demonstrated single peak of DFL on both sides, and they did not have any neurological complain either. One of them was investigated using X-ray, and the report came out normal, with no bony growth. The remaining 6 subjects having diagnosed CRM or neck pain demonstrated double or triple peaks of DFL.

Tables 4.2 indicate very conclusively that all subjects having diagnosed CRM had double or triple peaks of DFL, in at least one side, while all in the normal group had single peaks. Again, it can be seen that X-ray and MRI investigation carried out during this work also indicates some sort of spinal abnormality affecting the nerves in all the 9 subjects who demonstrated double or triple peaks of DFL.

If radiculopathy has to affect the thenar muscle, there should be compression of C7, C8 or T1 nerve roots. In Table 4.2 two subjects (EHS and SAL) had bony growth (osteophyte) at C7, as revealed by X-ray investigation, which may compress the nerve branch C7, and cause radiculopathy. There is also a case of cervical rib. However, in all others, disk space reduction coupled with disc bulging and compression on spinal cord are common at slightly higher levels of the vertebra. Therefore, it can be said that these cases had myelopathy, i.e., pressure on the spinal cord. This small study also indicates that myelopathy has affected more of the subjects than radiculopathy.

Another study was carried out on 24 median nerves of 12 patients with suspected cervical radiculopathy over a 9 month period at the Singapore General Hospital and

analysed at Dhaka (Rabbani et al., 2014). Initially only double peaks of DFL, prepared using 2ms bin intervals, were assumed to indicate radiculo-myelopathy. However, when compared with the MRI findings there was a significant percentage of false negatives; diagnosed as free of lesion through DFL, while MRI suggested otherwise. It was observed though that many of the false negatives had two adjacent frequency values (at a separation of 2ms) significantly high and with low values further out, which were considered as single peaks in this analysis. At this point the broad peaks of DFL were redefined to include such patterns of DFL, which were considered as marginal broad peaks. Through a comparison with the MRI findings a rule of thumb was made to define such a broad peak; it will be termed a broad peak if an adjacent (at a separation of 2 ms) frequency to a peak is more than one third the peak. This was considered in addition to the original definition of a broad peak. Thus the definition of broad peak was revised to include broad peaks as that where the adjacent frequency of occurrence was greater than one third of the peak frequency, or where non-zero frequency exists at 4 ms difference from the position of the peak .

Table 4.2: X-ray and MRI findings of subjects having double peak of DFL (Hossain et al., 2011)

Subject ID	Age (yrs)	X-ray findings (for whom done)	MRI findings (for whom done)
HFT	26	Mild ost: C5, DSR	----
CHA	26	Marginal ost: C4, DSR	---
EHS	36	Marginal ost C7, DSR	DB: C4-C5, C5-C6, SCC
AKT	46	Mild ost: C5-C6, DSR at C4-5 and C5-6	---
SAL	49	Ost: C5, C6, C7. DSR at C5-6	DB: C5-C6, SCC
HUQ	64	Mild ost: C4, C5, DSR at C3-4, C5-6, C6-7.	---
KSR	60		DB: C5-C6, SCC
ARA	25	Cervical Rib	
AAM	26	Normal	DB: C4-5, C5-6, SCC
Abbreviations:		Ost: Osteophyte	DB: Disc bulging
		DSR: Disc space reduction	SCC: Spinal cord compression

For the initial analysis only double peaks or distinct broad peaks of this distribution were assumed to indicate pathology. The correspondence with MRI assessment

however could be improved significantly through redefining a broad peak of the Distribution of F-latency as the pattern where the adjacent frequency of occurrence was greater than one third of the peak frequency. A third analysis was also performed where a case of sensori-motor neuropathy, not identified as radiculo-myelopathy by MRI, was also included as an abnormality.

The third analysis gave the best performance of the Distribution of F-latency giving correct predictions in 88% of cases corresponding to a sensitivity of 90% and positive predictive value of 95%. The specificity value was not significant as the number of negative cases in the study group was low.

To observe the effectiveness of DFL for diagnosis or screening of CRM a further study was carry out as a blind trial involving both MRI and DFL by Chowdhury et. al. in 2013. MRI is the standard investigation for the diagnosis of CRM. These investigations were carried out on both symptomatic and asymptomatic subjects. The Radiologist conducting MRI was not informed of the DFL findings. Also the investigator assessing the DFLs was unaware of the MRI results. This was done to keep the trial double blind and minimize bias.

A pool of 31 volunteers was chosen to take part in the investigation. The selection process was random. The pool was divided into two age groups. One group consisted of subjects aged from 25 to 50 and the other group consisted of subjects over 50. This grouping was done on the basis of the conventional understanding that cervical spondylosis was more prevalent in older age.

The DFL and MRI findings were evaluated separately (Chowdhury, 2013) and only brought together for comparison at the end of the investigation to ensure the double blind nature of the study. There were a few instances where the MRI findings were very subtle and judged to be within normal limits by the radiologist in spite of mild cord and root compression. At each level the severity of the defect was indicated by the number of stars (*) as shown in Table 4.3. The absence of star indicates normal condition. The data were also analysed based on two age groups as mentioned above.

Thus the results were tabulated and analyzed in the following four ways:

1. The whole data set with single star (*) considered as negative.
2. The whole data set with single star (*) considered as positive.

3. The group consisting of subjects aged between 20 and 50 yrs with single star (*) considered as positive.
4. The group consisting of subjects aged above 50 yrs with single star (*) considered as positive.

Table 4.3: Rules followed for MRI report interpretations

Factors	Fact	Conditions		
		Minimal / mild	Significant / Severe	Remarkable
Abutting disc				
Annular tear				
Disk bulge	Cord compression			
Disk extrusion	Cord indentation			
Disk herniation	Neural foraminal narrowing			
Disk height reduction	Nerve Root Impingement Thecal sac effacement	*	**	***
Facet hypertrophy				
Flavum hypertrophy	Thecal sac indentation			
Foraminal disk herniation				
Foraminal Osteophytosis				
Osteophytosis				
Right eccentricity				

From the above analysis the prediction capability of DFL were analysed in terms of Correctly predicted percentage, Wrongly predicted percentage, Sensitivity and Specificity. The results obtained from the above mentioned observation was summarized as Table 4.4 (Chowdhury et al., 2014).

Table 4.4: DFL as an indicator of CSN (Chowdhury et al., 2014)

Analysis	TP	TN	FP	FN	Correctly Predicted %	Wrongly Predicted %	Sensitivity %	Specificity %
1	18	11	29	4	47	53	82	28
2	45	2	2	13	76	24	78	50
3	29	2	2	11	70	30	73	50
4	16	0	0	2	89	11	89	***

The instances where the MRI reports indicated the deformity to be mild (indicated by single *) and was taken to indicate absence of neuropathy yielded results with a correct prediction score of only 47%. This was low as there was a high false positive score of 29 against true positive of 18 and true negative of 11. On the other hand the correct prediction score was significantly improved when the same MRI findings with mild compression were taken to indicate abnormality, raising the correct prediction score to 76%.

For the study of the two age groups, the lower age group (20-50yrs) gives the scores of correct prediction and sensitivity as 70% and 73% respectively while that for the older age group (50-70 yrs) were both 89%. The slightly low value for the lower age group was due to a rather large false negative score (11 out of 44) which reveals some limitations of the DFL technique. A close observation indicates that for most of these false negative cases the subject had compressions at multiple vertebral levels. If these compressions lead to a similar degree of delay shift of DFL through each of the nerve branches, the combined DFL would not show broad peak or double peak, thus leading to an erroneous conclusion. Therefore, this aspect of DFL needs to be looked into for future improvement. Even then the sensitivity score of 73% is good for a new, simple and low cost diagnostic method. For the elderly, the prediction rate and sensitivity are both high, both being 89%. Therefore, the efficacy of this technique for a screening test of elderly looks promising. The specificity for the younger age group was 50%, while it could not be obtained at all for the higher age group. This was because of the low incidence of actually negative cases. In the lower age group the true negative and false positives were both 2 while these were both zero for the higher age group.

The study carried out by Chowdhury (Chowdhury, 2013) showed that there is a very good relation between DFL and MRI findings with reasonably high sensitivity and moderate specificity. So it is very promising to use DFL as a screening tool for the detection of subclinical CRM.

4.5. Generalization of Hypothesis

In the nerve conduction clinic of Dhaka University, sometimes double peaks of DFL were observed in patients receiving stab injuries in the neighborhood of a nerve trunk in the arms. Although no rigorous scientific study has yet been taken up on such externally induced neuropathy, it was felt that the above hypothesis may be applied to

such cases as well. In such cases, the degeneration of nerve fibres may be anticipated in a part of the nerve trunk, while the rest remaining intact. Thus the affected or degenerated part of the nerve trunk will contribute to a delay shifted DFL compared to the unaffected part, and when combined, will give rise to a double peak (Rabbani, 2011b). Similarly, if a tumour in the spinal canal presses onto the spinal cord, a similar degeneration of peripheral nerve fibres will result contributing to a DFL with double peaks.

All the above point to the fact that if a part of the whole nerve trunk is affected, whatever be the cause, resulting in a reduction of their conduction velocity, double peaks of DFL are likely to be observed. This is schematically represented in Figure 4.11. Thus DFL can be an effective screening tool for neuropathy. Of course, absence of double peaks does not exclude all neuropathy, such as CTS, but presence of double peak definitely is an indicator of neuropathy.

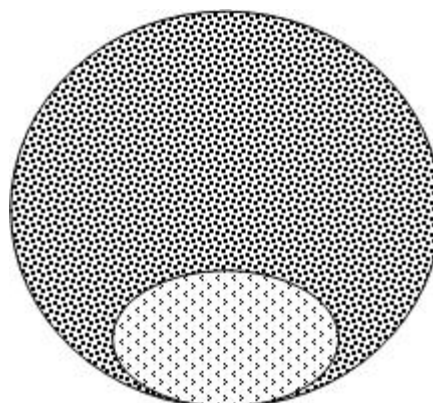


Figure 4.11: Schematic of segmental degeneration of fibres in a nerve trunk, hypothesised to cause double peak of DFL (Rabbani, 2011b).

Chapter 5: Statistics related to DCV and DFL

Statistical techniques and the scientific methods are inextricably connected. An experimental design cannot be complete without some thought being given to the statistical techniques that are going to be used. All experimental results have uncertainty attached to them.

In statistics a variable is some property with respect to which individuals, objects, medical images or scans, etc differ in some ascertainable way. A random variable has uncertainty associated with it. Nominal variables like pain or exertion are qualitative. Ordinal variables are some form of ranking or ordering. Nominal variables are often coded for in ordinal form. For example, patients with peripheral vascular disease of the lower limb might be asked to grade the level of pain they experience when walking on a treadmill on a scale from 1 to 4. In measurement, discrete variables have fixed numerical values with no intermediates. The heartbeat, a photon or an action potential would be examples of discrete variables. Continuous variables have no missing intermediate values. A chart recorder or oscilloscope gives a continuous display. In many circumstances the measurement device displays a discrete (digital) value of a continuous (analogue) variable.

5.1. Frequency distributions and its characterization

In many cases the clinical scientist is faced with a vast array of numerical data which at first sight appears to be incomprehensible. For example, a large number of values of blood glucose concentration obtained from a biosensor during diabetic monitoring. Some semblance of order can be extracted from the numerical chaos by constructing a frequency distribution. The difference between the smallest and largest values of the data set (the range) is divided into a number (usually determined by the size of the data set) of discrete intervals and the number of data points that fall in a particular interval is recorded as a frequency (number in interval/total number). Figure 5.1 gives an example of a frequency distribution obtained from 400 blood glucose samples. A normal level of blood glucose is 5 mmol/l, so the values shown are above the normal range.

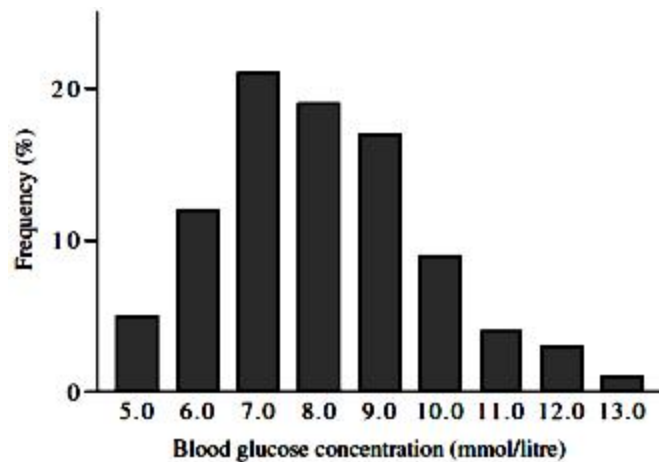


Figure 5.1: Frequency distribution obtained from 400 blood glucose samples

The data can always be summarized in terms of four parameters:

- A measure of central tendency.
- A measure of dispersion.
- A measure of skewness.
- A measure of kurtosis.

Central tendency says something about the ‘average value’ or ‘representative value’ of the data set, dispersion indicates the ‘spread’ of the data about the ‘average’, skew gives an indication of the symmetry of the data pattern, while kurtosis describes the convexity or ‘peakedness’ of the distribution.

There are four recognized measures of central tendency:

- Arithmetic mean.
- Geometric mean.
- Median.
- Mode.

The *arithmetic mean* uses all the data and is the ‘average’ value. Geometric mean is the ‘average’ value of transformed variables, usually a logarithmic transformation that is used for asymmetrical distributions. The *median* is a single data point, the ‘middle’ piece of data after it has been ranked in ascending order. The *mode* is the mid-point of the interval in which the highest frequency occurs.

5.2. Random sampling and Probability distributions

There are two types of probability: subjective and objective probability. The former is derived from past experiences and used it to make decisions such as when to cross the road or overtake when driving a car. The latter is based on the frequency concept of probability and can be constructed from studying idealized models. One of the favourites used by statisticians is the unbiased coin. There are two possible outcomes: a head or a tail. Each time the coin is thrown the chance or probability of throwing a head (or a tail) is $1/2$.

5.2.1. Random sampling

In a random sequence the result obtained from one trial has no influence on the results of subsequent trials. If you toss a coin and it comes down heads that result does not influence what you will get the next time you toss the coin. In the same way the numbers drawn in the national lottery one week have no bearing on the numbers that will turn up the following week! In a stochastic sequence, derived from the Greek word *stochos* meaning target, the events appear to be random but there is a deterministic outcome. Brownian motion of molecules in diffusion is an example of a 'stochastic sequence'.

In an experiment or trial the total number of possible outcomes is called the sample space. For example, if a single coin is thrown four times in succession, at each throw two possibilities only (a head or a tail) can occur. Therefore with four consecutive throws, each with two possible outcomes, the totality of outcomes in the trial is $2^4 = 16$. HHHT would be one possible outcome, TTHT would be another. To make sure for understanding it is worth writing out all 16 possibilities. If the total number of outcomes is 16 then the probability of each possibility is $1/16$. Therefore for the random sequence the sum of the probabilities of all possible outcomes in the sample space is unity (1). An important general rule: probabilities can never be greater than 1 and one of the possible outcomes must occur each time the experiment is performed. The outcome of a (random) trial is called an event. For example, in the coin tossing trial four consecutive heads, HHHH, could be called event A. Then we would use the notation probability of event A occurring, $P(A) = 1/16 = 0.0625$.

5.2.2. Gaussian distribution

A continuous random variable, x , can take an infinite number of values with infinitesimally small probability. However, the probability that x lies in some specified interval, for example the probability that $34 < x < 45$, is usually required. This probability, remembering that probability can never be greater than 1, is related directly to the area under the distribution curve. Because an arithmetic mean and a standard deviation can take an infinite number of values and any Gaussian curve can be summarized by these two parameters, there must be an infinite number of possible Gaussian distributions. To overcome this problem all Gaussian distributions are standardized with respect to an arithmetic mean of 0 and a standard deviation of 1 and converted into a single distribution, the standard Gaussian distribution. The transformation to a standard normal random variable is $z^* = (x - \text{mean})/\text{SD}$. With this formulation all those values of z^* that are greater than 1.96 (approximately 2 SD above the mean of zero for the standardized distribution) are associated with a probability—the area under the distribution—that is less than 0.025 or in percentage terms less than 2.5% of the total area under the curve. Similarly, because the mean is at zero, all those values of z that are less than -1.96 (approximately 2 SD below the

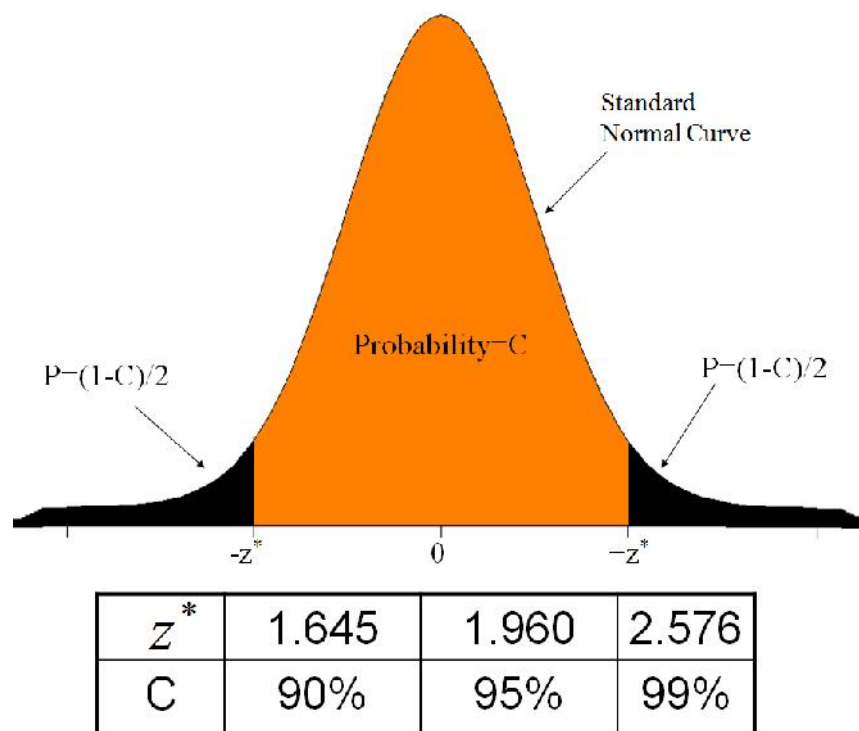


Figure 5.2: Confidence Interval for a Population Mean

mean of zero) are also associated with a probability of less than 0.025 or 2.5%. This means that any value of a random variable, x , assuming it has a Gaussian distribution, that transforms into a value of $z^* > 1.96$ or $z^* < -1.96$ for the standard distribution, has a probability of occurring which is less than 0.05. If z^* is known then the value of x that corresponds to this value of z^* can be obtained by a back transformation $x = (z^* \text{SD}) + \text{mean}$. Figure 5.2 shows the probability that the interval will capture the true parameter value in repeated samples of a distribution under the curve is 95%.

5.3. Performance of diagnostic test

To make out the relation between binary diagnosis test and the presence or absence of disease, a 2 by 2 contingency table construction is the primary prerequisite as follows:

Test	Gold standard test		Total
	Disease Positive	Disease Negative	
Positive	a (True positive) (TP)	b (False positive) (FP)	a + b
Negative	c (False negative) (FN)	d (True negative) (TN)	c + d
Total	a + c	b + d	N (a + b + c + d)

Common test used to assess performance are given as follows:

Sensitivity (SEN)

$$\frac{a}{a + c} \times 100 \quad \text{or} \quad \frac{TP}{TP + FN} \times 100$$

Remarks:

- i. Proportion of disease positive who are true positive.
- ii. Ability of a test to correctly diagnose the disease.
- iii. If SEN increases, FN decreases, so it is useful to exclude a diagnosis.
- iv. A sensitive test rarely miss the individual with disease.
- v. 100% sensitive test means all disease positive are true positive. So no chance of FN.

Specificity (SPE)

$$\frac{d}{b + d} \times 100 \quad \text{or} \quad \frac{TN}{FP + TN} \times 100$$

Remarks:

- i. Proportion of disease negative who are true negative.
- ii. Ability of a test to correctly identify the individual without disease.
- iii. If SPE increases FP decreases, so it is useful to confirm the diagnosis.
- iv. A specific test rarely misclassify an individual without disease as having the disease.
- v. 100% specific test means all disease negative are true negative. So no chance of FP.

Positive predictive value (PPV)

$$\frac{a}{a + b} \times 100 \quad \text{or} \quad \frac{TP}{TP + FP} \times 100$$

Remarks:

- i. Proportion of test positives that are truly disease positive.
- ii. If PPV increases FP decreases.
- iii. Probability of having disease when a person is test positive.

Negative predictive value (NPV)

$$\frac{c}{c + d} \times 100 \quad \text{or} \quad \frac{TN}{TN + FN} \times 100$$

Remarks:

- i. Proportion of test negatives that are truly disease negative.
- ii. If NPV increases FN decreases.
- iii. Probability of not having disease when a person is test negative.

Accuracy of efficacy

$$\frac{a + d}{N} \times 100 \quad \text{or} \quad \frac{TP + FN}{\text{Total population}} \times 100$$

Remarks:

- i. Proportion of all test results (positive and negative) that are correct.
- ii. Probability of correct diagnosis detected by the test.

Positive likelihood ratio (LR⁺)

$$\frac{\text{Probability of positive test result in a person with the disease}}{\text{Probability of positive test result in a person without the disease}}$$

$$= \frac{a/(a+c)}{b/(b+d)} = \frac{SEN}{1-SPE} = \frac{TP_{rate}}{FP_{rate}}$$

Remarks:

- i. Odds of positive test result in person with disease over that in person without disease.
- ii. LR⁺ = 1: test has no diagnosis value.
- iii. LR⁺ > 1: test has diagnosis value.
- iv. LR⁺ ≥ 10.0: test has high diagnosis value.

Negative likelihood ratio (LR⁻)

$$\frac{\text{Probability of negative test result in a person with the disease}}{\text{Probability of negative test result in a person without the disease}}$$

$$= \frac{c/(a+c)}{d/(b+d)} = \frac{1-SEN}{SPE} = \frac{FN_{rate}}{TN_{rate}}$$

Remarks:

- i. Odds of negative test result in person with disease over that in person without disease.
- ii. LR⁻ = 1: test has no diagnosis value.
- iii. LR⁻ < 1: test has diagnosis value.
- iv. LR⁻ ≤ 0.10: test has high diagnosis value.

Sensitivity and Specificity

It is obviously desirable to have a test with both SEN and SPE as close to 100% as possible. Unfortunately it is usually not possible; instead there is a trade off business between SEN and SPE of a diagnostic test. If one increases it is always at the cost of other. So if a test is highly sensitive, it will be less specific whether we aim for highly sensitive or highly specific test, depends on:

- i. The disease to be diagnosed.
- ii. Implication of FP and FN test result on patients.

Highly sensitive test is used in following situations:

- i. Easily treatable condition, here we need to decrease FN.
- ii. If penalty is high for missing a disease (serious but treatable disease), here we need to decrease FN.
- iii. To rule out a disease.
- iv. For screening followed by detailed investigation.

A highly sensitive test is most helpful when the test result is negative.

Highly specific test is used in following situations:

- i. Disease to be treated by major surgery, here we need to decrease FP.
- ii. To confirm the disease.
- iii. Serious but untreatable disease, here we need to decrease FP because it will bring on patient psychological steer.

A highly specific test is most helpful when the test result is positive.

5.4. ROC (Receiver Operator Characteristic) Curve

For diagnostic test based on continuous scale of measurement different cut off levels will result in different levels of SEN and SPE. Generally as the cutoff point decreases, SEN increases with corresponding decrease in SPE.

Constructions of ROC curve (a plot of SEN to 1 – SPE)

The value on the axis run from a probability of 0 to 1 (or 0 to 100%).

The dashed line represents a reference of a test with no diagnostic value. It corresponds to a test that is positive or negative just out of by chance; as if clinician merely flipped a coin and got it. At every point along this diagonal line the $SEN = 1 - SPE$ and $LR^+ = 1$. So a positive test result is equally likely for person with and without the disease. So a clinically useful diagnostic test will have a ROC curve far from this dashed diagonal line (to the left of diagonal line). Upper left corner is the best where $TP_{rate} = 1$ and $FP_{rate} = 0$ [$SEN = 100\%$, $SPE = 100\%$]. So ROC curve will go across the top of the grid area with AUROC (area under ROC curve) = 1. Towards the left hand side of curve there is a steep rise in SEN with a modest increase in 1 – PE (or modest decrease in SPE) which shows very favourable trade off.

PRESENT WORK

The present work will try to improve the efficacy of DFL in the diagnosis of Cervical spondylotic Radiculopathy and Myelopathy (CRM) by focusing on four major points which are presented in the next four chapters.

Chapter 6: Distribution of Conduction velocity from Measured F-wave latency and matching with standard DFL

6.1. Introduction

A peripheral nerve trunk has thousands of nerve fibres with different conduction velocities and their properties are adequately described through a statistical frequency distribution known as the Distribution of Conduction Velocity (DCV). For a proper assessment of neural health and diagnosis of neuropathy the DCV would have been an ideal parameter if it could be measured clinically. However, no established technique exists for the determination of DCV in a clinical setting. Our extended group at Dhaka University conceived and developed a simple method to obtain an approximate and relative DCV of motor nerve fibres in a peripheral nerve trunk as a mirror image of a new parameter, which was named by the group as Distribution of F-Latency (DFL).

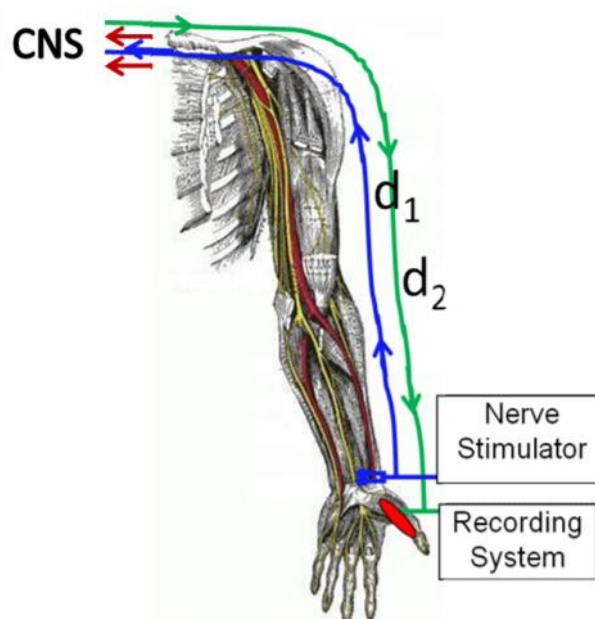


Figure 6.1: Stimulated signal travel through the median nerve

F-latency is a standard parameter widely measured in an EMG clinic as a late evoked EMG potential obtained through artificial stimulation of a peripheral nerve (Magladery and McDougal, 1950). For the median nerve, electrical stimulation is given at the wrist while the evoked potential from the Thenar muscle (APB muscle) at the base of the thumb is recorded using appropriate electrodes and instrumentation (Figure 6.1). The orthodromic (direction of the natural signal propagation) action

potentials along all the motor fibres contribute to a large compound muscle action potential from the APB muscle and is called the M-wave. The antidromic (opposite to the direction of the natural signal propagation) action potentials travel to the respective cell bodies at the vertebral roots (anterior horn cell) where nothing happens in most of the motor neurons. However a few percent of the cell bodies of these motor neurons backfire with an estimated delay of about 1 ms (Kimura, 1989) and then travels back to APB muscle causing a much smaller and delayed F-wave. Since the recruitment of motor neurons that contribute to the F-wave is random, different F-responses will have contributions from different motor nerve fibres with different conduction velocities. Therefore, the latencies, sizes and shapes of F-responses will vary from event to event (for multiple stimulations) for the same nerve of the same subject. Based on the above observations our extended group had proposed that a statistical frequency distribution DFL of the F-latencies is basically a reflection of the DCV of the motor nerve fibres that contribute to overall F-responses and they had established this through experiments on human subjects (Rabbani et al., 2007).

DFL involves obtaining multiple F-responses with a time interval of about 1 sec between stimulations and then making a statistical frequency distribution of the F-latency values thus obtained. This long time delay was chosen so that the physical mechanisms involved due to stimulation relax back their normal situations before the next stimulation. This would ensure that the physical mechanisms for each stimulation are independent of the previous event, or in other words, the events are random.

Furthermore, patterns of DFL have been related by our extended group to conditions of cervical radiculopathy (compression of the nerve roots) and myelopathy (compression of spinal cord), which we would refer to as Cervical spondylotic Radiculopathy and Myelopathy (CRM) in this work (Alam and Rabbani, 2010). Further work on this aspect has established the hypothesis on a stronger footing and has established DFL as a viable method for detection of CRM (Chowdhury, 2013, Chowdhury et al., 2014, Hossain et al., 2011, Rabbani, 2011b, Rabbani, 2011a, Rabbani et al., 2014). DFL with a single sharp peak has been related to normalcy while a broad peak, double peak or a triple peak was related to CRM. The broad peak has again been defined as the one where the frequency value at a bin adjacent to the peak is equal or greater than one third of the peak value (Rabbani et al., 2014).

Therefore, the pattern is very subtle, particularly for such a broad peak, which is very close in pattern to a single peak.

Since a considerable experience has been established in relating DFL patterns to CRM, it was thought that if DCVs have similar patterns then this experience can be used in the detection of CRM employing the method of obtaining DCV being proposed in the present work. In other words, we would like to see similar patterns, although inverted as a mirror image, for DFL and DCV. However, because of the inverse relationship between latency and velocity, this mirror image is not exact, a small variation is expected, particularly when discrete bin widths and not too large sample sizes are employed to obtain the frequency distribution.

To obtain DFL, 30 to 40 consecutive F-latencies are usually obtained through multiple stimulation of a peripheral nerve trunk with adequate intervals between stimulations, typically about 1 sec, as mentioned before.

In an earlier study Chowdhury (Chowdhury et al., 2014) applied about 40 supramaximal electrical stimulations to the median nerve at the wrist in sequence, with intervals of one second between each to obtain about 30 or more F-responses from the corresponding thenar muscle of 31 subjects, from both sides. An excess number of stimulations was given to each nerve since not all stimulations give rise to F-responses. These data were obtained using nerve conduction equipment made by our extended group which has been in use in a clinic over many years. The muscle was kept relaxed during the experiment. The actual number of stimulations given varied somewhat depending on the cooperation of the subject. The time sequence of the collected F-latencies from each nerve was maintained and recorded. The measurements were carried out at room temperature, which remained steady at or around 30°C. In the present work it is intended to obtain DCV from individual conduction velocity (CV) values that are obtained through converting the corresponding F-latencies. Data obtained experimentally by Chowdhury et al 2014 were used for the purpose. Then choosing an appropriate bin width, a frequency distribution of CV will be obtained which should be the desired DCV. Most of the DFLs obtained in our laboratory earlier used a bin width of 2 ms and a large experience has been built up on the analysis of its pattern for the detection of CRM as mentioned before (Chowdhury et al., 2014, Rabbani et al., 2007, Rabbani et al., 2014). Therefore, we could use that experience if a corresponding bin width for DCV

is chosen when analyzing individual CV values to obtain DCV, in order to obtain a similar, but mirror image pattern.

However, as mentioned before, the relationship between CV and Latency is non-linear; therefore, to correspond to a fixed bin width of DFL, the bin width for CV cannot be kept constant over the whole range. This will make the analysis difficult and we would like to have a fixed bin width for DCV as well. Therefore, the aim of the present work is to determine an optimized bin width for obtaining DCV from individual CV values while keeping the pattern of the DCV as close as to the mirror image of DFL, to aid the detection of CRM.

6.2. Methodology

As mentioned before, the present work used the data collected earlier by our extended group (Chowdhury, 2013, Chowdhury et al., 2014). However, the nerve lengths of the subjects were not measured during that study. Out of the 31 subjects used in that study, only 10 were available during the present work whose nerve length could be measured. Besides, out of the 20 median nerves of the 10 subjects, F-latency data were available for 18 nerves only, which was used in the present analysis. The data on the 18 median nerves came from 10 subjects, 1 female and 9 male, aged between 24 and 56 yrs with a mean of 33.25 yrs (± 12.26 yrs). The lengths of the nerve pathway from the stimulation site at wrist to the vertebral roots and then back to the relevant muscle at the base of the thumb were measured for all the subjects. Of course, some uncertainty would be involved as the nerve pathway is not accessible directly from outside, some estimation had to be incorporated.

To analyse the latency and the conduction velocity involved in an F-wave let us consider a supramaximal stimulation applied to the median nerve at the wrist (Figure 6.2). The orthodromic (direction of the natural signal propagation) action potentials along all the motor fibres contribute to a large compound muscle action potential, generated from the APB muscle at the base of the thumb, called the M-wave. The antidromic (opposite to the direction of the natural signal propagation) action potentials travel to the respective cell bodies at the vertebral roots (anterior horn cell) where nothing happens in most of the neurons. However a few percent of the motor neurons backfire with an estimated delay of about 1 ms (Kimura, 1989) and then travels back to APB muscle causing the much smaller and delayed F-wave.

We usually measure the latencies to the onset of the M-wave or the F-wave, and let these be represented by t_M and t_F . Therefore, the time of travel (t) from the wrist to the cell body in the spinal cord will be given by,

$$t = (t_F - t_M - 1)/2 \quad \dots (1)$$

The division by 2 appears since the F-wave action potential travels the corresponding distance twice.

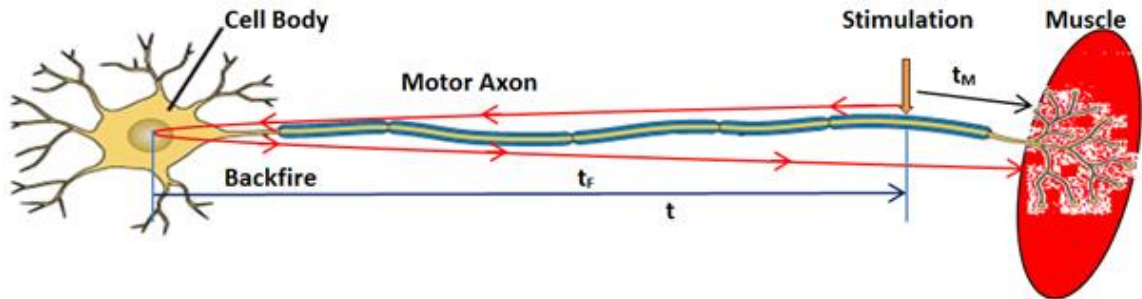


Figure 6.2: Schematic picture of nerve conduction due to artificial stimulation at a midpoint to illustrate latencies for M-wave and F-wave

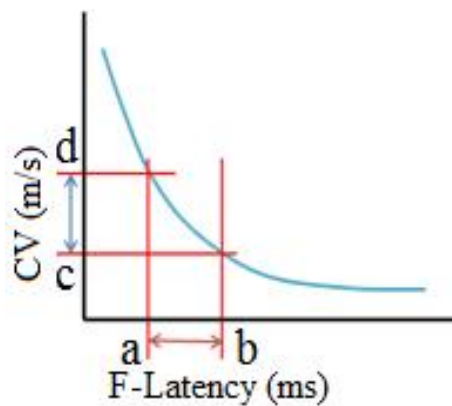


Figure 6.3: Non-linear curve of CV against F-latency illustrates problem with bin-width

If this distance is d then the Conduction velocity CV of the fastest fibre in the particular F-wave is given by,

$$CV = \frac{d}{t} \quad \dots (2)$$

This was given the name FWCV by Kimura (Kimura, 1989).

A relative DCV of such motor nerve fibres may be obtained by grouping them into a number of suitable bins in terms of velocity. However, as mentioned above, we would like to optimize this choice of the bin width so that the pattern of DFL has close resemblance to the mirror image pattern of DFL, typically obtained using a bin width of 2 ms. Since latency is inversely proportional to CV, if bin widths for DCV are

chosen to correspond to the constant F-latency bin over the whole range, varied bin widths for DCV will result, which is not a desired situation. This is illustrated in Figure 6.3. Suppose ab represents the bin width (shown exaggerated) for DFL. The corresponding bin width for DCV would be cd . Now as the bin location for DFL is shifted right or left keeping the range ab constant, the corresponding bin width for DCV will change.

However, when obtaining DCV from individual CV values, it is expected to use a fixed bin width. Therefore, in the present work we were looking for an optimized fixed bin width for DCV which would give a reasonable correspondence between the patterns of DFL and DCV for the same raw data of F-latencies. To elaborate this point, we wanted to fix the location of the bin group on the F-latency axis so that the corresponding bin width for DCV gives a reasonable pattern correspondence. With this aim four statistical parameters of the F-latency data were tried to identify the location of the bin group for DFL corresponding to which the bin width for DCV will be chosen. These are, for the range of non-zero values of F-latency, i) average of the minimum and maximum, ii) median, iii) mode and iv) weighted average. For the weighted average, the number of times a given F-latency repeated was considered for the average appropriately.

The corresponding bin widths for DCV using the above four parameters were obtained as follows. For the first parameter, we took the average of the maximum and minimum values of measured F-Latencies, which we denote by X . Similarly we took the average of the corresponding maximum and minimum CV values and denote this by Y . The desired bin width (W_V) for DCV to correspond to a bin width W_L of DFL (which is 2 ms for our study) is obtained using the formula,

$$W_V = \frac{Y}{X} \times W_L \quad \dots (3)$$

In a similar way replacing X and Y with the corresponding median, mode and weighted average values, we obtained the corresponding bin widths for DCV using the other three parameters.

Following the above methods we chose individual bin widths to generate DCVs for each of the 18 nerves based on the above four parameters and then tried to match the DFL and DCV curves visually. As indicated before, these curves are expected to be

approximate mirror images of each other, and we looked for pattern matching in view of the above.

Then we tried to compare the performances of the four chosen parameters. For this we studied each DCV pattern and the corresponding DFL pattern. If the DCV pattern appeared to be a good match of the mirror image pattern of the respective DFL we tagged it with a 'Y' for 'yes'. The ones that did not match were tagged 'N' for 'no'. The results were compiled in a table and the total numbers of correct matches ('Y') were counted corresponding to each of the four parameters. This value was used as a numerical figure to describe the quality of match for a particular method of obtaining the bin width for DCV. The parameter giving the maximum match was chosen as the one to use for obtaining bin width.

Finally, the mean of the chosen bin widths of the 18 nerves tested was obtained to give a reasonable value of bin width for DCV, expecting that this would give the best match for all other subjects too.

6.3. Results

Table 6.1 shows the individual bin widths calculated for DCV based on the four parameters described before for all the 18 nerves under study, with a fixed 2 ms bin width for DFL. It also shows the number of F-responses obtained from the particular nerve and an estimation of the nerve length. Table 6.4 shows representative DFLs and corresponding DCVs using bin widths calculated based on the four parameters respectively. The results of the visual matching of the DCV patterns with the corresponding DFL patterns are given in Table 6.2 (Y for a match, N for a non-match). The number of good matches for each of the four parameters was summed and the results are shown in Table 6.3. It can be seen that the median based bin width gave the best match, at 89% (16 out of 18 nerves).

Finally, the mean of the bin widths for the parameter 'median' to give the best match to DFLs with 2ms bin width was found to be 4.7 m/s (standard deviation: 0.5 m/s).

Table 6.1: Bin widths for DCV to correspond to a bin width of 2ms for DFL

Nerve ID	No of F-responses	Nerve Length (cm)	DCV Bin width, in m/s			
			$\frac{(\text{Max} - \text{Min})}{2}$	Median	Mode	Average
ABERRMF	30	156	5.41	5.47	4.51	5.40
BEGKMLMF	32	140	4.32	4.34	4.34	4.25
BEGKMRMF	28	142	3.84	4.25	4.35	3.93
HUSKLMF	35	168	4.06	4.11	4.17	4.07
HUSKRMF	22	170	4.68	4.63	4.63	4.60
KHAILMF	25	146	4.54	4.39	4.83	4.50
KHAIRMF	15	146	4.14	4.17	4.17	4.19
MAHALMF	35	144	5.35	5.24	5.24	5.31
MAHARMF	34	140	4.90	4.78	4.78	4.89
RAHOLMF	26	156	5.02	5.03	4.91	5.10
RAHORMF	27	156	4.73	4.91	4.91	4.88
SARTALMF	27	150	3.88	3.69	3.69	3.81
SARTARMF	18	148	3.78	4.16	4.28	4.02
YOUALMF	20	150	4.31	4.65	4.65	4.54
YOUARMF	32	156	4.71	5.02	4.94	5.06
ZAMMLMF	38	150	5.53	5.56	6.07	5.56
ZAMMRMF	31	144	4.98	4.82	4.82	5.06
ZIHMRMF	36	150	4.88	5.08	5.21	5.03

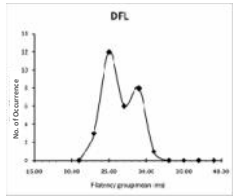
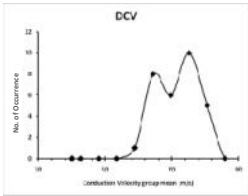
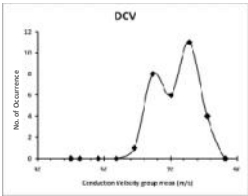
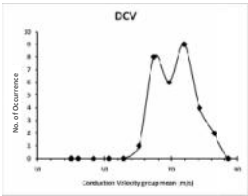
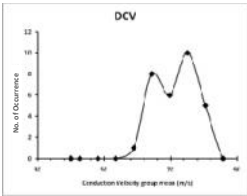
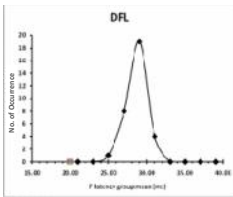
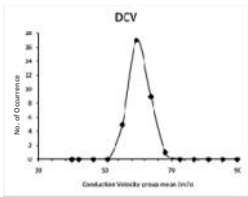
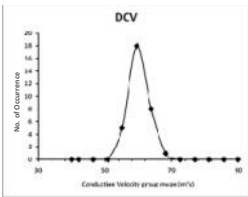
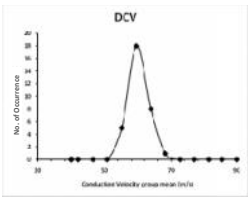
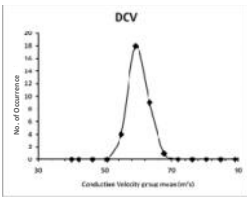
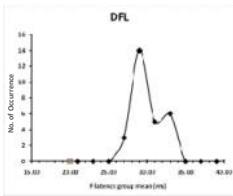
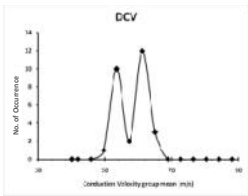
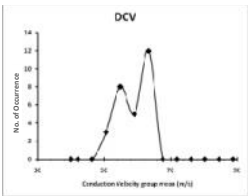
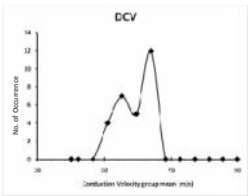
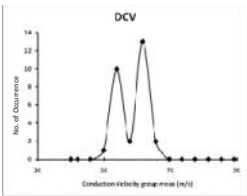
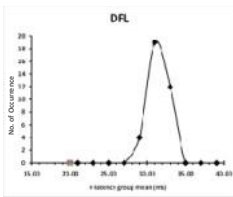
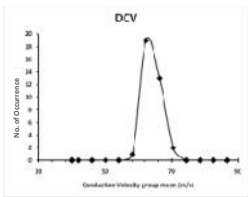
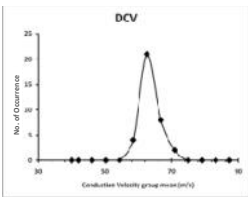
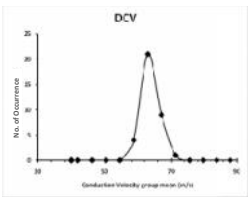
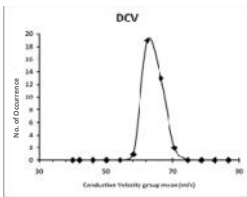
Table 6.2: Agreement of DCV patterns with corresponding mirror image of DFL patter, visual assessment (Y for a match, N for a non-match)

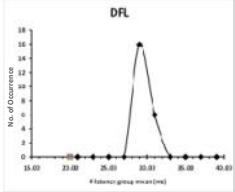
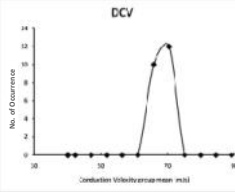
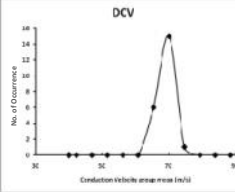
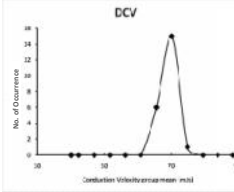
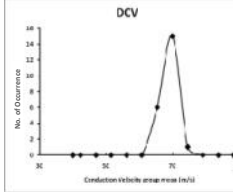
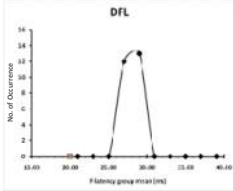
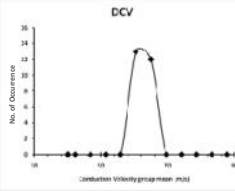
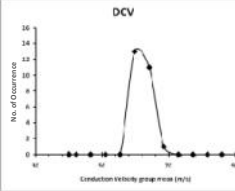
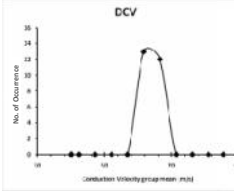
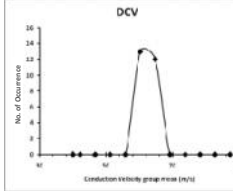
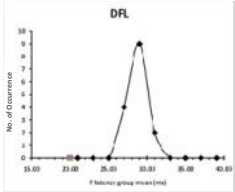
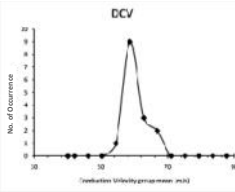
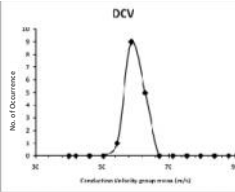
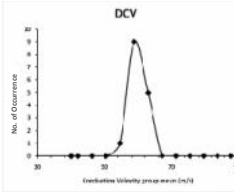
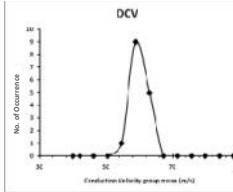
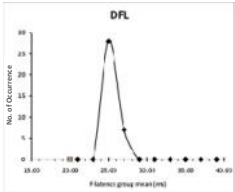
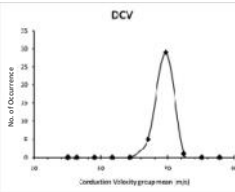
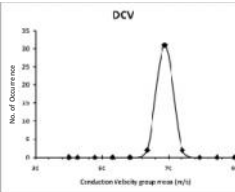
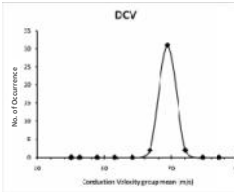
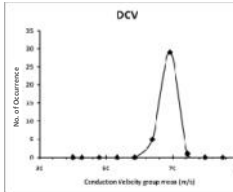
Nerve ID	DCV pattern matched with DFL pattern			
	$\frac{Min+Max}{2}$	Median	Mode	Average
ABERRMF	Y	Y	Y	Y
BEGKMLMF	Y	Y	Y	Y
BEGKMRMF	N	Y	Y	N
HUSKLMF	Y	Y	Y	Y
HUSKRMF	N	Y	Y	Y
KHAILMF	Y	Y	Y	Y
KHAIRMF	N	Y	Y	Y
MAHALMF	Y	N	N	Y
MAHARMF	Y	Y	Y	Y
RAHOLMF	N	N	N	N
RAHORMF	N	Y	Y	Y
SARTALMF	Y	Y	Y	N
SARTARMF	N	Y	Y	N
YOUALMF	N	Y	Y	N
YOUARMF	N	Y	Y	Y
ZAMMLMF	Y	Y	N	Y
ZAMMRMF	N	Y	Y	N
ZIHMRMF	Y	Y	Y	Y

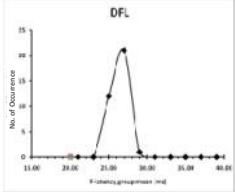
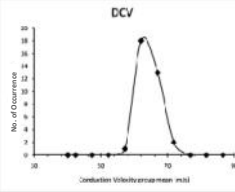
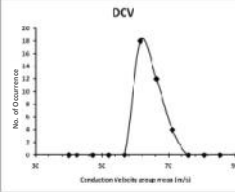
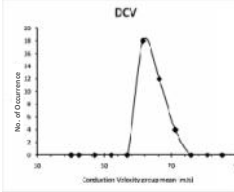
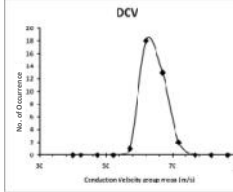
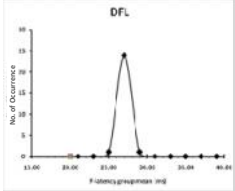
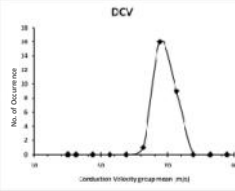
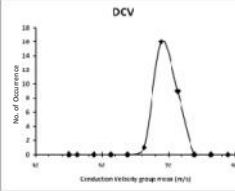
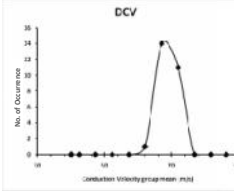
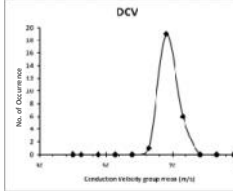
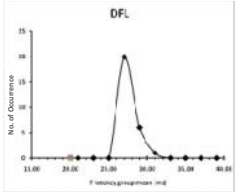
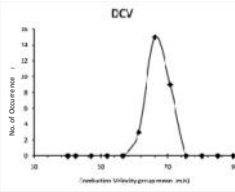
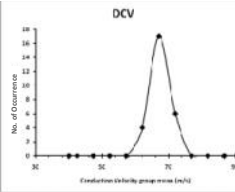
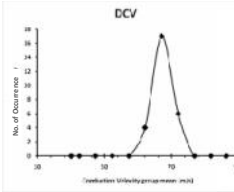
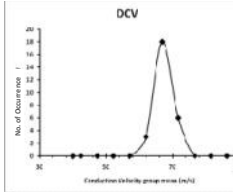
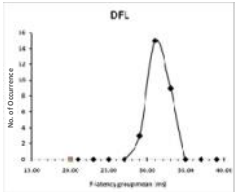
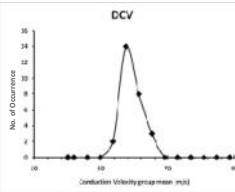
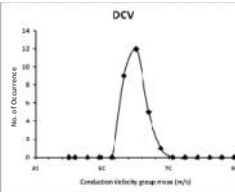
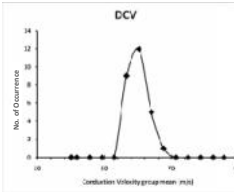
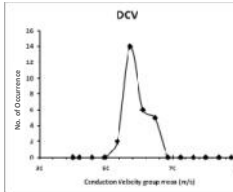
Table 6.3: Number of DCV pattern considered as a mirror of standard DFL pattern through visual assessment

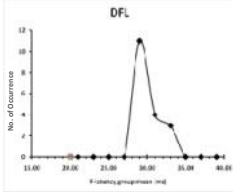
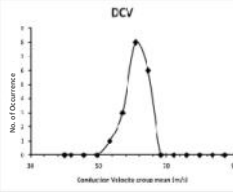
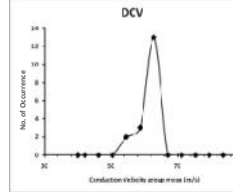
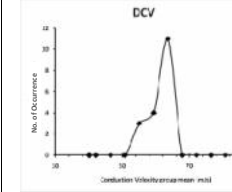
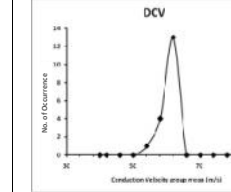
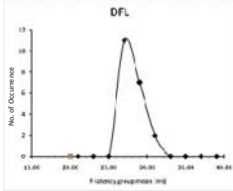
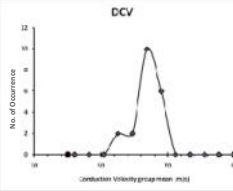
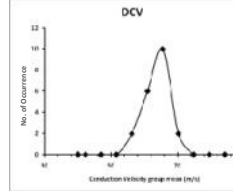
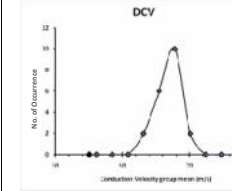
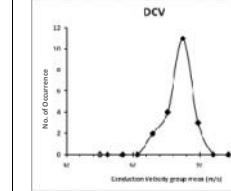
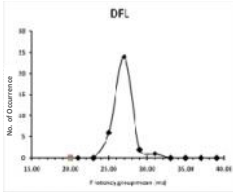
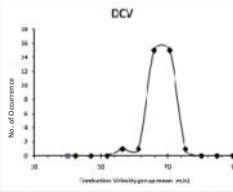
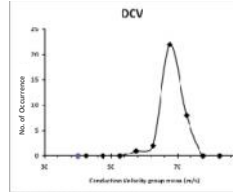
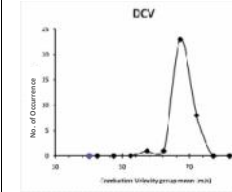
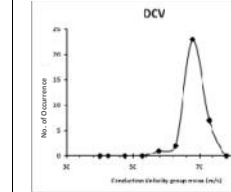
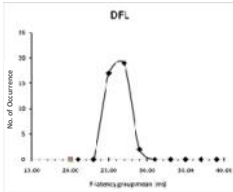
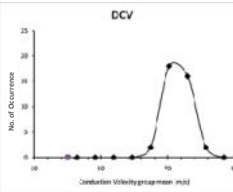
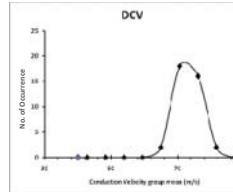
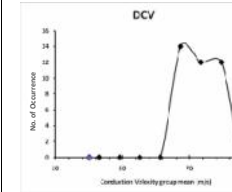
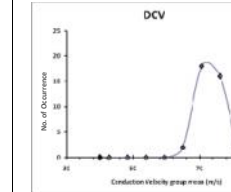
	$\frac{Min+Max}{2}$	Median	Mode	Average
Number of DFL Pattern	9	16	15	12
Percentage of total	50	89	83	67

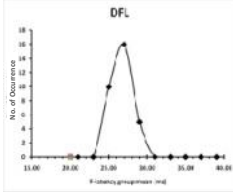
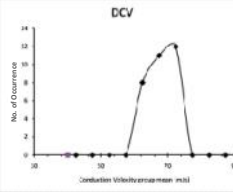
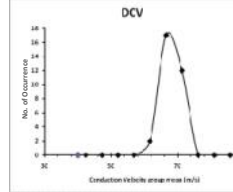
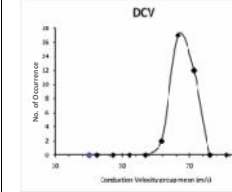
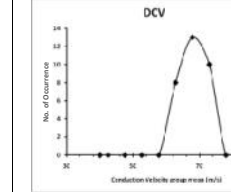
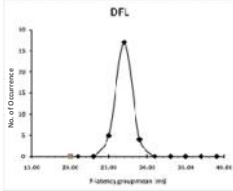
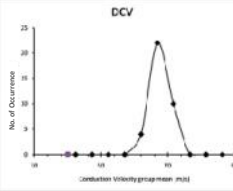
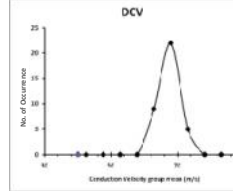
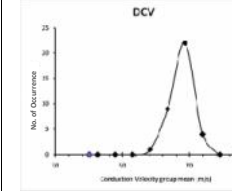
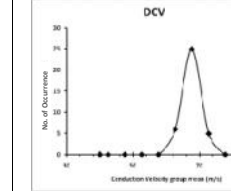
Table 6.4: Representative of DFL patterns and corresponding DCV patterns are obtained using four parameters to calculate bin width

Sl No.	Nerve ID	DFL Pattern	DCV Pattern			
			(Min+Max)/2	Median	Mode	Arithmetic Mean
1	ABERRMF					
2	BEGKMLMF					
3	BEGKRMRF					
4	HUSKLMF					

SI No.	Nerve ID	DFL Pattern	DCV Pattern			
			(Min+Max)/2	Median	Mode	Arithmetic Mean
5	HUSKRMF					
6	KHAILMF					
7	KHAIRMF					
8	MAHALMF					

SI No.	Nerve ID	DFL Pattern	DCV Pattern			
			(Min+Max)/2	Median	Mode	Arithmetic Mean
9	MAHARMF					
10	RAHOLMF					
11	RAHORMF					
12	SARTALMF					

SI No.	Nerve ID	DFL Pattern	DCV Pattern			
			(Min+Max)/2	Median	Mode	Arithmetic Mean
13	SARTARMF					
14	YOUALMF					
15	YOUARMF					
16	ZAMMLMF					

SI No.	Nerve ID	DFL Pattern	DCV Pattern			
			(Min+Max)/2	Median	Mode	Arithmetic Mean
17	ZAMRRMF	 <p>DFL graph for ZAMRRMF. The x-axis is Latency (group mean) (ms) from 13.00 to 43.00. The y-axis is No. of Occurrence from 0 to 18. The curve peaks at 25.00 ms with a frequency of approximately 17.</p>	 <p>DCV graph for ZAMRRMF (Min+Max)/2. The x-axis is Conduction Velocity (group mean) (m/s) from 30 to 90. The y-axis is No. of Occurrence from 0 to 14. The curve peaks at 70 m/s with a frequency of approximately 13.</p>	 <p>DCV graph for ZAMRRMF Median. The x-axis is Conduction Velocity (group mean) (m/s) from 30 to 90. The y-axis is No. of Occurrence from 0 to 16. The curve peaks at 70 m/s with a frequency of approximately 16.</p>	 <p>DCV graph for ZAMRRMF Mode. The x-axis is Conduction Velocity (group mean) (m/s) from 30 to 90. The y-axis is No. of Occurrence from 0 to 18. The curve peaks at 70 m/s with a frequency of approximately 17.</p>	 <p>DCV graph for ZAMRRMF Arithmetic Mean. The x-axis is Conduction Velocity (group mean) (m/s) from 30 to 90. The y-axis is No. of Occurrence from 0 to 14. The curve peaks at 70 m/s with a frequency of approximately 13.</p>
18	ZIHRRMF	 <p>DFL graph for ZIHRRMF. The x-axis is Latency (group mean) (ms) from 13.00 to 43.00. The y-axis is No. of Occurrence from 0 to 18. The curve peaks at 25.00 ms with a frequency of approximately 17.</p>	 <p>DCV graph for ZIHRRMF (Min+Max)/2. The x-axis is Conduction Velocity (group mean) (m/s) from 30 to 90. The y-axis is No. of Occurrence from 0 to 25. The curve peaks at 70 m/s with a frequency of approximately 22.</p>	 <p>DCV graph for ZIHRRMF Median. The x-axis is Conduction Velocity (group mean) (m/s) from 30 to 90. The y-axis is No. of Occurrence from 0 to 25. The curve peaks at 70 m/s with a frequency of approximately 22.</p>	 <p>DCV graph for ZIHRRMF Mode. The x-axis is Conduction Velocity (group mean) (m/s) from 30 to 90. The y-axis is No. of Occurrence from 0 to 25. The curve peaks at 70 m/s with a frequency of approximately 22.</p>	 <p>DCV graph for ZIHRRMF Arithmetic Mean. The x-axis is Conduction Velocity (group mean) (m/s) from 30 to 90. The y-axis is No. of Occurrence from 0 to 30. The curve peaks at 70 m/s with a frequency of approximately 25.</p>

6.4. Discussions

Investigation of nerve conduction are being carried out for quite a long time, but nothing more than the onset latency of evoked potentials have practical applications in quantitative evaluation till now. This diagnosis gives information only about the fastest group of nerve fibers while many diseases or disorders involve loss or slowing of conduction of the middle and slow nerve fibers which do not get detected in the existing methods. Therefore, the best diagnostic method would be one that gives a complete distribution of conduction velocity or DCV of a nerve trunk. The evoked potential waveshapes are expected to contain this information, but reproducible techniques are yet to be developed to extract the information, as desired.

As DFL owes its origin to DCV of motor nerve fibers as has been established through earlier work of our extended group, it was also suggested that an approximate relative DCV of motor nerves can be obtained directly as a mirror image of DFL. However, we wanted to obtain DCV directly from conduction velocity (CV) values obtained from each of the multiple F-responses used to obtain DFL. Since DFL have been used for quite some time in identifying Cervical spondylotic Radiculopathy or Myelopathy (CRM), a significant amount of experience has been accrued on the patterns of DFL. Therefore, our objective was to get a good match of the patterns of the mirror image of DFL and DCV. A challenge is the choice of a constant bin width for DCV as this choice can change the pattern of the distribution significantly if the total number of events (F-responses) are not too many. The objective of this chapter is to make a study that would help in choosing an appropriate bin width for obtaining the desired patterns of DCV using the above method.

Since our extended group has been using 2 ms bin width to obtain DFL from 30 to 40 F-responses we wanted to find the most appropriate bin width to correspond to the above choice when obtaining DCV from the F-wave conduction velocity values.

In Table 6.1 it was observed that to correspond to 2 ms bin width for DFL the bin width for conduction velocity varies somewhat for different subjects depending on what formulae we choose to obtain the bin width for DCV. The nerve length also played a role. Table 6.2 shows the quality of match between DFL and DCV for all the nerves tested. Table 6.3 shows the percentage of nerves for which a good match was obtained, using the four different bases for bin width calculation. It shows that out of

18 nerves, the best match was obtained for the median based bin width, at 89%. The next was for mode, at 83% while the other two based on averages are much less, at 50% and 67% respectively. This observation suggests that bin width calculation based on the median could be used to obtain an acceptable DCV pattern that would match with the corresponding DFL patterns.

Again, as a result of the present work we can say that the mean of the bin widths for the parameter 'median' to give the best match to DFLs with 2 ms bin width is 4.7 m/s. Therefore, this value can be used for obtaining DCVs for nerves of the upper limb (median and ulnar) from conduction velocity values obtained using multiple F-responses.

One of the major limitations of this study was the measurement of nerve length. The median nerve originates from the lateral and medial cords of the brachial plexus, and has contributions from ventral roots of C5, C6 & C7 (lateral cord) and C8 & T1 (medial cord) and passes through the carpal tunnel. The ones that are relevant for the present work were those derived from C7, C8 and T1 (Alam and Rabbani, 2010). It is impossible to measure the nerve length accurately; besides, those from the three roots will differ in length. Therefore, an approximate estimation was done with the help of anatomical reference points. However, an uncertainty of about 5 cm will lead to an error of about 3% since the total path length is of the order of 150 cm, which is negligible in this type of study.

It needs to be mentioned that a sample size of about 30 to 40 gives a representative distribution of a large population but these distributions will have a certain amount of uncertainty. The uncertainties are reduced if the sample sizes are made larger. In our case we cannot increase the sample size very much since it is uncomfortable and therefore unacceptable to patients. Therefore, we have to try to get the best from a sample size of 30 to 40 F-latencies.

The main aim of the present work was to obtain DCVs from multiple F-responses and to use their patterns in detecting CRM, which seems to work well, in comparison to the established patterns of DFL. Since both DFL and DCV are statistical techniques, some uncertainty will remain. Therefore, these methods are best to be used for screening of patients; those found positive will be required to go through further investigation. However, even the outcome of DFL or DCV may be improved through

the incorporation of some simple clinical tests carried out by Neurologists when the outcome of DFL or DCV will be very important.

Chapter 7: Study for Sample size and Bin Width for DFL (for detection of CRM)

7.1. Introduction

As mentioned before, the Biomedical Physics group of Dhaka University (our extended group) has conceptually related the occurrence of a particular F-latency to the percentage of fibres existing in a nerve trunk with the corresponding conduction velocity. For this they invoked probability statistics based on the physiology and physics of F-responses. Through these arguments they have conceptually related a frequency distribution of F-Latency, which they abbreviated as DFL, as an approximate mirror image of relative DCV of motor nerve fibres in a nerve trunk. This relationship allowed a simple experimental determination of DCV through DFL using conventional EMG/EP equipment, just measuring the F-latencies obtained through multiple stimulations at sufficient intervals (Rabbani, 2011a, Rabbani, 2012, Rabbani et al., 2007).

The above group has also shown that in Cervical Spondylotic Neuropathy involving both Radiculopathy (compression of nerve roots) and Myelopathy (compression of spinal cord), DFL has a broad peak, double or triple peaks, while for normal healthy subjects, DFL has a sharp single peak (Alam and Rabbani, 2010). They also showed that the distinction of a broad peak from a single peak is very subtle (Chowdhury, 2013, Rabbani et al., 2014). Therefore, getting a proper representative shape of DFL for a nerve trunk was very important in the diagnosis of Cervical spondylotic Radiculopathy and Myelopathy (CRM). Rabbani et al (Rabbani et al., 2014) had shown that for DFL using 2 ms bin width, if the frequency value of a point adjacent to the peak is greater or equal than one third the peak value then this can be considered as a broad peak representing an abnormality. Through this definition of a broad peak they were able to obtain a better predictive value for CRM against MRI findings.

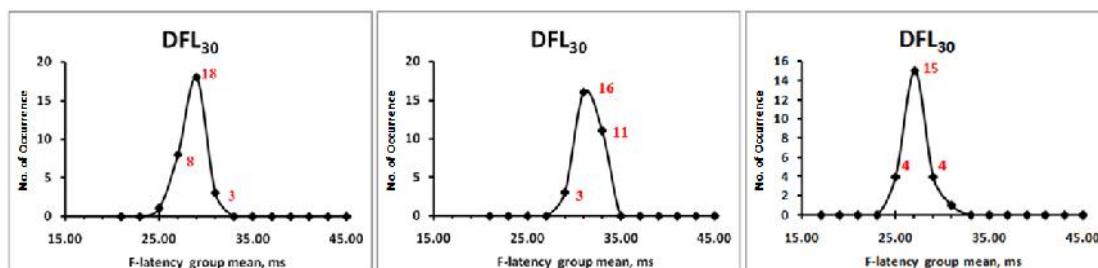


Figure 7.1: Broad peak observed in DFL pattern of three different nerves

Three DFL patterns with apparently single peaks but which are in fact broad peaks representing the presence of CRM are presented in figure 7.1. In the leftmost pattern it is observed that the peak value is 18 and the value of the nearest point to the left of the peak is 8, which is more than one third of 18. In this case we consider this as broad peak (Rabbani et al., 2014). Similarly in the middle DFL pattern the peak value is 16 and the value of the next point to the right is 11, which is also greater than one third of 16, and may be considered as a broad peak. In the rightmost DFL pattern the peak value is 15 and the next point to the left or right is 4 which is less than one third of 15. In this case the DFL pattern is considered as a single peak. The first two DFL patterns represent abnormality while the third represent normalcy in respect of CRM of the respective nerves.

It can be seen from the above three examples that the distinction between normal and abnormal patterns of DFL is very subtle, a little variation changes the interpretation. Therefore, the pattern of DFL, particularly with respect to CRM, should be very accurate. The aim of the study presented in this chapter was to find a minimum number of F-responses to give a reliable representative shape of DFL for the diagnosis of CRM.

To obtain a good representation the sample size should be large. If we could obtain, perhaps, a few hundred F-responses, the DFL would have been very accurate, but, electrical stimulation given to a patient to obtain F-response through supramaximal stimulus is not pleasant, in fact a little pain is felt. Therefore, for routine investigations, obtaining too many F-responses is not practical, limiting the number to less than 30 or 40 would be a realistic choice.

The most important parameters for the shape of a frequency distribution are the sample size (number of data points in a sample) and bin width because these two control the tradeoff between presenting a picture with too much detail ("undersmoothing") or too little detail ("oversmoothing") with respect to the true distribution. DFL and its shape, particularly for the subtle distinction between a broad peak and a single peak for the diagnosis of CRM being a recent development, not enough work has been done in determining the optimum sample size and bin width. Finding an appropriate combination of bin width and sample size with the target of keeping the sample size minimum is the aim of the study presented in this chapter.

In the present work the pattern of DFL is very important in detecting CRM and the distinction of patterns for single peaks and broad peaks is very subtle as has been mentioned before. Since the number of data points (F-latencies) that can be made available from a patient is limited, therefore, the choice of bin widths for typical ranges of F-latencies corresponding to typical sample sizes (number of F-latencies) is important.

In a data set with values falling within a certain range, the choice of bin width determines the number of bins or class intervals in a distribution generated using the data. This decision affects the shape of the frequency distribution if the number of data points is limited. There are some "rules of thumb" that can help us to choose an appropriate bin width though none of the rules is perfect.

In the work presented in this chapter we first introduce three popular rules that are used to calculate the number of required minimum bins corresponding to a particular sample size. We then use these rules to give us a guide for the choice of the appropriate sample sizes and bin widths, which we take as guides. Since our target is to minimize the number of stimulations (giving the patient less pain), we then sought if a lower number of data points than that obtained from the above guides can give us a reasonable clinical outcome for the diagnosis of CRM.

Since we tried several methods varying to some degree, we thought that it would be better if we present the methods and results together in the following section.

7.2. Methods, Observations and Results

Firstly, we present the relationship between the number of bins (or number of classes) and the bin width for a range of data points in a sample. The number of bins k can be calculated from a suggested bin width h as:

$$k = \frac{X_{max} - X_{min}}{h} = \frac{\text{Range (chronodispersion)}}{h} \dots \dots \dots (1)$$

where X_{max} and X_{min} correspond to the highest and lowest non zero values obtained in the data set, and the range of values is usually called the Chronodispersion in nerve conduction studies.

The most popular formulii for the relationship between the number of bins k and the number of samples n are given below:

- i. **Sturge's rule:** Herbert Sturges considered an idealised frequency histogram (for normally distributed data) and gave the relationship as (Sturges, 1926):

$$k = 1 + \log_2 n$$

If the data are not normal, additional classes may be required.

- ii. **Rice Rule:** (Lane, 2015):

$$k = [2n^{\frac{1}{3}}]$$

- iii. **Square Root rule** (Excel, 2015):

$$k = \sqrt{n}$$

In the experimental studies carried out at the department of Biomedical Physics and Technology, Dhaka University, the chronodispersion – the maximum difference between the fastest and the slowest F-Latency value for median nerves was found to be about 8 ms. Based on this value, the required sample sizes corresponding to different bin sizes, relevant to our study are given in Table 7.1 following the above three rules. Here the numbers of bins are calculated from assumed bin size using equation 1.

Table 7.1: Relationship between group bin numbers with sample sizes for a range value of about 8 ms

Group bin width h, (ms)	Number of Group bins k	Sample size, n		
		Sturge's rule	Rice Rule	Square Root Choice
0.5	16	32,768	512	256
1.0	8	128	64	64
1.5	6	32	27	36
2.0	4	8	8	16

Table 7.1 shows that if we increase the group bin width, the corresponding sample size decreases sharply. In our study, the sample size corresponds to the number of F-responses used, and we usually need more number of electrical stimulations as some stimulation does not give an F-response.

Electrical stimulations are not comfortable to patients. Therefore, the objective would be to obtain useful results giving the minimum number of stimulations. From our experience, we found that most patients can tolerate up to about 40 stimulations. Therefore, we feel the number of stimulations should be limited to this value so that the number of F-responses, or in other words the sample size, could be about 30. Therefore, Table 7.1 suggests that a choice of the last two bin widths, i.e., 1.5 ms and 2.0 ms would be practical.

Again, keeping the above bin widths fixed, we then studied how the requirement of sample size changes if the range of F-latencies differs from the assumed 8 ms above. Table 7.2 shows a relation between the group bin numbers and the sample size for two group bin width 1.5 ms and 2.0 ms with multiple ranges of F-latencies (chronodispersion), using the formulii (or formulas) given above.

It is impractical to use the number of samples to be less than at least twice that of the bin width value, therefore, we have shown values in Table 7.2 accordingly. We have also kept the fractions in the numerical values as obtained by the equations in order to have a feeling for the values, although these should be eventually full numbers.

Table 7.2: Relation between the bin widths and the sample sizes for different ranges of F-latency (chronodispersion)

Bin width (ms)	Range of F-latency (Chronodispersion) (ms)	Number of bins k	Sample size n		
			Sturge's Rule	Rice Rule	Square Root Choice
1.5	3	2.00	2.00	1.00	4.00
	4	2.67	3.17	2.37	7.11
	5	3.33	5.04	4.63	11.11
	6	4.00	8.00	8.00	16.00
	7	4.67	12.70	12.70	21.78
	8	5.33	20.16	18.96	28.44
2.0	4	2.00	2.00	1.00	4.00
	5	2.50	2.83	1.95	6.25
	6	3.00	4.00	3.38	9.00
	7	3.50	5.66	5.36	12.25
	8	4.00	8.00	8.00	16.00

The above table suggests the minimum sample size that would be required in order to represent a DFL pattern with a reasonable accuracy, which would be useful for the diagnosis of CRM.

However, although the above table gives the minimum sample sizes for different range values and bin widths, we wanted to examine how these actually fared in practical experiments, and whether lower sample sizes could be used.

To carry out the study mentioned above we used two data sets as mentioned below.

- i. Firstly, data obtained by our extended group on both median nerves of 31 subjects at the Department of Biomedical Physics and Technology earlier (Chowdhury, 2013). Those nerves that provided more than 30 F-responses were considered for this study. This resulted in a choice of 25 nerves from 16 subjects. The chosen 25 Median nerves came from 16 subjects, 5 female and 11 male, aged between 24 and 56 yrs with a mean of 33.25 yrs (\pm 12.26 yrs). These data were obtained using nerve conduction equipment made by our department which has been in use in a clinic over many years. All of the subjects had MRI done at the cervical region, and evaluated for Radiculopathy and/or Myelopathy.

The procedures followed by our extended group earlier to obtain these data were as follows. Informed consents were taken from the subjects prior to testing, and it was noted whether the patient had any history of cervical pain or prior diagnosis of CRM. To each of the median nerves of these subjects about 40 supramaximal electrical stimulations were applied at the wrist in sequence, with intervals of one second between each to obtain a minimum 30 non-zero F-responses from the corresponding Thenar muscle (abductor pollicis brevis-APB, at the base of the thumb). The muscle was kept relaxed during the experiment. The actual number of stimulations given varied, depending somewhat on the cooperation of the subject. Stimulations that did not produce any F-response were rejected. The time sequence of the collected F-latencies from each nerve was maintained and recorded. The measurements were carried out at room temperature, which remained steady at or around 30°C.

- ii. Secondly, we had collected about 200 or more F-responses each from 3 Median nerves of two subjects (both male), aged 41 and 42 yrs during this study. A commercial EMG/EP equipment, Nicolet EDX system developed and marketed by

CareFusion was used for this purpose. One of the subjects was uncooperative and data could only be collected from one hand only. As before, Informed consents were taken from the subjects prior to testing, and it was noted whether the patient had any history of cervical pain or prior diagnosis of CRM.

i. Analyses using about 30 raw data points for each of the 25 nerves

For the study using the first data set, the pattern of DFL obtained using the 30 F-latency values for each median nerve of each subject was taken to be the reference for that particular nerve. If there were more than 30 F-latencies in the raw data, the first 30 values were chosen for this reference. Next, from the raw F-latency values, the first 20 and the first 10 data values were chosen respectively for the study presented here. Effectively, this choice corresponds to random selection of the F-responses. This was done to mimic the actual physical process where random selections of nerve fibres occur in the backfiring of action potentials that produces the F-waves. Table 7.3 shows the minimum F-latencies and the Range (chronodispersion) values obtained for these three sample sizes, i.e., 30, 20 and 10 data points respectively, for all the 25 nerves.

It can be seen that the minimum F-latency for the sample size of 30 is at least equal or shorter than the corresponding ones for 20 and 10 sample sizes respectively. This is expected since for the larger sample size we expect to get contributions from most of the nerve fibres including those at the extreme ends of the velocity profile, while for smaller sample sizes, some of the fibres at the extreme ends may not contribute. So for a larger sample size, we expect to get the shortest and greatest F-latency values, resulting in the largest range or chronodispersion value. This we can also see from the right hand columns in the above table where values for a sample size of 30 is at least equal or greater than those of the corresponding sample sizes of 20 and 10 respectively.

For each nerve, we compared the shapes of the DFLs obtained using the randomly chosen 20 and 10 F-latency values with that of the DFL plotted from the 30 F-latency values, which is the reference in this case. If the shape of DFL for the smaller sample sizes match well with the reference (sample size: 30), we will infer that the chosen sample size (less than 30) may be acceptable in the particular case. The DFL patterns

as obtained are shown in Table 7.4a and 7.4b below corresponding to bin widths of 2.0 ms and 1.5 ms respectively.

Table 7.3: Minimum F-Latency and F chronodispersion with different sample sizes

SI No.	Patient ID	Age (yrs)	Sex	Minimum F-Latency (ms)			F Chronodispersion (ms)		
				30	20	10	30	20	10
1	ABERRMF0	25	M	23.2	23.2	24.2	6.8	6.8	3.8
2	AKTFLMF	55	F	28.8	28.8	28.8	4.6	4.6	4.6
3	AKTFRMF	55	F	33.1	33.1	33.1	5.5	5.5	5.5
4	BAPDRMF	55	M	25.6	26.2	27.8	4.4	3.8	2.2
5	BEGKMLMF	39	F	25.8	25.8	27.2	5.2	4.2	2.2
6	BIBLMF0	27	M	24.2	24.2	24.2	6.0	6.0	5.8
7	BIBRMF	27	M	25.2	25.2	25.2	6.8	4.8	2.4
8	CHUHALMF	56	M	24.6	24.6	24.6	8.4	8.4	8.4
9	CHUHARMF	56	M	24.8	25.4	25.4	7.4	6.8	6.8
10	DEYPLMF	26	M	24.6	24.6	24.6	2.6	2.6	2.2
11	DEYPRMF	26	M	25.6	26.2	26.2	4.2	3.6	3.6
12	HASSRMF	24	M	27.0	27.0	27.0	4.4	4.4	4.2
13	HUSKLMF	26	M	29.2	29.4	30.4	4.6	4.4	2.4
14	ISLNRMF	43	F	24.4	24.4	24.8	2.8	2.8	1.8
15	MAHALMF	26	M	24.4	24.4	24.6	2.4	2.4	2.2
16	MAHARMF0	26	M	24.8	24.8	24.8	3.0	3.0	3.0
17	PERSLMF	27	F	23.2	24.2	24.6	4.2	3.2	2.4
18	PERSRMF	27	F	24.4	24.4	24.6	4.4	4.4	3.4
19	SULRLMF0	24	F	21.4	21.4	21.6	3.0	3.0	2.2
20	SULRRMF	24	F	21.4	21.4	21.4	5.0	5.0	3.2
21	YOUARMF	30	M	25.2	25.2	26.0	6.4	6.4	5.6
22	ZAMMRMF	25	M	25.2	25.2	25.8	3.8	3.0	2.0
23	ZIHMLMF	25	M	25.0	25.0	25.4	7.0	5.0	3.8
24	ZIHMLMF0	25	M	25.6	25.6	25.6	3.6	3.4	3.0
25	ZIHMRMF	25	M	23.8	23.8	23.8	5.2	5.2	5.2

Table 7.4a: DFL patterns for different sample sizes with group bin of 2.0 ms

Sl. No.	Patient ID	DFL Pattern with		
		30 Data points	20 Data points	10 Data points
1	ABERRMFO			
2	AKTFLMF			
3	AKTRMF			
4	BAPDRMF			
5	BEGKMLMF			
6	BIBLMFO			
7	BIBRMF			

Sl. No.	Patient ID	DFL Pattern with		
		30 Data points	20 Data points	10 Data points
8	CHUHALMF	<p>DFL₃₀</p>	<p>DFL₂₀</p>	<p>DFL₁₀</p>
9	CHUHARMF	<p>DFL₃₀</p>	<p>DFL₂₀</p>	<p>DFL₁₀</p>
10	DEYPLMF	<p>DFL₃₀</p>	<p>DFL₂₀</p>	<p>DFL₁₀</p>
11	DEYPRMF	<p>DFL₃₀</p>	<p>DFL₂₀</p>	<p>DFL₁₀</p>
12	HASSRMF	<p>DFL₃₀</p>	<p>DFL₂₀</p>	<p>DFL₁₀</p>
13	HUSKLMF	<p>DFL₃₀</p>	<p>DFL₂₀</p>	<p>DFL₁₀</p>
14	ISLNRMF	<p>DFL₃₀</p>	<p>DFL₂₀</p>	<p>DFL₁₀</p>

Sl. No.	Patient ID	DFL Pattern with		
		30 Data points	20 Data points	10 Data points
15	MAHALMF			
16	MAHARMFO			
17	PERSLMF			
18	PERSRMF			
19	SULRLMFO			
20	SULRRMF			
21	YOUARMF			

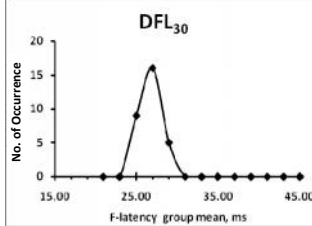
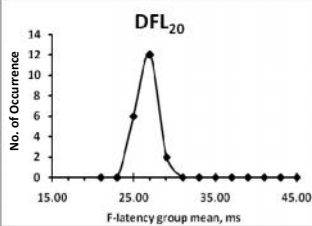
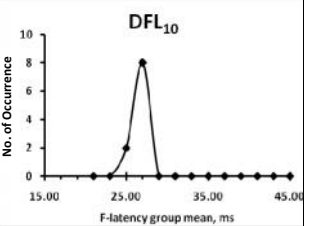
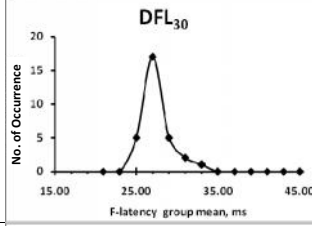
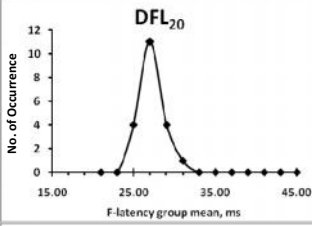
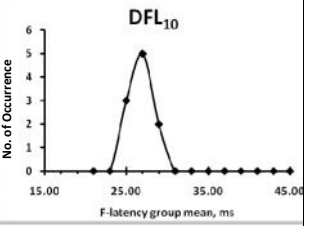
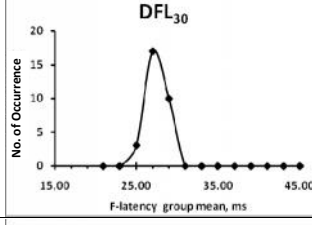
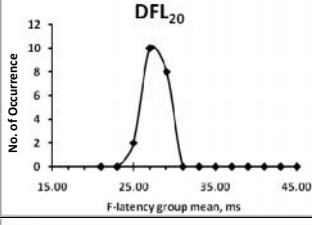
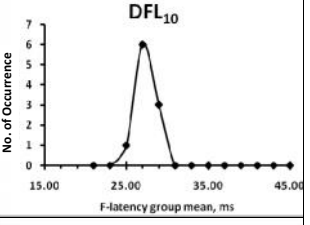
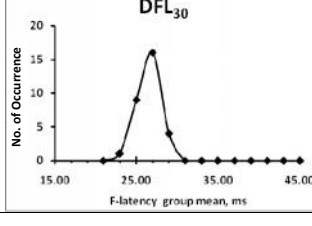
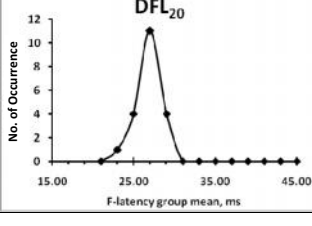
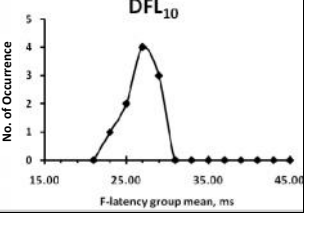
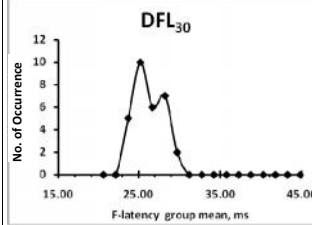
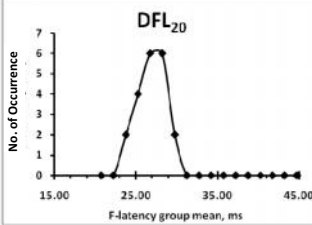
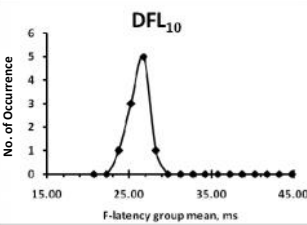
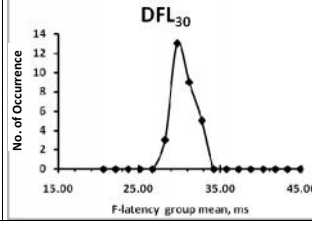
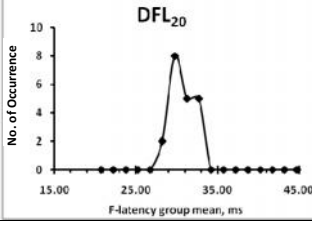
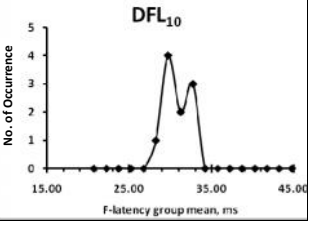
Sl. No.	Patient ID	DFL Pattern with		
		30 Data points	20 Data points	10 Data points
22	ZAMMRMF			
23	ZIHMLMF			
24	ZIHMLMFO			
25	ZIHMRMF			

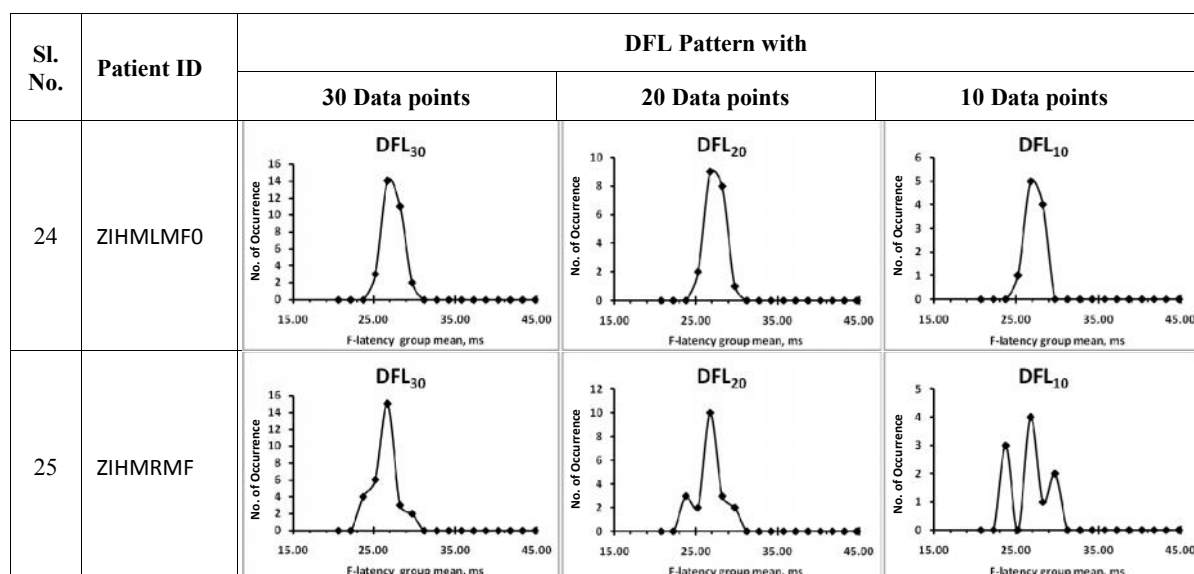
Table 7.4b: DFL patterns for different sample sizes with group bin of 1.5 ms

Sl. No.	Patient ID	DFL Pattern with		
		30 Data points	20 Data points	10 Data points
1	ABERRMFO			
2	AKTFLMF			

Sl. No.	Patient ID	DFL Pattern with		
		30 Data points	20 Data points	10 Data points
3	AKTFRMF			
4	BAPDRMF			
5	BEGKMLMF			
6	BIBLMFO			
7	BIBRMF			
8	CHUHALMF			
9	CHUHARMF			

Sl. No.	Patient ID	DFL Pattern with		
		30 Data points	20 Data points	10 Data points
10	DEYPLMF			
11	DEYPRMF			
12	HASSRMF			
13	HUSKLMF			
14	ISLNRMF			
15	MAHALMF			
16	MAHARMFO			

Sl. No.	Patient ID	DFL Pattern with		
		30 Data points	20 Data points	10 Data points
17	PERSLMF			
18	PERSRMF			
19	SULRLMFO			
20	SULRRMF			
21	YOUARMF			
22	ZAMMRMF			
23	ZIHMLMF			



It can be seen that the patterns have similarity for each of the three corresponding cases, however, for the sample size of 10, some deviations can be observed. Therefore, the above suggests that sample sizes of 30 and 20 are acceptable for typical subjects that we encounter in practice. Although we expected to see more distortion in the analyses using 1.5 ms bin width compared to that using 2.0 ms, in the above plots it is not so. These are almost as good as that for 2.0 ms bin width.

As mentioned before, for this study we tried to investigate the efficacy of DFL for the diagnosis of CRM. According to the simple method conceived and developed by our extended Dhaka University group and as mentioned before, a sharp single peak is considered to represent normalcy while a broad, double or multiple peak is considered to represent abnormality. Again, a broad peak is defined as the pattern in which the adjacent value to the peak is equal or greater than one third the peak value.

We therefore analyzed the patterns of DFL visually to identify whether each represent the presence of CRM (yes – ‘Y’) or absence of CRM (no – ‘N’). These results are presented in Table-7.5 below both for 1.5ms and 2ms bin widths respectively. Here, for the 2ms bin width, even a sample size of 5 each also shown.

Table 7.5: Comparative study of DFL_{30, 1.5}, DFL_{20, 1.5}, DFL_{10, 1.5}, DFL_{20, 2.0}, DFL_{10, 2.0} and DFL_{5, 2.0} patterns with diagnoses for CSN based on DFL_{30, 2.0} pattern.

[Double, Multiple or Broad peak indicates presence of CRM ('Y') and Single peak represent absence of CRM ('N')]

SI No.	Patient ID	DFL pattern with bin width 1.5 ms			DFL pattern with bin width 2.0 ms		
		30	20	10	30	20	10
1	ABERRMF0	Y	Y	Y	Y	Y	Y
2	AKTFLMF	Y	Y	Y	Y	Y	Y
3	AKTFRMF	Y	Y	Y	Y	Y	Y
4	BAPDRMF	Y	Y	Y	Y	Y	N
5	BEGKMLMF	Y	Y	Y	Y	Y	Y
6	BIBLMF0	Y	Y	Y	Y	Y	Y
7	BIBRMF	Y	Y	Y	Y	Y	Y
8	CHUHALMF	Y	Y	Y	Y	Y	Y
9	CHUHARMF	Y	Y	Y	Y	Y	Y
10	DEYPLMF	Y	Y	Y	Y	Y	Y
11	DEYPRMF	N	Y	Y	Y	Y	Y
12	HASSRMF	Y	Y	Y	Y	Y	Y
13	HUSKLMF	Y	Y	N	Y	Y	N
14	ISLNRMF	Y	Y	Y	Y	Y	Y
15	MAHALMF	N	N	N	N	N	N
16	MAHARMF0	Y	Y	Y	Y	Y	N
17	PERSLMF	Y	Y	Y	Y	Y	Y
18	PERSRMF	Y	Y	Y	Y	Y	Y
19	SULRLMF0	Y	Y	Y	Y	N	N
20	SULRRMF	Y	Y	Y	Y	Y	Y
21	YOUARMF	Y	Y	Y	Y	Y	Y
22	ZAMMRMF	Y	Y	Y	Y	Y	Y
23	ZIHMLMF	Y	Y	Y	N	Y	Y
24	ZIHMLMF0	Y	Y	Y	Y	Y	Y
25	ZIHMRMF	Y	Y	Y	Y	Y	Y

A summary of the prediction capabilities of the DFL technique is given in Table 7.6.

Table 7.6: Analysis for DFL pattern with different sample sizes and bin widths as an indicator for CRM

	DFL _{30, 1.5}	DFL _{20, 1.5}	DFL _{10, 1.5}	DFL _{20, 2.0}	DFL _{10, 2.0}
True Positive (TP)	22	23	22	16	14
True Negative (TN)	1	1	1	7	5
False Positive (FP)	1	0	1	0	2
False Negative (FN)	1	1	1	2	4
Correct Prediction (CP) %	92	96	92	92	76
Sensitivity (Sen) %	96	100	96	100	88
Specificity (Sp) %	50	50	50	78	56

From the above table, a quick observation reveals that DFL_{20, 2.0} (the first subscript denote the corresponding sample size and the next subscript denote the bin width) pattern has high values for all three indicators (CP, Sen, Sp) while others have low values of Specificity. On this basis we may say that DFL_{20, 2.0} provides us the best performance out of the 5 different patterns (DFL_{30, 1.5}, DFL_{20, 1.5}, DFL_{10, 1.5}, DFL_{20, 2.0}, DFL_{10, 2.0}) under test.

ii. Analyses using experiment giving about 200 raw data points

For the study using the second data set, we had collected 200 or more F-responses each from 3 Median nerves of two subjects, as mentioned before. The subjects were both male, aged 41 and 42 yrs. Informed consent was taken from the subjects prior to testing. Following a similar protocol as for the first data set as mentioned before, more than 200 supramaximal electrical stimulations were applied at the wrist in sequence to each of the median nerves of these subjects with one second interval. About 200 or more non zero F-latencies data were thus recorded for further analysis. Since patient cooperation was limited for such study involving so many stimulations, we performed this study only on two volunteers, one of them again refusing to have the study on both hands. The basic data and analyses showing mean and minimum F-latency and the Range (Chronodispersion) relevant to the whole data sets are given in Table 7.7.

Table 7.7: Basic information with a large sample data (about 200 or more) for three Median Nerves

Nerve ID	Age (yrs)	Sex	Number of Samples	Mean F-Latency (ms)	Minimum F-Latency (ms)	F Chronodispersion (ms)
N1	41	M	196	27.20	24.60	6.60
N2	42	M	240	26.30	24.00	6.30
N3	42	M	168	26.71	24.40	8.30

This large number of data for each nerve provided us with an opportunity to generate multiple data sets with different sample numbers randomly in order to study the statistical variation between different random samples with the same sample size and to establish a minimum number of samples for the detection of CRM.

Although 200 F-latencies would allow us to choose smaller bin widths, but since we were interested in 40 or less stimulations keeping view of the practical aspects as mentioned before, we kept the bin width study limited to 1.5 ms and 2.0 ms as in the study with the data from 25 nerves presented earlier in this chapter.

From the 200 or so raw data values for each nerve, 5 sets of 40 F-latency values were randomly obtained (using “RANDBETWEEN” random generator function of EXCEL2007) from which individual DFLs were obtained. The frequency of occurrence of each of these DFLs was normalized with respect to the respective peak value, so that the peak value became unity. This would allow easy visual comparison of the DFLs of all the 5 sets when plotted on the same graph. The same was also done to get 5 sets of data each for 5, 10, 20 and 30 F-latencies, independently. The mean of the corresponding 5 sets of F-latencies and the Range (Chronodispersion) are shown in Table 7.8.

Table 7.8: Comparing the 5 Minimum F-latencies mean and 5 F-Chronodispersion mean for different sample sizes

Nerve ID	Mean of 5 F-Latencies Mean (ms)					Mean of 5 F-Chronodispersion Mean (ms)				
	40	30	20	10	5	40	30	20	10	5
N1	27.11	27.03	27.10	27.16	27.45	6.08	5.74	5.64	3.74	3.14
N2	26.32	26.26	26.48	26.33	26.01	4.14	4.26	4.08	3.30	2.22
N3	26.48	26.69	26.82	26.78	26.80	7.92	7.74	7.66	5.28	2.68

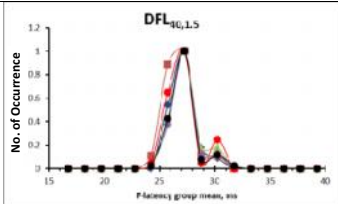
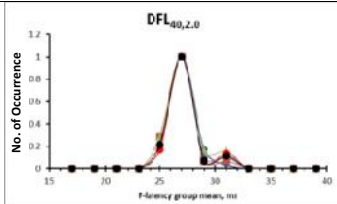
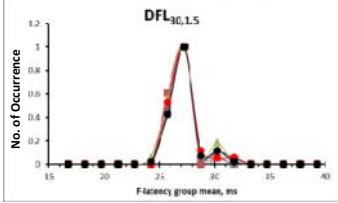
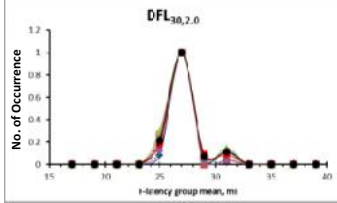
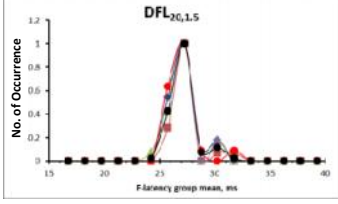
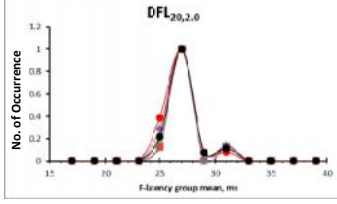
Because of the 5 samples taken in each category, in effect these mean values are for 5 times the sample size in each case, i.e., for 200, 150, 100, 50 and 25 F-responses

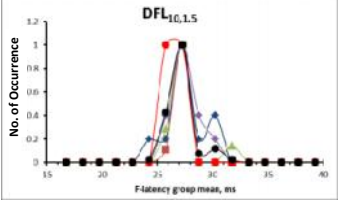
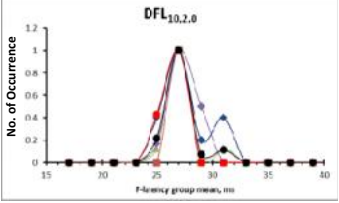
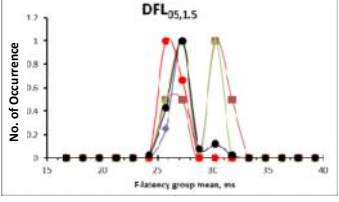
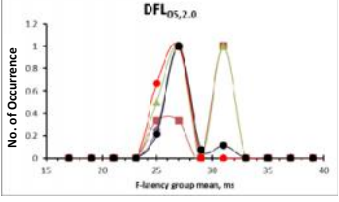
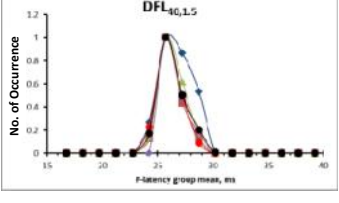
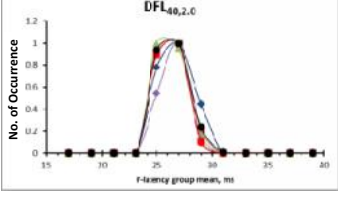
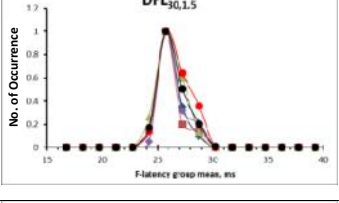
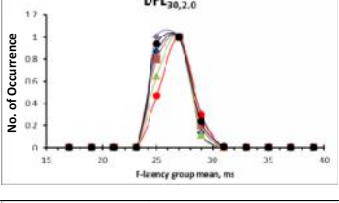
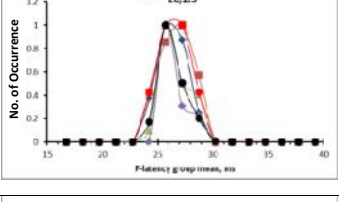
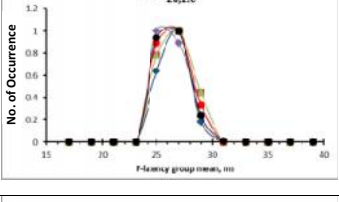
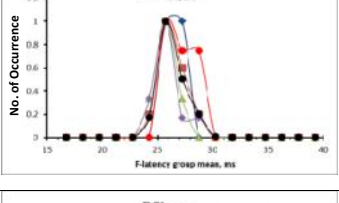
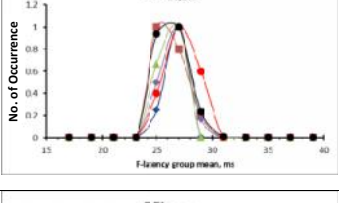
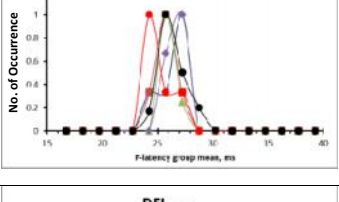
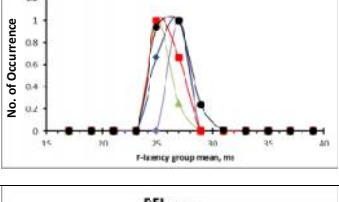
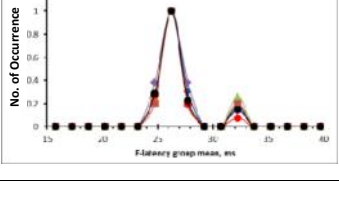
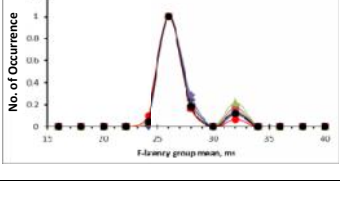
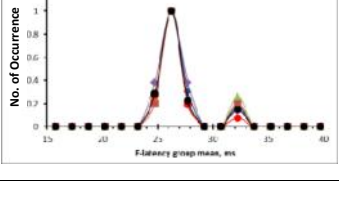
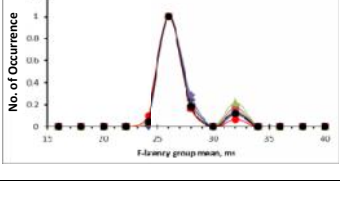
respectively. Therefore, for F-latency means all the values are very close, because the smallest size, i.e., 25 is a reasonably large number in statistical sense. On the other hand for the Range (Chronodispersion), obviously the larger sample sizes are likely to contain the contributions of the fibres with extremes of conduction velocity, which is apparent from the table.

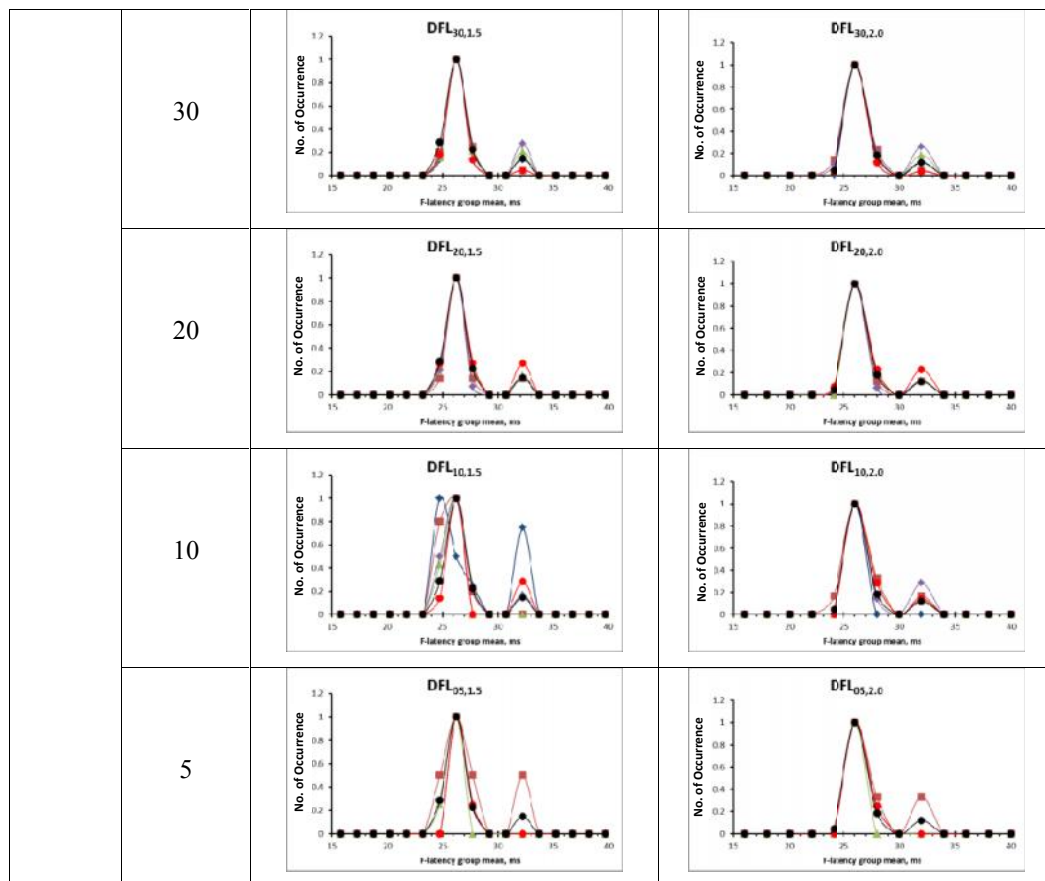
The data sets obtained were used to make a comparative study of the variation in DFL between different samples of the same size and bin width, and their comparison to the DFL obtained using the whole data set, having a sample size of around 200. The last one is the most reliable DFL under the present circumstances for each nerve, and may almost be considered as giving the population values, in other words the standard reference for that particular nerve. Thus all other DFLs for smaller sample sizes may be compared with these appropriate references to assess their accuracy.

These comparative plots are shown for the three nerves in Tables 7.9. Here, different coloured lines were used to represent the different data sets. In each graph the black line represents the respective reference DFL, for about 200 data points. Again, different DFL sets were plotted for bin widths of 1.5 ms and 2.0 ms.

Table 7.9: Comparative study of 5 Different DFL patterns for randomly selected sample of 40, 30, 20, 10 and 5 [Black line represents the total number of data points and five different coloured lines (Red, Green, Blue, Purple, Brown) represent five randomly chosen data sets from total number of data points, DFL₄₀ stands for sample size 40, DFL₃₀ stands for sample size 30, DFL₂₀ stands for sample size 20 DFL₁₀ stands for sample size 10, DFL₅ stands for sample size 5]

Nerve ID	Sample size	Bin width 1.5 ms	Bin width 2.0 ms
N1	40		
	30		
	20		

	10		
	5		
N2	40		
	30		
	20		
	10		
	5		
	40		
N3	40		



All the above DFL plots show the following:

- i. For any fixed bin width, the clustering of the different DFLs are better as the sample sizes increase from 5 to 40. For the smaller sample sizes, particularly for sample sizes of 10 and 5 the DFLs are more scattered.
- ii. For the same sample size, the DFLs are more clustered for 2.0 ms bin width compared to that for 1.5 ms bin width.

Both the above behaviours are expected based on common statistical arguments. However, in order to come to a decision regarding the sample size and bin width to be used for DFL study, particularly to highlight subtle patterns as for broad peaks due to CRM, we may suggest taking sample sizes more than 20 if the bin width is either 1.5 ms or 2 ms.

Correlation Coefficient between DFL patterns with different sample sizes

In order to determine the matching of the DFL patterns using different sample sizes with that of the corresponding larger samples (size: about 200) we determined the respective correlation coefficients. These are presented in Table 7.10.

Table 7.10: Correlation coefficient of 5 Different DFL patterns for randomly selected sample of 40, 30, 20, 10 and 5 with DFL pattern for large sample value (200) with bin size 2.0 ms

Sample Size →	Nerve ID	No of Obs.	Correlation Coefficient				
			40	30	20	10	5
N1	1	1	0.990	0.999	0.993	0.925	0.979
	2	2	0.943	0.984	0.987	0.949	0.548
	3	3	0.993	0.992	0.995	0.976	0.796
	4	4	0.997	0.997	0.982	0.955	0.979
	5	5	0.979	0.993	0.978	0.915	0.819
N2	1	1	0.949	0.982	0.961	0.919	0.681
	2	2	0.998	0.963	0.891	0.997	0.960
	3	3	0.994	0.992	0.984	0.960	0.948
	4	4	0.985	0.982	0.973	0.941	0.836
	5	5	0.994	0.987	0.936	0.905	0.495
N3	1	1	0.997	0.997	0.993	0.906	0.971
	2	2	0.999	0.992	0.997	0.988	0.976
	3	3	0.995	0.998	0.999	0.976	0.907
	4	4	0.995	0.989	0.993	0.980	0.990
	5	5	0.997	0.995	0.993	0.974	0.990

It can be seen that most of the values are close to 1 except a few for sample sizes of 5. However, to scrutiny further, we took a threshold of 0.95 for making a distinction between the quality of correlation, higher the better. On this basis the findings are presented in Table 7.11 below.

Table 7.11: Number of samples with correlation coefficient equal or greater than 0.95 with the data for 200 samples being the reference

No. of samples with $r \geq 0.95$	Sample Size				
	40	30	20	10	5
	14	15	14	9	8

From the above table it can be envisaged that if the sample size is greater than 20, the matching with the reference data (200 samples) is significantly better than that for 10 and 5 sample sizes.

7.3. Discussions

The main idea of the work presented in this chapter is to determine the minimum sample size and corresponding practical bin widths that would give reliable patterns of DFL, particularly for the detection of Cervical Spondylotic Radiculopathy and

Myelopathy (CRM) for which the distinction between patterns for normal DFL and abnormal DFL is very subtle.

The minimum sample size depends on the number of non-zero bins or groups present in the collected F-latencies. Since the number of bins to make a distribution (DFL) equals the ratio of the range (chronodispersion) and the bin width, range is important. For a particular bin width, the more the range is, the more should be the sample size for a representative pattern of the distribution. Therefore, ideally, the range should be a determinant in the choice of the sample size, but this is only possible after the data is taken and analysed, which will require repeat testing on patients, and is not desirable. Therefore, based on typical maximum values obtained from patients, a reasonable sample size should be chosen. For a normal nerve, this will give a more than adequate sample size, but for a patient with abnormality it should at least give the expected indication.

The work presented in this chapter dealt with these aspects in some detail in respect of practical data of F-latencies obtained from human subjects. Although some standard statistical formulii were used to determine the minimum sample size, these were used as initial guides only. Based in these guides and practical considerations of range (Chronodispersion) values of F-latencies and tolerance of human subjects to stand the discomfort produced by multiple electrical stimulations, we decided to use bin widths of 1.5ms or 2.0ms. However, the main judgment was based on the ability to distinguish between normal and abnormal DFL from real human subjects for the detection of CRM.

We used two independent sets of data to make the above judgment. One used data collected from 25 median nerves of 16 persons earlier by members of our extended group. These had more than 30 but less than 40 F-latencies each.

DFL patterns were generated for both 1.5 ms and 2.0 ms bin widths. We considered the DFL patterns obtained using 30 F-latencies (sample size) and 2.0 ms bin width (DFL_{30, 2.0}) as the respective reference for each nerve.

The highest value of correct prediction, 96%, occurred for a sample size of 20 with a bin width of 1.5 ms. For the same sample size with a bin width of 2.0 ms, the value was 92%. Even for a sample size of 30 and bin width of 1.5ms, the correct prediction value was 92%. However, the slight decrease in the predictive value for a sample size

of 10 and bin width 2 ms (76%), being much less than that for a sample size of 20. Although the sensitivity values (detected positives out of all positives – all abnormal cases) for the DFLs with 20 sample size and a bin width of 1.5 ms or 2.0 ms are 100%, on the other hand the specificity values (detected false negatives out of all negatives – all normal cases) for DFL with sample size 20 and a bin width of 2.0 ms is much higher (78%) than the rest of the DFLs with sample size 30, 20, 10 and a bin width of 1.5 ms (50%). Finally in order to come to a decision regarding the sample size and bin width to be used for DFL study, particularly to highlight subtle patterns as for broad peaks due to CRM, we may suggest taking sample sizes more than 20 if the bin width is either 1.5 ms or 2 ms.

To test the reproducibility of DFL, multiple (5 each) DFL patterns with sample sizes of 40, 30, 20 10 and 5 respectively were generated from a large number (about 200 or more) of recorded non-zero F-latency values from three nerves of two subjects. The bin sizes chosen were 1.5 ms and 2 ms. DFLs were generated with the whole sets of data points (about 200) for each nerve and these patterns were considered as the respective reference patterns. Later individually 40, 30, 20, 10 and 5 data points were used randomly from about 200 or more non-zero F-responses for each of the three nerves. Several attempts were taken to verify each of these patterns. Comparing the obtained patterns it was observed that most of the attempts matched with the standard pattern for each of the three nerves with the sample sizes 40, 30 and 20 data values, bin width 1.5 ms and 2.0 ms. Some of the patterns with 10 and 5 data points also matched with the standard pattern, but not all.

It can be seen from Table 7.8 that the Range (Chronodispersion) values for sample sizes of 40, 30 and 20 were the highest for the nerve N3 and smallest for N1, while N2 had intermediate values, but close to those for N3. This was true for both bin-sizes, 1.5ms and 2.0 ms. The corresponding DFLs had double peaks for N2 and N3, while N1 had single peaks. This supports the hypothesis originally put forward that due to CRM the DFL patterns from different nerve branches spread out more than that for cases without CRM.

Table 7.9 shows a comparison of the different DFL patterns, where the black solid line represents the standard pattern and the coloured solid lines represent the five different sample sizes. This was again done for two different bin widths 1.5ms and 2.0 ms. It can be seen that for any fixed bin width, the clustering of the different DFLs are

better as the sample sizes increase from 5 to 40. For the smaller sample sizes, particularly for sample sizes of 10 and 5 the DFLs are more scattered. Again for the same sample size, the DFLs are more clustered for 2.0 ms bin width compared to that for 1.5 ms bin width. This shows that grouping into either 1.5ms or 2.0 ms are acceptable for sample sizes of 20 or more.

Table 7.11 shows that when the data for sample sizes of 40, 30, 20, 10 and 5 were compared with that for a sample size of 200, which was taken as the reference, it seems very clear that sample sizes above 20 gave matching values in almost all the random samples for the three nerves while these fell short for sample sizes of 10 and 5. However, this result depends on the choice of the threshold at 0.95 which was rather arbitrary. Still this table gives an indication which is useful.

The study presented in this chapter allows us to choose a sample size with confidence that may give a good diagnosis of CRM based on the patterns of DFL. Combining all the study presented in this chapter, we may state that a sample size give a representative DFL if the bin width is chosen to be 1.5 ms or 2.0 ms.

Chapter 8: Effect of bin shifting on DFL for the detection of Cervical Spondylotic Radiculopathy and Myelopathy (CRM)

8.1. Introduction

A peripheral nerve trunk consists of thousands of nerve fibres with varying conduction velocities, which can be well described by distribution of conduction velocity (DCV). If a motor nerve is electrically stimulated, action potentials are generated within the individual nerve fibres, which travelling to the connected muscle (called orthodromic conduction) elicit a compound muscle action potential, or an M-response, that can be recorded using surface electrodes. From the stimulation site the action potentials also travel in the opposite direction (called antidromic conduction) to their respective cell bodies located in the spinal cord. In most of the motor nerve cells these antidromic potentials simply die down. However, a few percent of the cell bodies backfire after a short delay and send fresh action potentials down the nerve fibres to the muscle. These in effect produce a delayed compound muscle action potential called the F-response (Fox and Hitchcock, 1987, Magladery and McDougal, 1950, Mayer and Feldman, 1967, McLeod and Wray, 1966), which is very much reduced in amplitude with respect to the M-response because of the small number of fibres involved. F-latencies obtained from multiple stimulations vary in latency, size and shape because of random backfiring of the cell bodies. Recruitment of fibres for F-response would depend on DCV for motor fibres directly (Rabbani et al., 2007). Being a random process, they hypothesised that a frequency distribution of F-latencies (DFL) from such multiple F-Latencies would be an approximate mirror image of the corresponding DCV. This new neurophysiological parameter DFL obtained from evoked EMG responses have previously been reported to be useful in the detection of Cervical spondylotic Radiculopathy and Myelopathy (CRM) (Alam and Rabbani, 2010, Hossain et al., 2011, Rabbani et al., 2014).

There are usually two major causes for CRM. One is called Radiculopathy in which nerve branches coming out of the spinal cord (nerve root) may be compressed in the narrow channels or gaps created by the vertebral bones. This compression may be caused by bony growth in the vertebra (osteophyte), or herniation of inter-vertebral disc. Either of these compressions leads to Radiculopathy. The other cause of CRM is Myelopathy in which one side of the spinal cord is directly pressed onto, mostly by a

bulging or herniated intervertebral disc. This compression may also be caused by tumours or other changes in the spinal column. Such compression affects the descending nerve fibres located in the specific region of the spinal cord which in turn may affect the peripheral nerve fibres onto which these descending nerve fibres terminate.

Recently a double blind study was performed to ascertain the efficacy of DFL in the detection of CRM using MRI findings as the benchmark (Chowdhury, 2013, Chowdhury et al., 2014) which showed that DFL can predict CRM to a high degree of reliability.

In our laboratory DFL is obtained by grouping F-latency data into 2 ms bins and then plotting a frequency polygon. The resulting polygon shapes are sorted into two categories: i) single peak and ii) broad peak or multiple peaks. The first category was taken to represent normalcy while the second category was taken to represent CRM. Different types of DFL typically obtained are shown in Figure 8.1-8.5.

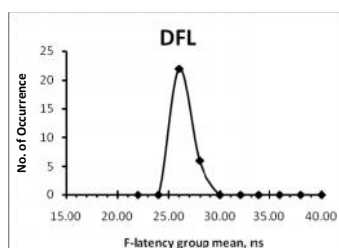


Figure 8.1: Single Peak

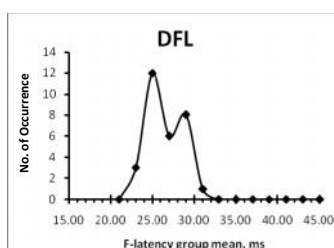


Figure 8.2: Double Peak

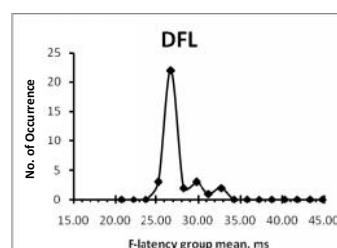


Figure 8.3: Triple Peak

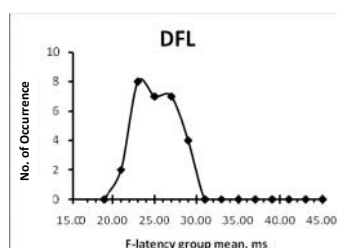


Figure 8.4: Broad Peak

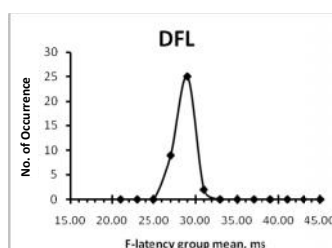


Figure 8.5: Broad Peak

A single peak was defined as the polygon which has a single high value (peak) while the adjacent values (at intervals of 2 ms) are very small as shown in Figure 8.1. Double or triple peaks were also visually determined simply, as shown in Figures 8.2 and 8.3. A broad peak was defined where significant non-zero frequency exists at a difference of two bin separation (here, 4ms) from the position of the peak, with the intermediate bin having a significantly high frequency value as shown in Figure 8.4. A recent work carried out in Singapore (Rabbani et al., 2014) has helped improve the

definition of a broad peak with relation to the occurrence of CRM. According to this definition, if any of the adjacent frequency values was greater than one third of the peak frequency (as in Figure 8.5) then it would be considered a broad peak as well. Comparing figures 8.1 and 8.5, it is obvious that there is a very small difference in between these shapes while it is very critical to distinguish a single peak from a broad peak for the diagnosis of CRM.

During the present work it was observed that while making the frequency polygons of DFL, if the starting point for the grouping into the 2 ms bins is changed by 1 ms (half the bin width), then the pattern sometimes changed from a single peak to a broad peak, or from a broad peak to double peak, or vice versa, for the same raw data points. This poses a difficulty regarding the decision on the diagnosis of CRM which relies on these shapes of the DFL polygon. For this reason the present work was taken up to systematically study the effect of this shift in the starting value of the bins of earlier data and how the inferences from the slightly different patterns may be combined to get a better decision for the diagnosis of CRM.

8.2. Methodology

The study was performed on the data obtained in an earlier study (Chowdhury, 2013) which was carried out on 62 median nerves of 31 subjects with age ranging from 20yrs to 70yrs with a mean of 37.66 yrs (± 14.55 yrs). MRI reports indicating CRM were also available for most of the subjects. However, both median nerves of two individual subjects and one each of two other individuals had insufficient MRI information and these were excluded from the present study. So this study essentially included data from 56 median nerves of 29 subjects.

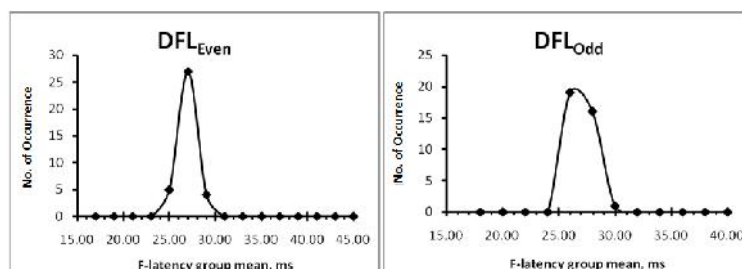


Figure 8.6: DFL_{even} and DFL_{odd} for one nerve of a subject demonstrate single peak and broad peak respectively after shifting the bin starting point

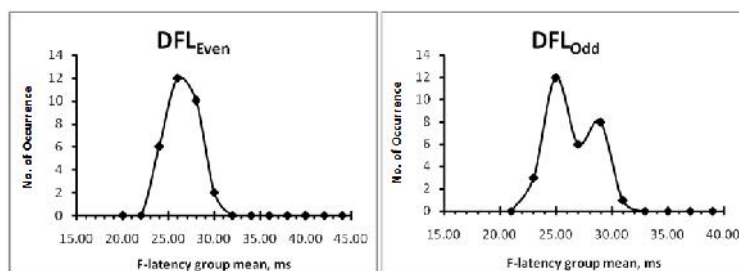


Figure 8.7: DFL_{even} and DFL_{odd} for one nerve of a subject demonstrate broad peak and double peak respectively after shifting the bin starting point

Frequency distribution for a continuous variable is usually performed choosing appropriate bins or groups. All the previous work in our laboratory used a bin size of 2 ms to obtain a DFL polygon. Typical values of F-latency for median nerves from adult subjects vary between 20 ms and 35 ms. In the previous work bin values were chosen at intervals (all in ms) 20^+-22 , 22^+-24 , ... so on. Here the starting value is an even number and let us name the DFL thus obtained as DFL_{even} . We would like to see what changes in shape occurs, particularly with respect to the detection of CRM, if a 1ms shift is made in the choice of the bins, i.e. if the bins were chosen at intervals (all in ms) 21^+-23 , 23^+-25 , ... so on. Let us name the DFL thus obtained as DFL_{odd} . Figures 8.6 and 8.7 shows the polygon shapes for two nerves of two subjects for both DFL_{even} and DFL_{odd} where the shapes change between the classifications considered for diagnosis in the present work as mentioned before. Particularly in Figure 8.6, the difference is very subtle. In one, it is a single peak based on our new definition mentioned above (Rabbani et al., 2014) while the other is a broad peak.

Since the patterns change through this process of bin shifting, we were interested to see if any combination of the decisions based on these changed patterns can improve the diagnostic ability of DFL. We considered two approaches, one using logical OR operation and the other using logical AND operation on the decisions given by the two patterns as a result of bin shifting. These were to be compared with the decisions given by the MRI findings which have been considered as the gold standard in the previous study (Chowdhury et al., 2014).

For these logical operations the diagnosis based on DFL and MRI were assigned the letters 'Y' and 'N' to represent the presence of CRM (yes) and absence of CRM (no) respectively. As already mentioned, if the DFL shows a single peak, we interpret this as normal, i.e. the diagnosis is a 'no' indicated by 'N'. If a DFL gave broad, double or triple peak, the diagnosis is a 'yes' indicated by 'Y'. For each nerve of a subject, these

diagnoses were made with both DFL_{even} and DFL_{odd} . The MRI findings were similarly assigned ‘Y’ or ‘N’ values based on the findings of the radiologist which were taken from the earlier work (Chowdhury et al., 2014). It needs to be mentioned that in this earlier work DFL gave a better efficacy if even mild findings of MRI were taken to represent CRM, which was also chosen for this work.

The diagnosis based on individual shapes of DFL_{even} and DFL_{odd} and the two mentioned combinations (OR and AND) were performed. These four sets of diagnosis were then compared with the MRI findings. This gave us a way to identify which of the diagnoses gave the best performance for DFL.

To determine the predictive capabilities of the above diagnoses based on DFL we determined the following parameters from the relevant tables: true positives (TP), true negatives (TN), false positives (FP) and false negatives (FN). These parameters were then analysed to obtain values of correct prediction (CP) or efficacy, Sensitivity (Sen) and Specificity (Sp) defined as (all expressed in percentage):

$$CP = (TP+TN)/\text{Total number}$$

$$\text{Sen} = TP/(TP+FN)$$

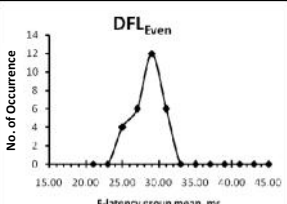
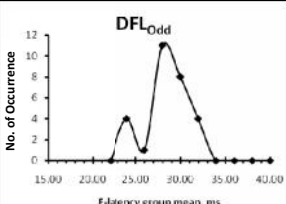
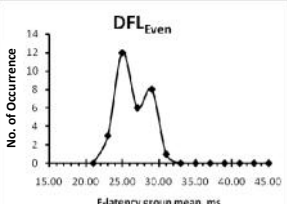
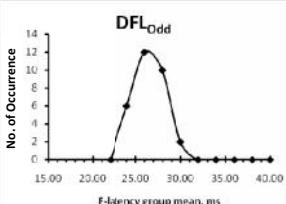
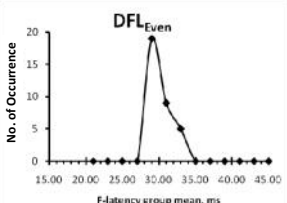
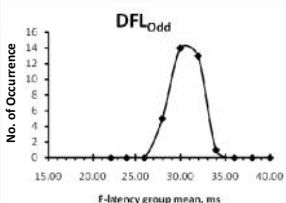
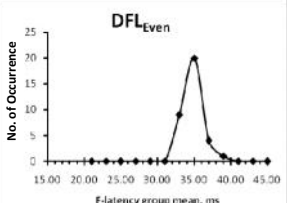
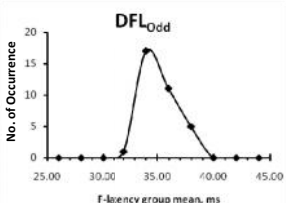
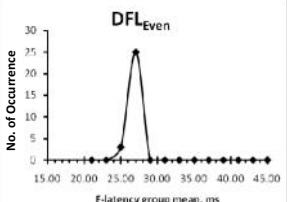
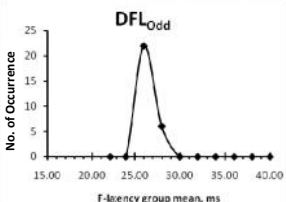
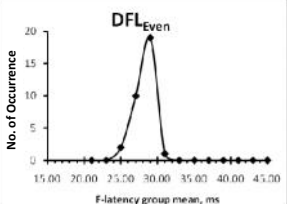
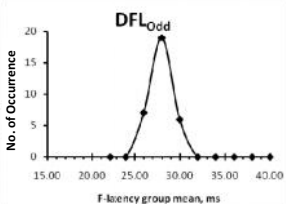
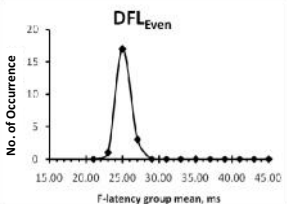
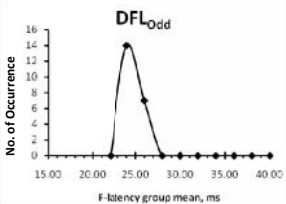
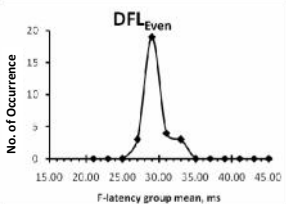
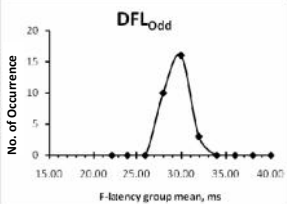
$$\text{Sp} = TN/(TN+FP).$$

The higher the value for each, the better is the performance of the new test regime, here of DFL.

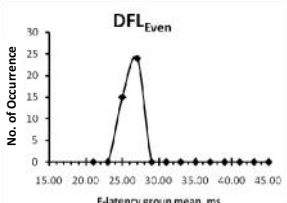
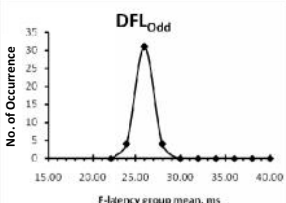
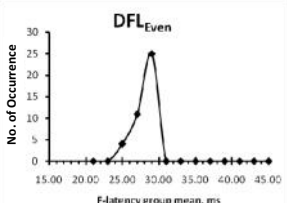
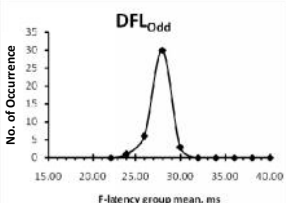
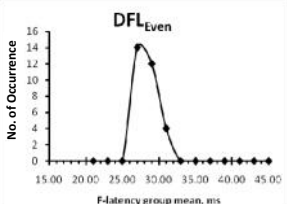
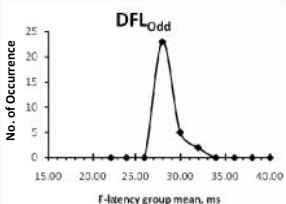
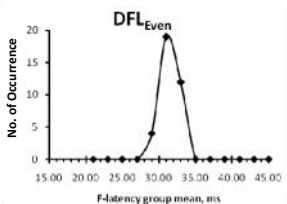
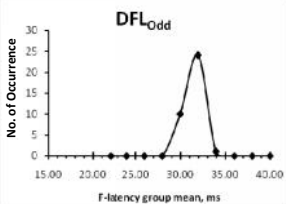
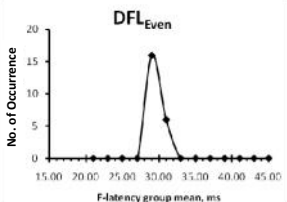
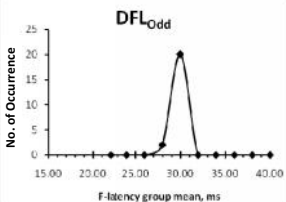
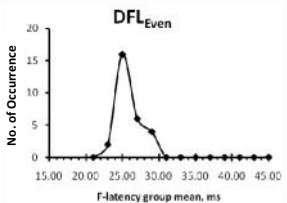
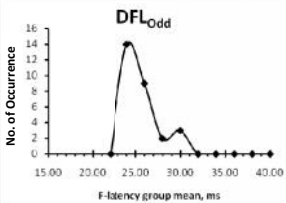
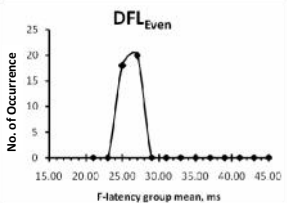
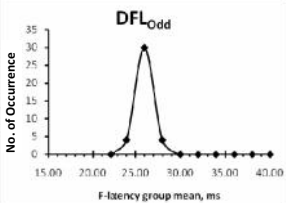
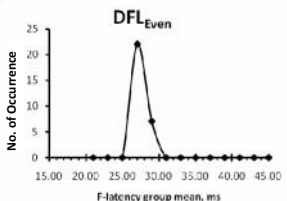
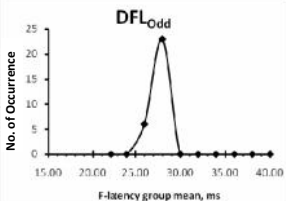
8.3. Results

Corresponding DFLs based on the starting point, i.e., DFL_{even} and DFL_{odd} are presented in table 8.1. These show the pattern changes obtained because of this shift in the starting point. The comparative DFL findings for 56 median nerves corresponding to MRI based on ‘Y’ and ‘N’ are presented in Table 8.2. The predictive analysis of DFL as an indicator for CRM is presented in Table 8.3.

Table 8.1: Effect of bin shifting of the starting point on DFL pattern

Sl. No.	Subject ID	Age	Sex	Distribution of F-Latencies (DFL) pattern for Bin starting point from	
				Even number	Odd number
1	ABERLMF	25	M		
2	ABERRMF0	25	M		
3	AKTFLMF	55	F		
4	AKTFRMF	55	F		
5	BAPDLMF	55	M		
6	BAPDRMF	55	M		
7	BEGALMF	26	F		
8	BEGARMF	26	F		

Sl. No.	Subject ID	Age	Sex	Distribution of F-Latencies (DFL) pattern for Bin starting point from	
				Even number	Odd number
9	BEGKMLMF	39	F		
10	BEGKMRMF	39	F		
11	BIBLMF	27	M		
12	BIBRMF	27	M		
13	CHUHALMF	56	M		
14	CHUHARMF	56	M		
15	DEYCNLMF	63	M		
16	DEYCNRMF	63	M		

Sl. No.	Subject ID	Age	Sex	Distribution of F-Latencies (DFL) pattern for Bin starting point from	
				Even number	Odd number
17	DEYPLMF	26	M		
18	DEYPRMF	26	M		
19	HASSRMF	24	M		
20	HUSKLMF	26	M		
21	HUSKRMF	26	M		
22	ISLNLMF	43	F		
23	ISLNRMF	43	F		
24	JABALMF	60	M		

Sl. No.	Subject ID	Age	Sex	Distribution of F-Latencies (DFL) pattern for Bin starting point from	
				Even number	Odd number
25	JABARMF	60	M		
26	KHAILMF	23	M		
27	KHAIRMF	23	M		
28	LATNNLMF	22	F		
29	LATNNRMF	22	F		
30	MAHALMF	26	M		
31	MAHARMF	26	M		
32	MAMALMF	29	M		

Sl. No.	Subject ID	Age	Sex	Distribution of F-Latencies (DFL) pattern for Bin starting point from	
				Even number	Odd number
33	MAMARMF	29	M		
34	MIAMMLMF	32	M		
35	MIAMMRMF	32	M		
36	PERSLMF	27	F		
37	PERSRMF	27	F		
38	RAHALMF	37	M		
39	RAHARMF0	37	M		
40	RAHOLMF	38	M		

Sl. No.	Subject ID	Age	Sex	Distribution of F-Latencies (DFL) pattern for Bin starting point from	
				Even number	Odd number
41	RAHORMF	38	M		
42	RAHSLMF0	53	M		
43	RAHSRMF0	53	M		
44	RAYLMF	50	F		
45	RAYRMF	50	F		
46	SARTALMF	62	M		
47	SARTARMF	62	M		
48	SULRLMF	24	F		

Sl. No.	Subject ID	Age	Sex	Distribution of F-Latencies (DFL) pattern for Bin starting point from	
				Even number	Odd number
49	SULRRMF	24	F		
50	UDDKRMF	64	M		
51	YOUALMF	30	M		
52	YOUARMF	30	M		
53	ZAMMLMF	25	M		
54	ZAMMRMF	25	M		
55	ZIHMLMF	25	M		
56	ZIHMRMF0	25	M		

Table 8.2: Comparative study between MRI and DFL findings for CRM

Sl. No.	Subject ID	CRM from MRI	CRM from	
			DFL _{even}	DFL _{odd}
1	ABERLMF	Y	Y	Y
2	ABERRMF	Y	Y	Y
3	AKTFLMF	Y	Y	Y
4	AKTFRMF	Y	Y	Y
5	BAPDLMF	Y	N	N
6	BAPDRMF	Y	Y	N
7	BEGALMF	Y	N	Y
8	BEGARMF	Y	Y	Y
9	BEGKMLMF	Y	Y	Y
10	BEGKMRMF	Y	Y	Y
11	BIBLMF	Y	Y	N
12	BIBRMF	Y	Y	Y
13	CHUHALMF	Y	Y	Y
14	CHUHARMF	Y	Y	Y
15	DEYCNLMF	Y	Y	Y
16	DEYCNRMF	Y	Y	Y
17	DEYPLMF	Y	Y	N
18	DEYPRMF	Y	Y	N
19	HASSRMF	Y	Y	Y
20	HUSKLMF	Y	Y	Y
21	HUSKRMF	Y	Y	N
22	ISLNLMF	Y	Y	Y
23	ISLNRMF	Y	Y	N
24	JABALMF	Y	Y	Y
25	JABARMF	Y	Y	Y
26	KHAILMF	N	Y	N
27	KHAIRMF	Y	Y	Y
28	LATNNLMF	Y	N	Y
29	LATNNRMF	Y	Y	Y
30	MAHALMF	Y	N	N
31	MAHARMF	Y	Y	Y
32	MAMALMF	Y	Y	Y
33	MAMARMF	Y	Y	Y
34	MIAMMLMF	Y	Y	N
35	MIAMMRMF	Y	Y	Y
36	PERSLMF	Y	Y	Y
37	PERSRMF	N	Y	Y
38	RAHALMF	Y	Y	Y
39	RAHARMF	Y	N	N
40	RAHOLMF	Y	N	Y
41	RAHORMF	Y	N	N
42	RAHSLMF	Y	Y	Y
43	RAHSRMF	Y	Y	Y
44	RAYLMF	Y	Y	Y
45	RAYRMF	Y	N	Y
46	SARTALMF	Y	Y	Y
47	SARTARMF	Y	Y	Y
48	SULRLMF	Y	N	N
49	SULRRMF	Y	Y	Y
50	UDDKRMF	Y	N	N
51	YOUALMF	Y	Y	Y
52	YOUARMF	Y	Y	Y
53	ZAMMLMF	N	Y	Y
54	ZAMMRMF	N	Y	Y
55	ZIHMLMF	Y	Y	Y
56	ZIHMRMF	Y	N	Y

Table 8.3: Analysis for DFL as an indicator for CRM

	DFL _{even}	DFL _{odd}	Logical Operation	
			OR	AND
True Positive (TP)	41	39	46	34
True Negative (TN)	0	1	0	1
False Positive (FP)	4	3	4	3
False Negative (FN)	11	13	6	18
Correct Prediction (CP) %	73	71	82	63
Sensitivity (SEN) %	79	75	88	65
Specificity (SPE) %	0	25	0	75

It needs to be noted that to obtain reliable figures for specificity we need a significant number of subjects with true negative values. From Table 8.2 it can be seen that there are only 4 cases out of 56 having a true negative value. Therefore the Specificity values obtained here are not significant and should not be considered for an evaluation of the method.

A quick observation of Table 8.3 reveals that the OR combination of DFL_{even} and DFL_{odd} gives the best overall performance.

8.4. Discussions

The work on DFL (a statistical frequency distribution of F-latencies from multiple F-responses) is already established for CRM detection by our extended group at Dhaka University and foreign collaborators in the earlier years. Recently it was observed that if the starting point of DFL is shifted by half the bin width then the polygon pattern changes and a detailed study of its effect in the predictive capability of DFL was felt, and this was therefore, taken up in the present work. Since DFL is used as a screening tool for CRM diagnosis depending upon the polygon shapes, choice of polygon pattern is important. Since DFL is used as a screening tool for CRM diagnosis depending upon the polygon shapes, choice of polygon pattern is important.

Table 8.3 summarises the outcome of this specific study carried out on 56 median nerves. The efficacy or correct prediction improved significantly, from 73% and 71% of the individual results of DFL_{even} and DFL_{odd} to 82% if we took the OR of the two. On the other hand this value decreased significantly to 63% if we took the AND of the

two. The sensitivity figure also improved (from 79% and 75% to 88%) for OR operation while it decreased to 65% for AND operation. The specificity seems to favour the AND operation but a close observation of the raw data would indicate that there are not enough data to obtain a reliable value of specificity. From Table 8.2 it can be seen that there are only 4 cases out of 56 having a true negative value which is the most important parameter for a calculation of specificity. Therefore, the present data set does not allow us to obtain a value of specificity with any degree of reliability, and this parameter should not be considered for an evaluation of the proposed methods. These points to the requirement of obtaining a data set with a significant population with True Negative CRM, as indicated by MRI. In spite of this limitation it can be safely said that an OR operation of DFL_{even} and DFL_{odd} could be useful for a better diagnosis of CRM using DFL.

A closer look at the raw data indicates that most subjects chosen for this study (Chowdhury et al., 2014) were in the age range 20-50 yrs and apparently did not have any clinical symptoms of CRM. Most of them were initially thought to be normal. However, both DFL and MRI indicated otherwise. The medical community usually holds that people under the age of 50 yrs usually do not have CRM, but the work of Chowdhury et al, improved upon by the present work, seem to contradict the conventional notion. This is very important from a public health point of view and a rigorous epidemiological study needs to be carried out in order to ascertain this pathology in our population based on differences of age, living style, physical strains involved in their work, etc.

Chapter 9: Quantitative analysis of DFL pattern to identify single and broad peaks

9.1. Introduction

Distribution of F-Latency (DFL), introduced by the Dhaka University biomedical physics group, and its application in the detection of Cervical spondylotic Radiculopathy and Myelopathy (CRM) (Rabbani et al., 2007, Rabbani, 2011b), is the focus of this thesis. The pattern of DFL (in the form of a frequency polygon) is characterized visually to identify cases of CRM as described in chapter 4. The shapes of the resulting polygons are sorted into two categories: i) single peak and ii) broad peak or multiple peaks. The first category was taken to represent normalcy while the second category was taken to represent CRM (Alam and Rabbani, 2010). The DFL pattern with double or multiple peak can easily be diagnosed as CRM. However, based on a comparison with MRI studies Rabbani et al showed that the distinction of a broad peak that indicates the presence of CRM from a single peak that indicates normalcy is very subtle (Rabbani et al., 2014). This has also been discussed in detail in previous chapters of this thesis. For a DFL pattern made up using a bin width of 2 ms, the broad peak was defined as the pattern where the frequency value at a bin adjacent to that of the peak is equal or greater than 1/3 rd the value of the peak. Therefore, identifying the correct representative shape of DFL for a nerve trunk is very important for the detection of CRM.

Since the shape of the broad peak is frequently skewed, and the peak is less sharp than a single peak, we wanted to study the possibility of using two common parameters of the DFL patterns - Skewness and Full Width Half Maximum (FWHM). These are expected to characterize DFL broad peak for the diagnosis of CRM more accurately. If this is successful, this could also lead to automated disease identification. Besides, it may be possible to extract further information on the nature of compression or degeneration of the several nerve branches that contribute to a particular DFL.

Skewness

Skewness is a measure of symmetry, or more precisely, the lack of symmetry. A distribution, or data set, is symmetric if it looks the same to the left and right of the center point.

In probability theory and statistics, skewness is a measure of the extent to which a probability distribution of a real-valued random variable "leans" to one side of the mean. The skewness value can be positive or negative, or even undefined.

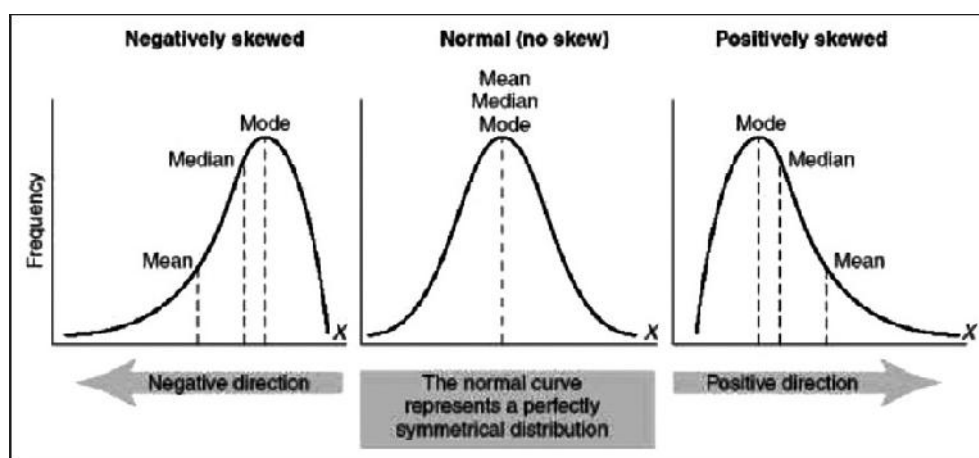


Figure 9.1: Statistically distributed curve with negatively skewed (left), zero skewed (middle) and positively skewed (right)

The qualitative interpretation of the skew is complicated. For a unimodal distribution, negative skew indicates that the tail on the left side of the pattern is longer or fatter than the right side. Conversely, positive skew indicates that the tail on the right side is longer or fatter than the left side. In cases where one tail is long but the other tail is fat, skewness does not obey a simple rule. For example, a zero value indicates that the tails on both sides of the mean balance out, which is the case both for a symmetric distribution, and for asymmetric distributions where the asymmetries even out, such as one tail being long but thin, and the other being short but fat. Figure 9.1 shows the three different types of skewness for three different distributions.

If the distribution is symmetric then the mean is equal to the median and the distribution will have zero skewness. If, in addition, the distribution is unimodal, then the mean = median = mode.

Full Width at Half Maximum (FWHM)

Full width at half maximum (FWHM) is an expression of the extent of a function, given by the difference between the two extreme values of the independent variable at which the dependent variable is equal to half of its maximum value. The Gaussian or normal distribution plays a central role in all of statistics and probabilities theory and is the mostly used distribution in all the sciences including neuroscience. FWHM

essentially gives the sharpness of a Gaussian distribution, and may therefore, be of use in the identification of broad peaks of DFL.

9.2. Methodology

For studying the skewness, DFL patterns with single peak and broad peak were chosen from the study done earlier (Chowdhury, 2013) on 62 median nerves of 31 subjects, which were also used for much of the study of this thesis presented earlier. Isolating DFL patterns with single peak from this set of data, we chose 19 median nerves of 16 subjects. Similarly isolating DFL pattern with broad peak we chose 33 median nerves of 24 subjects. It needs to be mentioned that for all the DFL patterns, the sample size was 20 and the bin size was 2 ms.

Using Microsoft Excel 2007 the skewness of the individual DFL polygons were obtained. The outcomes of the analysis are presented in the results section of this chapter.

For studying the Full Width at Half Maximum (FWHM), the same data sets that used for studying Skewness were used.

Developing a simple program in Microsoft Excel 2007 the FWHM of the individual DFL were obtained. The outcomes of the analysis are presented in the results section of this chapter.

Student t-test is performed based on null hypothesis. For Skewness this is a two-tail test and for FWHM it is a one-tail test. For both of the analysis we are testing at the 5% (0.05) level of significance. The analysis is presented in the result section of this chapter.

9.3. Results

Table 9.1 shows the respective skewness and FWHM values of DFLs with single peak (identified visually, based on the definitions mentioned in the introduction section) for 19 median nerves of 16 subjects. Table 9.2 shows the respective skewness and FWHM values of DFL with double peak for 33 median nerves of 24 subjects.

In chapter 8, it was shown that depending upon bin starting point, DFL pattern may change from a single peaked to a broad peaked one. For this reason some of the nerve-IDs are same in both of the table 9.1 and 9.2 with different DFL patterns. There

the final decision regarding CRM was taken using an OR of these two outcomes. However, in the present chapter we are interested in the patterns of DFL, not its interpretation in relation to CRM, we are just interested in the patterns – whether a curve is to be classified as having a single peak or a broad peak.

For the curves which give a single peak when starting from a certain F-latency value and a broad peak when starting from a value 1ms different, the skewness values are same since both the curves are derived from the raw data set, not the DFL pattern as such. On the other hand, FWHM values are derived from the DFL patterns, so this pattern may change for different starting points of DFLs, even though obtained from the same raw data set.

Table 9.1: Skewness and FWHM of DFL with single peak (19 median nerves of 16 subjects)

Sl. No.	Nerve ID	DFL Pattern	Skewness	FWHM (ms)
1	BAPDLMF		0.39	2.06
2	BAPDRMF		-0.84	2.63
3	BEGALMF		0.53	2.30
4	BIBLMF		-0.63	2.13

Sl. No.	Nerve ID	DFL Pattern	Skewness	FWHM (ms)
5	DEYPLMF	<p>DFL₂₀ histogram for DEYPLMF. The x-axis is 'F-latency group mean, ms' (15.00 to 45.00) and the y-axis is 'No. of Occurrence' (0 to 16). The distribution is unimodal and slightly left-skewed, peaking at 25ms with 14 occurrences.</p>	-0.47	2.57
6	DEYPRMF	<p>DFL₂₀ histogram for DEYPRMF. The x-axis is 'F-latency group mean, ms' (15.00 to 45.00) and the y-axis is 'No. of Occurrence' (0 to 16). The distribution is unimodal and slightly right-skewed, peaking at 25ms with 14 occurrences.</p>	0.29	2.55
7	HUSKRMF	<p>DFL₂₀ histogram for HUSKRMF. The x-axis is 'F-latency group mean, ms' (15.00 to 45.00) and the y-axis is 'No. of Occurrence' (0 to 20). The distribution is unimodal and left-skewed, peaking at 25ms with 18 occurrences.</p>	-0.45	2.13
8	ISLNRMF	<p>DFL₂₀ histogram for ISLNRMF. The x-axis is 'F-latency group mean, ms' (15.00 to 45.00) and the y-axis is 'No. of Occurrence' (0 to 16). The distribution is unimodal and slightly right-skewed, peaking at 25ms with 14 occurrences.</p>	0.13	2.44
9	KHAILMF	<p>DFL₂₀ histogram for KHAILMF. The x-axis is 'F-latency group mean, ms' (15.00 to 45.00) and the y-axis is 'No. of Occurrence' (0 to 20). The distribution is unimodal and symmetric, peaking at 25ms with 16 occurrences.</p>	0.00	2.33
10	LATNNLMF	<p>DFL₂₀ histogram for LATNNLMF. The x-axis is 'F-latency group mean, ms' (15.00 to 45.00) and the y-axis is 'No. of Occurrence' (0 to 20). The distribution is unimodal and left-skewed, peaking at 25ms with 18 occurrences.</p>	-0.23	2.20
11	MAHALMF	<p>DFL₂₀ histogram for MAHALMF. The x-axis is 'F-latency group mean, ms' (15.00 to 45.00) and the y-axis is 'No. of Occurrence' (0 to 20). The distribution is unimodal and slightly right-skewed, peaking at 25ms with 18 occurrences.</p>	0.19	2.21

Sl. No.	Nerve ID	DFL Pattern	Skewness	FWHM (ms)
12	MIAMMLMF	<p>DFL₂₀</p> <p>No. of Occurrence</p> <p>F-latency group mean, ms</p>	1.32	2.30
13	RAHARMF0	<p>DFL₂₀</p> <p>No. of Occurrence</p> <p>F-latency group mean, ms</p>	0.52	2.63
14	RAHOLMF	<p>DFL₂₀</p> <p>No. of Occurrence</p> <p>F-latency group mean, ms</p>	0.22	2.12
15	RAHORMF	<p>DFL₂₀</p> <p>No. of Occurrence</p> <p>F-latency group mean, ms</p>	0.95	2.36
16	RAYRMF	<p>DFL₂₀</p> <p>No. of Occurrence</p> <p>F-latency group mean, ms</p>	-0.10	2.50
17	SULRLMF	<p>DFL₂₀</p> <p>No. of Occurrence</p> <p>F-latency group mean, ms</p>	-0.03	2.33
18	UDDKRMF	<p>DFL₂₀</p> <p>No. of Occurrence</p> <p>F-latency group mean, ms</p>	0.57	2.13

Sl. No.	Nerve ID	DFL Pattern	Skewness	FWHM (ms)
19	ZIHMRMF0	<p>DFL₂₀</p> <p>No. of Occurrence</p> <p>F-latency group mean, ms</p>	0.04	3.05

Table 9.2: Skewness and FWHM of DFL with broad peak (33 median nerves of 24 subjects)

Sl. No.	Nerve ID	DFL Pattern	Skewness	FWHM (ms)
1	AKTFLMF	<p>DFL₂₀</p> <p>No. of Occurrence</p> <p>F-latency group mean, ms</p>	0.25	4.29
2	AKTFRMF	<p>DFL₂₀</p> <p>No. of Occurrence</p> <p>F-latency group mean, ms</p>	0.88	2.91
3	BAPDRMF	<p>DFL₂₀</p> <p>No. of Occurrence</p> <p>F-latency group mean, ms</p>	-0.84	2.63
4	BEGALMF	<p>DFL₂₀</p> <p>No. of Occurrence</p> <p>F-latency group mean, ms</p>	0.53	3.14
5	BEGKMLMF	<p>DFL₂₀</p> <p>No. of Occurrence</p> <p>F-latency group mean, ms</p>	0.03	3.42

Sl. No.	Nerve ID	DFL Pattern	Skewness	FWHM (ms)
6	BIBLMF	<p>DFL₂₀</p> <p>No. of Occurrence</p> <p>F-latency group mean, ms</p>	-0.63	3.78
7	DEYCNLMF	<p>DFL₂₀</p> <p>No. of Occurrence</p> <p>F-latency group mean, ms</p>	-0.06	3.05
8	DEYCNRMF	<p>DFL₃₀</p> <p>No. of Occurrence</p> <p>F-latency group mean, ms</p>	0.70	4.00
9	DEYPLMF	<p>DFL₂₀</p> <p>No. of Occurrence</p> <p>F-latency group mean, ms</p>	-0.47	3.14
10	DEYPRMF	<p>DFL₂₀</p> <p>No. of Occurrence</p> <p>F-latency group mean, ms</p>	0.29	2.75
11	HASSRMF	<p>DFL₂₀</p> <p>No. of Occurrence</p> <p>F-latency group mean, ms</p>	1.09	4.40
12	HUSKLMF	<p>DFL₂₀</p> <p>No. of Occurrence</p> <p>F-latency group mean, ms</p>	0.41	3.20

Sl. No.	Nerve ID	DFL Pattern	Skewness	FWHM (ms)
13	HUSKRMF	<p>DFL₂₀</p> <p>No. of Occurrence</p> <p>F-latency group mean, ms</p>	-0.45	2.75
14	ISLNRMF	<p>DFL₂₀</p> <p>No. of Occurrence</p> <p>F-latency group mean, ms</p>	0.13	3.5
15	JABALMF	<p>DFL₂₀</p> <p>No. of Occurrence</p> <p>F-latency group mean, ms</p>	-0.13	2.75
16	JABARMF	<p>DFL₂₀</p> <p>No. of Occurrence</p> <p>F-latency group mean, ms</p>	0.28	2.75
17	KHAILMF	<p>DFL₂₀</p> <p>No. of Occurrence</p> <p>F-latency group mean, ms</p>	0.00	3.78
18	LATNNLMF	<p>DFL₂₀</p> <p>No. of Occurrence</p> <p>F-latency group mean, ms</p>	-0.23	3.78
19	MAHARMF0	<p>DFL₂₀</p> <p>No. of Occurrence</p> <p>F-latency group mean, ms</p>	-0.08	3.78

Sl. No.	Nerve ID	DFL Pattern	Skewness	FWHM (ms)
20	MIAMMLMF	<p>DFL₂₀</p> <p>No. of Occurrence</p> <p>F-latency group mean, ms</p>	1.32	2.40
21	PERSLMF	<p>DFL₂₀</p> <p>No. of Occurrence</p> <p>F-latency group mean, ms</p>	0.49	3.50
22	PERSRMF	<p>DFL₂₀</p> <p>No. of Occurrence</p> <p>F-latency group mean, ms</p>	0.48	5.26
23	RAHALMF0	<p>DFL₂₀</p> <p>No. of Occurrence</p> <p>F-latency group mean, ms</p>	-0.21	3.50
24	RAHOLMF	<p>DFL₂₀</p> <p>No. of Occurrence</p> <p>F-latency group mean, ms</p>	0.22	3.38
25	RAHSLMF0	<p>DFL₂₀</p> <p>No. of Occurrence</p> <p>F-latency group mean, ms</p>	0.68	3.71
26	RAYRMF	<p>DFL₂₀</p> <p>No. of Occurrence</p> <p>F-latency group mean, ms</p>	-0.10	3.14

Sl. No.	Nerve ID	DFL Pattern	Skewness	FWHM (ms)
27	RAYRMF	<p>DFL₂₀</p> <p>No. of Occurrence</p> <p>F-latency group mean, ms</p>	-0.10	3.14
28	SARTALMF	<p>DFL₂₀</p> <p>No. of Occurrence</p> <p>F-latency group mean, ms</p>	-0.15	4.00
29	SULRRMF	<p>DFL₂₀</p> <p>No. of Occurrence</p> <p>F-latency group mean, ms</p>	0.40	3.35
30	ZAMMLMF	<p>DFL₂₀</p> <p>No. of Occurrence</p> <p>F-latency group mean, ms</p>	0.06	3.78
31	ZAMMRMF	<p>DFL₂₀</p> <p>No. of Occurrence</p> <p>F-latency group mean, ms</p>	-0.48	3.20
32	ZIHMLMF	<p>DFL₂₀</p> <p>No. of Occurrence</p> <p>F-latency group mean, ms</p>	0.22	3.14
33	ZIHMRMF0	<p>DFL₂₀</p> <p>No. of Occurrence</p> <p>F-latency group mean, ms</p>	0.04	4.00

Table 9.3: Statistical analysis of Skewness and FWHM for single and broad peaks of DFL

	No. of nerves	Skewness (mean \pm SD)	FWHM (mean \pm SD), ms
Single peak	19	0.13 \pm 0.53	2.37 \pm 0.25
Broad Peak	33	0.14 \pm 0.48	3.43 \pm 0.60
t-value	----	0.08	9.08
Test of Significance (P value)	----	>> 0.20	<< 0.01
Preliminary choice of threshold for identification of broad peak	----	None	> 2.5

Table 9.3 shows that there is no significant difference of the skewness between the DFL pattern with single peak and broad peak since the p value (of the two classes being the same) is far greater than 20%. On the other hand, there is a highly significant difference of the FWHM between the DFL pattern with single peak and broad peak since the p value (of the two classes being the same) is far less than 1%.

9.4. Discussions

Distribution of F-latencies (DFL) has already been established as a means to detect Cervical Spondylotic Radiculopathy and Myelopathy (CRM) with confidence by the group at Dhaka University in the earlier years. Double and broad peaks of DFL indicate CRM, while a sharp single peak indicate normalcy. Double peaks are fairly easy to identify but the broad peaks are not, some time they look very similar to single peaks. In an earlier work (Rabbani et al., 2014) it was shown that a DFL for which the value of the frequency at the peak is less than or equal to 3 times that of an adjacent frequency value may be considered to be a broad peak as it gave a good matching with the diagnosis based on MRI. Therefore, the distinction between the patterns of normal and abnormal DFL is very subtle specially in the case of broad peak.

In the present chapter we tried to find an alternative means to distinguish a broad peak from a single peak. The study in the present chapter tried to find if two commonly used parameters, skewness and full width at half maximum (FWHM), can characterize the shapes to detect CRM.

From Table 9.3 we can see that the Skewness is not very different for the two patterns of DFL, but FWHM is significantly different. This indicates that FWHM may be used

as a parameter to distinguish single and broad peaks of DFL. The success of FWHM and failure of Skewness is somewhat expected since it was observed that the same raw data may give both single peak or broad peak of DFL depending on the starting point of DFL, and Skewness is derived from the raw data. On the other hand FWHM is derived from the DFL pattern itself; therefore, it is likely to represent the shape of DFL well.

The last row in Table 9.3 gives a possible threshold for taking a decision regarding distinction of single peaks and broad peaks using FWHM. A preliminary choice of 2.5 ms as the threshold for FWHM was identified observing the data. If the value of FWHM is less than 2.5 ms we may take the DFL as having a single peak, and if it is greater, we may identify it as a broad peak. However, this is a preliminary choice. A much larger study needs to be taken up to find a threshold value with greater accuracy.

Thus the study presented in this chapter has been able to identify that FWHM can be used effectively to identify whether a DFL has a single peak or a broad peak, but not Skewness.

Summary and Conclusion

The present work tried to improve the efficacy of Distribution of F-Latency (DFL) in the diagnosis of Cervical Radiculopathy and Myelopathy (CRM) with a limited number of data in a sample (30 to 40 F-responses), as this will be clinically acceptable. The overall research work as described in the earlier chapters can be summarized below:

Chapter 6: Distribution of Conduction Velocity (DCV) of nerve fibres in a peripheral nerve is necessary for a proper assessment of neural health and diagnosis of neuropathy. It was established earlier that as DFL owes its origin to DCV, an approximate DCV of motor nerves may be obtained directly as a mirror image of DFL. In the present work we obtained conduction velocities (CV) directly from the 30 to 40 F-responses and then tried to compute DCV from these CV values. However, since a large experience has been built up through earlier work of our extended group in relating the shapes of DFL obtained from the median nerve to Cervical Radiculopathy and Myelopathy, we wanted to obtain DCVs that show similar but laterally inverted (mirrored) shapes. For this the bin width used to obtain the frequency distribution is very important as the number of samples is limited. Our extended group used 2 ms bin width to obtain DFL, so we tried to determine the most appropriate bin width for computing DCV from CVs so that the above mentioned features are retained. We studied this aspect varying the bin widths of DCVs for data obtained from many human subjects. For this we related the typically used 2ms bin width of DFL for each nerve to the average of the maximum and minimum values, median and mode values of the corresponding CV data. It was found that by relating the median value of CV to the 2ms bin width used for DFL, the best result for DCV may be obtained.

Chapter 7: An important part of this study was the sample size of DFL, i.e., to find out how many F-latencies are adequate to make a DFL for a particular bin size, particularly to make it effective in the detection of CRM. Two independent sets of data were used to make the judgment in between normal and abnormal DFL patterns. One used data collected from 25 median nerves of 16 persons earlier by members of our extended group. These had more than 30 but less than 40 F-latencies each. Another set of data were generated from a large number (about 200 or more) of

recorded non-zero F-latency values from three nerves of two subjects, obtained during the present work. For both of the cases bin sizes were chosen at 1.5ms and 2ms. Combining all the study it was found that a minimum sample of 20 F-latencies can give a representative for the detection of CRM if the bin width is chosen at 1.5ms or 2.0ms.

Chapter 8: Broad or double peaked patterns of DFL have already been established for detection of CRM by our extended group at Dhaka University and its foreign collaborators earlier, as against sharp single peaks which represent normalcy. During the present work it was observed that if the starting point of DFL is shifted by half the bin width (by 1ms where the bin width is 2ms, used mostly in the DFL work) then the DFL peak pattern may in some cases change from single to broad, or broad to double or vice-versa. This happens as the number of samples (F-latencies) involved is low, typically about 30 to 40. The measurement of F-latencies requires giving reasonably strong electrical stimulations to nerves which is unpleasant and a patient would not cooperate if the number is increased much beyond the above figures. The above observation regarding the change of pattern of DFL created a great uncertainty in the prediction of CRM, particularly for the changes between single and broad peak patterns as this changes the prediction altogether. In order to remove this uncertainty we carried out a detailed analysis on the data obtained from many human subjects earlier. The study was performed on the quality of prediction using DFLs obtained using the individual DFLs, and a combined result of the two shifted DFL patterns through a logical OR and a logical AND operation, where a 'Yes' corresponded to the presence of CRM. The predictions were adjudged against MRI findings which is the 'gold standard' at present for detecting CRM. It was found from our study that a logical OR operation gave the best result.

Chapter 9: In this chapter we tried to find alternative means of characterizing DFL patterns quantitatively, particularly between the single and broad peaks as the difference is very subtle, and it has an important bearing on the prediction of CRM as discussed before. We tried two common parameters – Skewness and Full Width Half Maximum (FWHM) – for this purpose. We calculated these values for single and broad peaked patterns of DFLs obtained from many subjects and performed statistical t-tests to determine if any of these parameters can distinguish between these two

patterns significantly. It was found that skewness could not distinguish the patterns at all while FWHM could do it very well at a very high level of significance. From an observation of the FWHM values from both the groups, a preliminary threshold value was chosen at 2.5ms; a larger value would indicate a broad peak, giving an indication that this is a case of CRM. Of course a study involving a large number of data needs to be carried out to determine an accurate value of the threshold.

The present study strengthens our confidence in characterizing the DFL patterns both qualitatively and quantitatively for the diagnosis of CRM. DFL can be measured using standard EMG equipment which can be made at a much lower cost in comparison with MRI machines, investigation using which is considered as the 'gold standard of the day' in the diagnosis. Portable EMG units based on Laptop computers are also available. Therefore, such portable equipment for measuring DFL can be distributed widely.

The present work builds up sufficient knowledge and confidence in the use of DFL for specific determination of CRM which will go a long way in the diagnosis of neural disorders, contributing to public health, and the society in general.

References

- ACKIL, A. A., SHAHANI, B. R. & YOUNG, R. R. (1981) Sural nerve conduction studies and late responses in children undergoing hemodialysis. *Arch Phys Med Rehabil.*, 62, 487-491.
- ALAM, M. J. & RABBANI, K. S. (2010) Possible detection of cervical spondylotic neuropathy using Distribution of F-latency (DFL), a new neurophysiological parameter. *BMC Research Notes*, 3.
- ALFONSI, E., MERLINI, G. P., GIORGETTI, A., CERONI, M., PICCOLO, G., AGOSTINIS, C. & SAVOLDI, F. (1987) Temperature-related changes in sensory nerve conduction: studies in normal subjects and in patients with paraproteinaemia. *Electromyogr. Clin. Neurophysiol.*, 27, 277-282.
- ANDERSEN, H., STALBERG, E. & FALCK, B. (1997) F-wave latency, the most sensitive nerve conduction parameter in patients with diabetes mellitus. *Muscle Nerve*, 20, 1296 - 1302.
- ANDERSEN, K. (1985) Surface recording of orthodromic sensory nerve action potentials in median and ulnar nerves in normal subjects. *Muscle Nerve*, 8, 402-408.
- ARASAKI, K. (1992) Maximal and minimal motor nerve conduction velocities determined by a collision method: correlation with axonal conduction velocity of type-identified motor units. *J. Neurol. Sci.*, 110, 131-138.
- ARASAKI, K., IJIMA, M. & NAKANISHI, T. (1991) Normal maximal and minimal motor nerve conduction velocities in adults determined by a collision method. *Muscle Nerve*, 14, 647-653.
- ARGYROPOULOS, C. J., PANAYIOTOPOULOS, C. P. & SCARPALEZOS, S. (1978) F- and M-wave conduction velocity in amyotrophic lateral sclerosis. *Muscle Nerve*, 1, 479 - 485.
- ASBURY, A. K. & JOHNSON, P. C. (1978) *Pathology of Peripheral Nerve*, Philadelphia, London, Toronto, W.B. Saunders.
- ASHWORTH, N. L., MARSHALL, S. C. & SATKUNAM, L. E. (1998) The effect of temperature on nerve conduction parameters in carpal tunnel syndrome. *Muscle Nerve*, 21, 1089-1091.
- BARKER, A. T., BROWN, B. H. & FREESTON, I. L. (1979) Modeling of an active nerve fiber in finite volume conductor and its application to the calculation of surface action potentials. *IEEE Trans Biomed Eng.*, 26, 53-56.
- BARWICK, D. & FAWCETT, P. R. W. (1988) The clinical physiology of neuromuscular disease. IN WALTON, S. (Ed.) *Disorders of Voluntary Muscle*. Edinburgh, Churchill Livingstone.
- BEHSE, F. (1990) Morphometric studies on the human sural nerve. *Acta Neurol. Scand.*, 82, 5-38.
- BEHSE, F. & BUCHTHAL, F. (1971) Normal sensory conduction in the nerves of the leg in man. *J. Neurol. Neurosurg. Psychiatry*, 34, 404-414.
- BERGER, A. R. & SCHAUMBURG, H. H. (1995) Human peripheral nerve disease (peripheral neuropathies). IN WAXMAN, S. G., KOCISIS, J. D. & STYS, P.

- K. (Eds.) *The Axon: Structure, Function and Pathophysiology*. New York, Oxford, Oxford University Press.
- BERTHOLD, C. H. & RYDMARK, M. (1995) Morphology of normal peripheral axons. IN WAXMAN, S. G., KOCSIS, J. D. & STYS, P. K. (Eds.) *The Axon: Structure, Function and Pathophysiology*. New York, Oxford, Oxford University Press.
- BISCHOFF, C., SCHOENLE, P. W. & CONRAD, B. (1992) Increased F- Wave duration in patients with spasticity. *Electromyogr Clin Neurophysiol*, 32, 449-453.
- BOSTOCK, H., SEARS, T. A. & SHERRATT, R. M. (1981) The effects of 4-aminopyridine and tetraethylammonium ions on normal and demyelinated mammalian nerve fibres. *J. Physiol.*, 313, 301-315.
- BOSTOCK, H., SHERRATT, R. M. & SEARS, T. A. (1978) Overcoming conduction failure in demyelinated nerve fibres by prolonging action potentials. *Nature*, 274, 385-387.
- BRADLEY, W. (1978) Editorial: The F-wave determination controversy. *Muscle Nerve*, 1, 180.
- BUCHTHAL, F. & ROSENFALCK, A. (1966) Evoked action potentials and conduction velocity in human sensory nerves. *Brain Res.*, 3, 1-122.
- BURKE, D., ADAMS, R. W. & SKUSE, N. F. (1989) The effects of voluntary contraction on the H reflex of human limb muscles. *Brain*, 112(Pt 2), 417-433.
- BURKE, D., MOGYOROS, I., VAGG, R. & KIERNAN, M. C. (1999) Temperature dependence of excitability indices of human cutaneous afferents. *Muscle Nerve*, 22, 51-60.
- CADDY, D. J., KRANZ, H. & WESTERMAN, R. A. (1981) Electrophysiological determination of peripheral nerve conduction velocity distribution. IN KIDMAN, A., TOMKINS, J. & WESTERMAN, R. (Eds.) *New Approaches to Nerve and Muscle Disorders*. Amsterdam, Excerpta Medica.
- CAI, F. C. & ZHANG, J. M. (1997) Study of nerve conduction and late responses in normal Chinese infants, children, and adults. *J. Child Neurol.*, 12, 13-18.
- CARUSO, G., MASSINI, R., CRISCI, C., NILSSON, J., CATALANO, A., SANTORO, L., BATTAGLIA, F., CRISPI, F. & NOLANO, M. (1992) The relationship between electrophysiological findings, upper limb growth and histological features of median and ulnar nerves in man. *Brain*, 115, 1925-1945.
- CHOWDHURY, E. A. (2013) Study of the efficacy of the Distribution of F-latency (DFL) in the diagnosis of cervical spondylosis. *M.Phil. Thesis*.
- CHOWDHURY, E. A., RAHMAN, M. O. & RABBANI, K. S. (2014) Comparing DFL and MRI findings. *Bangladesh Journal of Medical Physics*, 6.
- CHRONI, E. & PANAYIOTOPOULOS, C. P. (1993a) F tacheodispersion. *J. Neurol. Neurosurg. Psychiatry*, 56, 1103-1108.
- CHRONI, E. & PANAYIOTOPOULOS, C. P. (1993b) F tacheodispersion: quantitative analysis of motor fiber conduction velocities in patients with polyneuropathy. *Muscle Nerve*, 16, 1302-1309.

- CLAUSSEN, G. C., ODABASI, Z. & OH, S. J. (1996) Near nerve sensory conduction study in chronic sensory demyelinating neuropathy. *Muscle Nerve*, 19, 1219-1220.
- CONRAD, B., ASCHOFF, J. C. & FISCHIER, M. (1975) Der diagnostische Wert der F-Wellen-Latenz. *J Neurol*, 210, 151-159.
- CUMMINS, K. L. & DORFMAN, L. J. (1981) Nerve fiber conduction velocity distributions: studies of normal and diabetic human nerves. *Ann. Neurol.*, 9, 67-74.
- CUMMINS, K. L., DORFMAN, L. J. & PERKEL, D. H. (1979a) Nerve fiber conduction-velocity distributions. II. Estimation based on two compound action potentials. *Electroencephalogr Clin Neurophysiol*, 46, 647-658.
- CUMMINS, K. L., PERKEL, D. H. & DORFMAN, L. J. (1979b) Nerve fiber conduction-velocity distributions. I. Estimation based on the single-fiber and compound action potentials. *Electroencephalogr Clin Neurophysiol*, 46, 634-646.
- DAUBE, J. R. (1996) Compound muscle action potentials. IN DAUBE, J. (Ed.) *Clinical Neurophysiology*. Philadelphia, Davis.
- DAWSON, G. D. (1956) The relative excitability and conduction velocity of sensory and motor nerve fibres in man. *J Physiol.*, 131, 436-451.
- DELISA, J. A., LEE, H. J., BARAN, H. M. & SPILHOLZ, N. (1994) F wave in the lower extremity. IN JA DELISA, HJ LEE, HM BARAN & SPILHOLZ, N. (Eds.) *Manual of Nerve Conduction Velocity and Clinical Neurophysiology*. New York, Raven Press.
- DENGLER, R., STEIN, R. B. & THOMAS, C. K. (1988) Axonal conduction velocity and force of single human motor units. *Muscle Nerve*, 11, 136-145.
- DEVRIES, L. S. (1996) Neurological assessment of the preterm infant. *Acta Paediatr.*, 85, 765-771.
- DORFMAN, L. J., CUMMINS, K. L. & ABRAHAM, G. S. (1982) Conduction velocity distributions of the human median nerve: Comparison of methods. *Muscle Nerve*, 5, 148-153.
- DROZDOWSKI, W., KOCHANOWIEZ, J. & BANIUKIEWICZ, E. (1998) F wave occurrence in patients after stroke. *Neurol Neurochir Pol.*, 32, 1341-1352.
- EISEN, A., HOIRCH, M., WHITE, J. & CLANE, D. (1984) Sensory group la proximal conduction velocity. *Muscle Nerve*, 7.
- EISEN, A., SCHOMER, D. & MEIMED, C. (1977a) An electrophysiological method for examining lumbosacral root compression. *Can J Sci Neurol*, 4, 117-123.
- EISEN, A., SCHOMER, D. & MELMED, C. (1977b) The application of F-wave measurements in the differentiation of proximal and distal upper limb entrapments. *Neurology*, 27, 662-668.
- EXCEL, M. (2015) EXCEL 2007: Histogram.
- FISHER, M. A. (1982) F response latency determination. *Muscle Nerve*, 5, 730-734.

- FISHER, M. A. (1983) Cross correlation analysis of F response variability and its physiological significance. *Electroencephalogr Clin Neurophysiol*, 23, 329-339.
- FISHER, M. A. (1992) H reflexes and F-waves: physiology and clinical indications. *Muscle Nerve*, 15, 1223-1233.
- FISHER, M. A., HOFFOR, B. & HULTIMOL, C. (1994) Normative F wave values and the number of recorded F waves. *Muscle Nerve*, 17, 1185-1189.
- FISHER, M. A., SHAHANI, B. T. & YOUNG, R. R. (1978) Assessing segmental excitability after acute rostral lesions. I. The F response (Minneapolis). *Neurology*, 28, 1265-1271.
- FOWLER, C. J. (1993) Electromyography and nerve conduction. IN CD BINNIE, R COOPER, CJ FOWLER, F MAUGUIERE & PRIOR, P. (Eds.) *Clinical Neurophysiology: EMG, Nerve Conduction and Evoked Potentials*. Oxford, Butterworth-Heinemann.
- FOX, J. E. & HITCHCOCK, E. R. (1987) F wave size as a monitor of motor neuron excitability: Effect of deafferentation. *J Neurol. Neurosurg. Psychiatry*, 50 453-459.
- FRANSSSEN, H. & WIENEKE, G. H. (1994) Nerve conduction and temperature. Necessary warming time. *Muscle Nerve*, 17, 336-344.
- FRANSSSEN, H., WIENEKE, G. H. & WOKKE, J. H. (1999) The influence of temperature on conduction block. *Muscle Nerve*, 22, 166-173.
- FRASER, J. L. & OLNEY, R. K. (1992) The relative diagnostic sensitivity of different F-wave parameters in various polyneuropathies. *Muscle Nerve*, 15, 912-918.
- GARDNER, E. P., MARTIN, J. H. & JESSELL, T. M. (2000) The bodily senses. IN KANDEL, E. R., SCHWARTZ, J. H. & JESSELL, T. M. (Eds.) *Principles of Neural Science*. New York, McGraw-Hill.
- GASSER, H. S. (1941) The classification of nerve fibers. *Ohio J. Sci.*, 41, 145.
- GASSER, H. S. & ERLANGER, J. (1927) The role played by the sizes of the constituent fibers of a nerve trunk in determining the form of its action potential wave. *Am. J. Physiol.*, 80, 522.
- GILLIATT, R. W. (1978) Sensory conduction studies in the early recognition of nerve disorders. *Muscle Nerve*, 1, 352-359.
- GILLIATT, R. W., HOPF, H. C., RUDGE, P. & BARAITSER, M. (1976) Axonal velocities of motor units in the hand and foot muscles of the baboon. *J. Neurol. Sci.*, 29, 249-258.
- GUILOFF, R. J. & MODARRES-SADEGHI, H. (1991) Preferential generation of recurrent responses by groups of motor neurons in man. Conventional and single unit F-wave studies. *Brain*, 114 (Pt 4), 1771-1801.
- HANSEN, K. & SCHLIACK, H. (1962) *Segmentale Innervation*, Stuttgart, Thieme.
- HARAYAMA, H., SHINOZAWA, K., KONDO, H. & MIYATAKE, T. (1991) A new method to measure the distribution of motor conduction velocity in man. *Electroencephalogr Clin Neurophysiol*, 81, 323-331.

- HAYMAKER, W. & WOODHALL, B. (1953) *Peripheral Nerve Injuries*, Philadelphia, W. B. Saunders.
- HEIDENREICH, F. & VINCENT, A. (1998) Antibodies to ion-channel proteins in thymoma with myasthenia, neuromyotonia, and peripheral neuropathy. *Neurology*, 50, 1483-1485.
- HODGKIN, A. L. (1958) Ionic movements and electrical activity in giant nerve fibres. *Proceedings of the Royal Society B*, 148, 1-37.
- HOFFMAN, P. (1922) *Untersuchungen uber die Eigenreflexe (Sehnenreflexe), Menschlicher Muskeln*, Springer.
- HOPF, H. C. (1962) Untersuchungen uber die unterschiede in der leitgeschwindigkeit motorischer nervenfasern beim menschen. *Deutscher Z. Nervenerkrankungen*, 183, 579-588.
- HOROWITZ, S. H. & KRARUP, C. (1992) Conduction studies of the normal sural nerve. *Muscle Nerve*, 15, 374-383.
- HOSSAIN, M. I., CHOWDHURY, E. A., MAMUN, A. A., SALAM, A., BAIG, T. N. & RABBANI, K. S. (2011) Use of Distribution of F-latency (DFL) in the Detection of Cervical Spondylotic Neuropathy. *Bangladesh Journal of Medical Physics*, 4, 37-42.
- INGRAM, D. A., DAVIS, G. R. & SWASH, M. (1987) Motor nerve conduction velocity distributions in man: results of a new computer-based collision technique. *Electroencephalogr. Clin. Neurophysiol.*, 66, 235-243.
- KADRIE, H., YATES, S. K., MILNER-BROWN, H. S. & BROWN, W. F. (1976) Multiple point electrical stimulation of ulnar and median nerves. *J. Neurol. Neurosurg. Psychiatry*, 39, 973-985.
- KAJI, R. (2003) Physiology of conduction block in multifocal motor neuropathy and other demyelinating neuropathies. *Muscle Nerve*, 27, 285-296.
- KIERNAN, M. C., CIKUREL, K. & BOSTOCK, H. (2001a) Effects of temperature on the excitability properties of human motor axons. *Brain*, 124, 816-825.
- KIERNAN, M. C., HART, I. K. & BOSTOCK, H. (2001b) Excitability properties of motor axons in patients with spontaneous motor unit activity. *J. Neurol. Neurosurg. Psychiatry*, 70, 56-64.
- KIMURA, J. (1974) F-wave velocity in the central segment of the median and ulnar nerves: A study in normal subjects and in patients with Charcot-Marie-Tooth disease. *Neurology*, 24, 539-546.
- KIMURA, J. (1976) A method for estimating the refractory period of motor fibers in the human peripheral nerve. *J. Neurol. Sci.*, 28, 485-490.
- KIMURA, J. (1978) Proximal versus distal slowing of motor nerve conduction velocity in the Guillain-Barre syndrome. *Ann Neurol*, 3, 344-350.
- KIMURA, J. (1983) *Electrodiagnosis in Diseases of Nerve and Muscle: Principles and Practices*, Philadelphia, Davis.
- KIMURA, J. (1989) *Electrodiagnosis in diseases of nerve and muscle: Principles and practice*, Philadelphia, F.A. Davis company.

- KIMURA, J. (1993) Nerve conduction studies and electromyography. IN PJ DYCK, PK THOMAS, JW GRIFFIN, PA LOW & PODULSO, J. (Eds.) *Peripheral Neuropathy*. Philadelphia, Saunders.
- KIMURA, J. (2001) *Electrodiagnosis in Diseases of Nerve and Muscle: Principles and Practice*, New York, Oxford University Press.
- KIMURA, J., BOSCH, P. & LINDSAY, G. M. (1975) F-wave conduction velocity in the central segment of the peroneal and tibial nerves. *Arch Phys Med Rehabil.*, 56, 492-497.
- KIMURA, J. & BUTZER, J. F. (1975) F-wave conduction velocity in Guillain -Barre syndrome: Assessment of nerve segment between axilla and spinal cord. *Arch Neurol*, 32, 524-529.
- KIMURA, J., BUTZER, J. F. & VAN ALLEN, M. W. (1974) F-wave conduction velocity between axilla and spinal cord in the Guillain-Barré syndrome. *Trans. Am. Neurol. Assoc.*, 99, 52-62.
- KIMURA, J., YAMADA, T. & STEVLAND, N. P. (1979) Distal slowing of motor nerve conduction velocity in diabetic polyneuropathy. *J Neurol Sci*, 42, 291-302.
- KING, D. & ASHBY, P. (1976) Conduction velocity in the proximal segments of a motor nerve in the Guillain-Berre syndrome. *J Neurol Neurosurg Psychiatry*, 39, 538-544.
- KOHARA, N., KIMURA, J., KAJI, R., GOTO, Y., ISHII, J., TAKIGUCHI, M. & NAKAI, M. (2000) F-wave latency serves as the most reproducible measure in nerve conduction studies of diabetic polyneuropathy: multicentre analysis in healthy subjects and patients with diabetic polyneuropathy. *Diabetologia*, 43, 915-921.
- LABBOK, A. (1937) Anatomische Untersuchungen and Typen des Kreuzabschnittes der Trunci sympathici. *Anat. Anz.*, 85, 14.
- LACHMAN, T., SHAHANI, B. T. & YOUNG, R. R. (1980) Late responses as aids to diagnosis in peripheral neuropathy. *J Neurol Neurosurg Psychiatry*, 43.
- LANE, D. M. (2015) Online Statistics Education: A Multimedia Course of Study (<http://onlinestatbook.com/>) (chapter 2 "Graphing Distributions", section "Histograms"). Rice University.
- LEE, R. G., ASHBY, P., WHITE, D. G. & AGUAYO, A. J. (1975) Analysis of motor conduction velocity in the human median nerve by computer simulation of compound muscle action potentials. *Electroencephalography and Clinical Neurophysiology*, 39, 225-237.
- LEFEBVRE D' AMOUR, M., SHAHANI, B. T., YOUNG, R. R. & BIRD, K. T. (1979) The importance of studying sural nerve conduction and late responses in the evaluation of alcoholic subjects. *Neurology*, 29, 1600-1604.
- LEIFER, L. J. (1981) Nerve-fiber conduction velocity distributions: Motor nerve studies using collision neurography. *Prog. Clin. Biol. Res*, 52, 233-263.
- LEIFER, L. J., MEYER, M., MORF, M. & PETRIG, B. (1977) Nerve bundle conduction velocity distribution measurement and transfer function analysis. *Proc IEEE* 65:747-755, 1977. *Proc. IEEE*, 65, 747-755.

- LETZ, R. & GERR, F. (1994) Covariates of human peripheral nerve function: In: Nerve conduction velocity and amplitude. *Neurotoxicol. Teratol.*, 16, 95-104.
- LIVESON, J. A. & MA, D. M. (1992) Late responses. IN JA LIVESON & MA, D. (Eds.) *Laboratory Reference for Clinical Neurophysiology*. Philadelphia, Davis.
- LORENTE DE NO (1947) A Study of Nerve Physiology. *Stud. Rockefeller Inst. Med Res.*, 384-482.
- MAGLADERY, J. W. & MCDUGAL, J. D. B. (1950) Electrophysiological studies of nerve and reflex activity in normal man. *Bull John Hopkins Hosp.*, 86, 265-290.
- MARRA, T. R. (1987) F wave measurements: A comparison of various recording techniques in health and peripheral nerve disease. *Electroencephalogr Clin Neurophysiol*, 27, 33-37.
- MAYER, R. F. & FELDMAN (1967) Observations on the nature of F wave in man. *Neurology*, 17, 147-156.
- MCLEOD, J. G. & WRAY, S. H. (1966) An experimental study of the F wave in the baboon. *J Neurol. Neurosurg. Psychiatry*, 29, 196-200.
- MOGYOROS, I., KIERNAN, M. C., BURKE, D. & BOSTOCK, H. (1997) Excitability changes in human sensory and motor axons during hyperventilation and ischaemia. *Brain*, 120, 317-325.
- MOGYOROS, I., KIERNAN, M. C., BURKE, D. & BOSTOCK, H. (1998) Strength-duration properties of sensory and motor axons in amyotrophic lateral sclerosis. *Brain*, 121, 851-859.
- NAKANISHI, T., TAMAKI, M. & ARASAKI, K. (1989) Maximal and minimal motor nerve conduction velocities in amyotrophic lateral sclerosis. *Neurology*, 39, 580-583.
- NAKANISHI, T., TAMAKI, M., MIZUSAWA, H., AKATSUKA, T. & KINOSHITA, T. (1986) An experimental study for analyzing nerve conduction velocity. *Electroencephalogr. Clin. Neurophysiol.*, 63, 484-487.
- NEWSOM-DAVIS, J. (1997) Autoimmune neuromyotonia (Isaacs' syndrome): an antibody-mediated potassium channelopathy. *Ann. N Y Acad. Sci.*, 835, 111-119.
- NOBREGA, J. A., MANZANO, G. M., NOVO, N. F. & MONTEAGUDO, P. T. (2000) F-waves and conduction velocities range *Electromyogr. Clin. Neurophysiol.*, 40, 327-329.
- ODABASI, Z., OH, S. J., CLAUSSEN, G. C. & S., K. D. (1999) New near-nerve needle nerve conduction technique differentiating epicondylar from cubital tunnel ulnar neuropathy. *Muscle Nerve*, 22, 718-723.
- OH, S. J. (1993) Anatomical guide for common nerve conduction studies. IN OH, S. (Ed.) *Clinical Electromyography: Nerve Conduction Studies*. Baltimore, Williams & Wilkins.
- OH, S. J. (2002) Nerve conduction velocity tests: their clinical applications. IN BERTORINI, T. E. (Ed.) *Clinical Evaluation and Diagnostic Tests For Neuromuscular Disorders*. Boston, Butterworth Heinemann.

- OH, S. J., JOY, J. L. & KURUOGLU, R. (1992) Chronic sensory demyelinating neuropathy": chronic inflammatory polyneuropathy presenting as a pure sensory neuropathy. *J. Neurol. Neurosurg. Psychiatry*, 55, 677-680.
- OH, S. J., KIM, H. S. & AHMAD, B. K. (1985) The near-nerve sensory nerve conduction in tarsal tunnel syndrome. *J. Neurol. Neurosurg. Psychiatry*, 48, 999-1003.
- OH, S. J., MELO, A. C. & LEE, D. K. (2001) Large-fiber neuropathy in distal sensory neuropathy with normal routine nerve conduction. *Neurology*, 56, 1570-1572.
- OUVRIER, R. A., MCLEOD, J. G. & CONCHIN, T. (1987) Morphometric studies of sural nerve in childhood. *Muscle Nerve*, 10, 47-53.
- PAINTAL, A. S. (1965) Effects of temperature on conduction in single vagal and saphenous myelinated nerve fibres of the cat. *J. Physiol.*, 180, 20-49.
- PAINTAL, A. S. (1966) The influence of diameter of medullated nerve fibres of cats on the rising and falling phases of the spike and its recovery. *J. Physiol.*, 184, 791-811.
- PANAYIOTOPOULOS, C. P. (1979) F chronodispersion: A new electrophysiologic method. *Muscle Nerve*, 2, 68-72.
- PANAYIOTOPOULOS, C. P. & CHRONI, E. (1996) F-waves in clinical neurophysiology: a review, methodological issues and overall value in peripheral neuropathies. *Electroencephalogr. Clin. Neurophysiol.*, 101, 365-374.
- PANAYIOTOPOULOS, C. P. & LAGOS, G. (1980) Tibial nerve H-reflex and F-wave studies in patients with uremic neuropathy. *Muscle Nerve*, 3, 423-426.
- PANAYIOTOPOULOS, C. P., S., S. & NASTAS, P. E. (1978) Sensory: (1a) and F-wave conduction velocity in the proximal segment of the tibial nerve. *Muscle Nerve*, 1, 181-189.
- PANAYIOTOPOULOS, C. P. & SCARPALEZOS, S. (1977) F-wave studies on the deep peroneal nerve. Part 2. 1. Chronic renal failure. 2. Limb-girdle muscular dystrophy. *J Neurol Sci*, 31, 331-341.
- PANAYIOTOPOULOS, C. P., SCARPALEZOS, S. & NASTAS, P. E. (1977) F-wave studies on deep peroneal nerve. Part 1. Control subjects. *J Neurol Sci*, 31, 319-329.
- PEARSON, K. & GORDON, J. (2000) Spinal reflexes. IN KANDEL, E. R., SCHWARTZ, J. H. & JESSELL, T. M. (Eds.) *Principles of Neural Science*. New York, McGraw-Hill.
- PEIOGLOU-HARMOUSSI, S., FAWCETT, P. R. W., HOWEL, D. & BARWICK, D. D. (1987) F-response frequency in motor neuron disease and cervical spondylosis. *J Neurol Neurosurg Psychiatry*, 50, 593-599.
- PIERRAT, V., EKEN, P., TRUFFERT, P., DUQUENNOY, C. & DEVRIES, L. S. (1996) Somatosensory evoked potentials in preterm infants with intrauterine growth retardation. *Early Hum. Dev.*, 44, 17-25.

- PITT, M. C. (1996) A system-based study of the variation in the amplitude of the compound sensory nerve action potential recorded using surface electrodes. *Electroencephalogr. Clin. Neurophysiol.*, 101, 520-527.
- PRESTON, D. C., VENKATESH, S., SHEFNER, J. M. & LOGIGIAN, E. L. (1994) Submaximal stimuli activate different nerve fiber populations at different sites. *Muscle Nerve*, 17, 381-385.
- RABBANI, K. S. (2011a) Distribution of F-Latency (DFL) - a new nerve conduction parameter Recent developments and possibilities. *Biomedical Engineering, Editors – Ramesh R. Galigekere et. al., Narosa Publishing House, India*, 137-142.
- RABBANI, K. S. (2011b) Hypotheses to Explain the Occurrence of Multiple Peaks of DFL in Nerve Conduction Measurement. *Bangladesh Journal of Medical Physics*, 4, 27-36.
- RABBANI, K. S. (2012) Neuro-physiological measurements for diagnosis using evoked responses. *Bangladesh J of Med Phys*, 5.
- RABBANI, K. S., ALAM, M. J. & SALAM, A. (2007) Frequency Distribution of F-Latencies (DFL) has Physiological Significance and Gives Distribution of Conduction Velocity (DCV) of Motor Nerve Fibres With Implications for Diagnosis. *J. Biol. Phys.*, 33, 291-303.
- RABBANI, K. S., STEVENS, J. C., WILSON, A. J. & COCHRANE, T. (1989) Development of a microcomputerised electrophysiology system with signal averaging capability. *J. of Bangladesh Academy of Science*, 13, 209.
- RABBANI, K. S., YASSIN, N. & LO, Y. L. (2014) Identification of Cervical Spondylotic Radiculo-Myelopathy using Distribution of F-Latency (DFL), a new nerve conduction parameter. *Bangladesh J of Med Phys*, 7, 34-45.
- RABBEN, O. K. (1995) Sensory nerve conduction studies in children. Age-related changes of conduction velocities. *Neuropediatrics*, 26, 26-32.
- RIVNER, M. H., SWIFT, T. R. & MALIK, K. (2001) Influence of age and height on nerve conduction. *Muscle Nerve*, 24, 1134-1141.
- ROSENFALCK, A. (1978) Early recognition of nerve disorders by near-nerve recording of sensory action potentials. *Muscle Nerve*, 1, 360-367.
- ROSENFALCK, P. & ROSENFALCK, A. (1975) Electromyography - sensory and motor conduction. *Findings in Normal subjects*. Rigshospitalet, Copenhagen, Laboratory of Clinical Neurophysiology.
- RUTKOVE, S. B. (2001) Effects of temperature on neuromuscular electrophysiology. *Muscle Nerve*, 24, 867-882.
- SERRA, J., CAMPERO, M., OCHOA, J. & BOSTOCK, H. (1999) Activity-dependent slowing of conduction differentiates functional subtypes of C fibres innervating human skin. *J. Physiol.*, 515, 799–811.
- SHEHAB, D. K., KHURAIKET, A. J., BUTINAR, D., ABRAHAM, M. P. & JABRE, J. F. (2001) Effect of gender on orthodromic sensory nerve action potential amplitude. *Am. J. Phys. Med. Rehabil.*, 80, 718–720.
- SOLDERS, G., ANDERSSON, T., BORIN, Y., BRANDT, L. & PERSSON, A. (1993) Electroneurography index. A standardized neurophysiological method

- to assess peripheral nerve function in patients with polyneuropathy. *Muscle Nerve*, 16, 941-946.
- STÅLBERG, E. (1966) Propagation velocity in human muscle fibers in situ. *Acta Physiol. Scand.*, 70 (Suppl. 287), 1-112.
- STEGEMAN, D. F. & DE WEERD, J. P. C. (1982) Modelling compound action potentials of peripheral nerves in situ. II. A study of the influence of temperature. *Electroencephalogr. Clin. Neurophysiol.*, 54, 516-529.
- STURGES, H. (1926) The choice of a class-interval. *J. Amer. Statist. Assoc.*, 21, 65-66.
- SUNDERLAND, S. (1978) *Nerves and Nerve Injuries*, New York, Churchill Livingstone.
- THOMAS, P. K., SEARS, T. A. & GILLIATT, R. W. (1959) The range of conduction velocity in normal motor nerve fibers to the small muscles of the hand and foot. *J. Neurol. Neurosurg. Psychiatry*, 22, 175-181.
- TROJABORG, W. (1992) Sensory nerve conduction. Near-nerve recording. . *Meth. Clin. Neurophysiol. (DANTEC)*, 3, 17-40.
- TROJABORG, W., MOON, A., ANDERSEN, A., ANDERSEN, B. B. & TROJABORG, N. S. (1992) Sural nerve conduction parameters in normal subjects related to age, gender, temperature, and height: a reappraisal. *Muscle Nerve*, 15, 666-671.
- TSAI, C. T., CHEN, H. W. & CHANG, C. W. (2003) Assessments of chronodispersion and tacheodispersion of F waves in patients with spinal cord injury. *Am J Phys Med Rehabil*, 82, 498-503.
- VINCENT, A., JACOBSON, L., PLESTED, P., POLIZZI, A., TANG, T., RIEMERSMA, S., NEWLAND, C., GHORAZIAN, S., FARRAR, J., MACLENNAN, C., WILLCOX, N., BEESON, D. & NEWSOM-DAVIS, J. (1998) Antibodies affecting ion channel function in acquired neuromyotonia, in seropositive and seronegative myasthenia gravis, and in antibody-mediated arthrogryposis multiplex congenita. *Ann. N Y Acad. Sci.*, 841, 482-496.
- WAGNER, A. L. & BUCHTHAL, F. (1972) Motor and sensory conduction in infancy and childhood: reappraisal. *Dev. Med. Child Neurol.*, 14, 189-216.
- WEBER, F. (1998) The diagnostic sensitivity of different F wave parameters. *J Neurol Neurosurg Psychiatry*, 65, 535-540.
- WULFF, C. H. & GILLIATT, R. W. (1979) F waves in patients with hand wasting caused by a cervical rib and band. *Muscle Nerve*, 2, 452-457.
- YOUNG, R. R. & SHAHANI, B. T. (1978) Clinical value and limitations of F-wave determination. *Muscle Nerve*, 1, 248-250.